ABSTRACT

ZHENGJIA, WANG. Nanolayer Self-Assembly on Ionic Fiber. (Under the direction of Peter J. Hauser).

The application of electrostatic self-assembly techniques in textiles has been explored. The layer-by-layer and atomic layer deposition have been used as new methods of textile modification. The use of layer-by-layer and atomic layer deposition offer the possibility of achieving fully conformal, uniform functionalization of textile fibers of any shape. The optimum processing conditions that allow the selective and controlled deposition of organic, inorganic, and metallic substances on textile substrates via self-assembled nanolayers and atomic layer deposition techniques have also been investigated. However, non-uniform surface and irregular shapes in yarns and fibers, especially the natural fibers increase the difficulties of these applications. Recent studies stated the feasibility of using electrostatic self-assembly on cationic cotton substrates.

The goal of this research was to determine the charge density on ionic cotton fibers, which directly affect the electrostatic self-assembly. The ionic cotton fabric was produced after treatment of the substrate with a salt of chloroacetic acid or 3-chloro-2-hydroxypropyltrimethyl ammonium chloride. This research also provides a better understanding of layer-by-layer adsorption behaviors of positively or negatively charged polymer solutions on ionic cellulose films as measured by quartz microgravimetry. At neutral solution pH the adsorption of polyelectrolytes on ultrathin cellulose films was found to depend mainly on the charge density of the adsorbing macromolecule and that of the substrates. At the same adsorption condition,

the thickness and surface excess (surface concentration) of the adsorbed species are controlled by the nature of the substrate and polyelectrolyte solution.

Nanolayer Self-assembly on Ionic Fiber

by
Zhengjia Wang

A dissertation submitted to the Graduate Faculty of
North Carolina State University
in partial fulfillment of the
requirements for the Degree of
Doctor of Philosophy

Fiber and Polymer Science

Raleigh, North Carolina

2009

APPROVED BY:

_____	_____
Orlando Rojas	Xiangwu Zhang
_____	_____
Stephen Michielsen	Peter Hauser
	Chair Advisory Committee

BIOGRAPHY

I was born in Xuzhou located in Jiangsu province of China. I completed my high school education from Jiujiang No. 2 Middle School in 1999 to join the Bachelor of Technology program in Fiber and Textile Processing in Zhejiang Sci-Tech University and graduated in 2003. In 2006, I got my master degree of Textile Chemistry in Zhejiang Sci-Tech University under the direction of Dr. Jiangzhong Shao. I joined North Carolina State University in August 2006 to pursue a Ph.D program in Fiber and Polymer Science and started my research in ionic fibers under the direction of Drs. Peter J. Hauser and Orlando Rojas.

ACKNOWLEDGEMENTS

I would like to express my deepest appreciation to my major professor Peter J. Hauser not only for his invaluable help and encouragement throughout the completion of this research, but also for his continued friendship and kindness. I would also like to thank my committee members Orlando Rojas, Stephen Michielsen, and Xiangwu Zhang for their helpful comments and support.

My thanks also go to Deusanilde Silva for her help with the QCM-D, and many graduate students and peoples in paper science and textile for their help in the lab. Thanks to Kristin Cannon, for her continuing help since the first day I was in Textile department.

Thanks and appreciation is also due to the National Textile Center and North Carolina state University for their financial support and research facilities for this work.

Very special thanks go to my parents for their emotional support and understanding throughout all these years. A special thanks also to my boyfriend Yao Peng for keeping my smile and always standing with me.

TABLE OF CONTENTS

LIST OF FIGURES

LIST OF TABLES

CHAPTER 1: INTRODUCTION

1.1 Purpose of Research

Surface modification is an important element of textile manufacturing. The final properties of a textile material are critical in determining how they perform for their given end use. Electrostatic self-assembly (ESA) deposition is a new method for depositing nano-scale thin films of various materials, or creating hybrid composite structures in which functional nanometer-to-micrometer sized particles are incorporated within organic films. This method has been successfully used in the semiconductor industry and become popular field of scientific research. However, little research has been done involving the use of textiles as substrates for these processes. This research work has investigated charge distribution of ionic fibers, which is an important factor in nanolayer self-assembly process, the control of surface properties and the structure of the assembled films, such as the films morphology and film thickness. This research also aimed at better understanding of the polyelectrolytes self-assembly deposition on ionic cotton.

1.2 Challenges

The electrostatic self-assembly process has not been implemented in textile materials as they pose a number of unique problems that are not found when using traditional substrates such as silicon wafers or gold particles. These problems include non-uniform surfaces and irregular shapes in yarns and fibers, especially the natural fibers [1]. In addition, no detailed understanding about charge density of ionic fibers

would obstruct further study of nanolayer self-assemblies on ionic fibers. Moreover, no single theory is available to provide a complete description of the self-assembly process and deeper understanding of the specificity of ion-ion and ion-substrate interactions remains a challenge.

1.3 Research objectives

The benefits of utilizing electrostatic self-assembly in textiles include: Flexibility, the properties of the modified textile that can be tailored to a specific application through the control of the number and composition of the self-assembled nanolayers; Compatibility, the process that can be readily incorporated into existing textile manufacturing infrastructure; Durability, the method which is particularly tolerant to defects, as the layered structures have the ability to self-heal; and its Environmental Friendliness, the water-based process without expensive or hazardous solvent, or any vacuum system, and large excesses of the polyion solutions.

For this goal, our research is mainly divided into two tasks, based on different scales we are interested in.

Task 1: study the total charge and surface charge of ionic cotton. The charges of the substrate in ESA technique are significant caused by electrostatic action. Different treatment concentrations may influence the distribution of total and surface charge. By knowing the characterization of layer-by-layer deposition process that happened on the cationic cotton surface, we could provide more information about substrate for the future work.

Task 2: study the process of electrolytes layer-by-layer deposition on ionic cotton films by QCM-D. This task involves three steps: building polyelectrolyte multilayers on cellulose films; calculating the masses of adsorption and the film thicknesses; and comparing their differences due to the different surface charge.

2 LITERATURE REVIEW

2.1 Textile Finishing

In the textile manufacturing process, finishing is the final step to determine the final properties of a textile material. Wet processes are commonly applied in many finishing methods. However, before a fiber, fabric, or nonwoven is packaged, any operation used to change the appearance or properties can be considered a finishing procedure. A finish includes the usage chemicals and mechanical devices. The former changes the properties of the textile, and the latter changes the surface of the material. Therefore, textile finishing is often divided into two different categories: chemical and mechanical [2]. In chemical finishing, water is normally used as the medium for applying chemicals that alter the textile substrate in some way. For example, the application of polyvinyl chloride as a low surface energy film to make a fabric waterproof [3]. Any operation that improves fabric appearance or function by physical manipulation using some type of machinery is mechanical finishing. For example, a fabric is passed between two rolls under pressure to increase the luster of a fabric. This mechanical finishing is named calendaring [3]. However, it is hard to clearly distinct chemical and mechanical finishing since chemical finishing normally requires the use of some machinery while mechanical finishing may use water or steam during processing. However, these two methods can be easily classified by determining what aspects, chemical or mechanical, impart the desired characteristics to the material [2, 3].

Large quantities of water are used in many traditional methods of textile finishing. The water and any remaining chemicals require further processing to remove from the fabric. There is currently an effort in the textile industry to develop finishing techniques that are able to recycle some of the used chemicals and decrease the use of water at the same time [3].

The finishes and methods used to treat the materials are determined by the types of fiber being treated. Therefore, it is often difficult to define textile finishing as a step-by-step process. In general, products consisting of natural fibers require more processing than synthetic fibers. At the same time, the different synthetic fibers can require very diverse finishing procedures [3].

Textile finishes can be divided into functional and aesthetic finishes. Finishes that alter fiber or fabric performance, maintenance, durability, safety, and environmental resistance can be considered as functional finishes. Functional finishes are generally applied specifically to alter properties related to care, comfort, and durability. Most functional fabric properties are imparted by using chemical and wet processing methods [2, 3].

Some common functional finishes can be seen in the list below [3]:

• Antimicrobial

• Antistatic

• Durable press

• Flame resistant/retardant

• Soil release/resistant

• Water proof/repellent

• Wrinkle recovery

Aesthetic finishes are finishes used to modify the appearance or hand of a fiber or fabric. They can alter the texture, luster, or drape of a textile material [3]. Mechanical and chemical processes may be used to impart an aesthetic finish, this type of finishing with a greater emphasis being placed on mechanical processes [2].

The above is only a belief review of textile finishing. Many different chemicals and processes are used in the finishing of textile materials. Layer-by-layer deposition is also a type of textile finishing to give fibers more functionality.

2.2 Layer-by-Layer Self-Assembly

In 1991, Decher first introduced electrostatic layer-by-layer assembly through non-covalent interactions in the area of polymer thin film [4, 5]. This method is widely applied in a myriad of materials because of the ability to create highly tailored polymer thin films with a nearly unlimited range of functional groups incorporated within the structure of the film. Meanwhile this adsorption process is inexpensive and accessible. In these decades, the impact on the use of lay-by-layer electrostatic adsorption in the polymer thin film area has become more evident. In this still-expanding research field, scientists concentrate on new applications and a greater knowledge and control of the structure of the assembled films, such as the films morphology, film thickness and surface properties.

2.2.1 The Langmuir-Blodgett Technique

Until the 1990s, the creation of molecularly controlled nanostructured films is dominated by Langmuir-Blodgett (LB) technique. This technique consists of a system in which monolayer are formed on a non-solvent surface. The monolayer is then transported to a solid support. In the 1960s, Kuhn et al. performed initial work on synthetic nanoscale heterostructures by using LB technique [4]. These experiments were the first real nanomanipulations. They allowed for the mechanical handling of individual molecular layers with a very high degree of precision.

As the LB technique became widely used, several disadvantages with the process appeared. Special equipments required in the LB technique are often expensive and difficult to maintain. With regard to size and topology, substrate selection is also strict [4]. Because of the various problems with the LB technique, the development of a process to create nanolayer films with well defined layers on any type of substrate has been a subject of much interest.

2.2.2 Electrostatic Self-assembly

An excellent basis for the creation of nanolayer films is provided by the electrostatic attraction between oppositely charged molecules. This is due to the fact that it has the least steric demand of all chemical bonds [4]. Therefore, starting in the early 1990s, Decher et al. began to work on a realistic method of the electrostatic self-assembly of nanolayers [6-9]. They experimented with rod-like molecules with ionic groups at both ends, polyelectrolytes, and various other charged materials in aqueous

solution [4]. The process developed by Decher et al. has greatly increased popularity since its introduction, because of its simplicity and feasibility. Polyelectrolytes and charged nanoobjects can be used to create the nanolayers [10] on many kinds of substrates. Figure 2.1 was used by Decher in his original publication in Science to describe the process in details [7]. This technique is based on the alternating adsorption of multiple charged cationic and anionic species. The basic process involves dipping a positively charged substrate into a dilute aqueous solution of an anionic polyelectrolyte and allowing the anionic polymer to adsorb on the surface, in order to reverse the charges of the substrate surface. The negatively charged coated substrate is rinsed to remove the loosely polymer and then dipped into a solution of cationic polyelectrolyte, which adsorbs and re-creates a positively charged surface. By such sequential adsorptions of anionic and cationic polyelectrolytes, the multilayer films are created [11]. Some researchers studied the adsorption of polyelectrolytes and found although these polymers are somewhat associated in solution, they uncoil on adsorption to a charged surface, and can form quite stable multilayer films. When the films are exposed to air drying or storage in other solvents, rearrangements occur rapidly on the surface. Therefore, continuous dipping methods have been used to obtain the most stable and uniform films [11].

Theoretically, the adsorption of charged molecules which consist of more than one equal charge allows for opposite charge reversal on the surface. This behavior implies that (1) the repulsion of equally charged molecules leads to self-regulation of

adsorption and restriction of the deposition to a single layer; (2) oppositely charged molecules can be adsorbed in a second step on the top of the first adsorbed layer. Adsorption of the opposite charged molecules alternately occurs to form multilayer structures on the surface of a substrate [4].

Multilayer films may be composed of polyions, charged molecular objects, and/or colloidal objects. In theory, substrate size and topology have no limitations due to the fact that the process involves adsorption from a solution. Nanolayer films have been created on objects of a variety of different sizes [4].

Decher's work determined that the use of polyelectrolytes was advantageous when compared to various other small molecules. While good adhesion of a layer to the base substrate depends on a particular number of ionic bonds, the overcompensation of the surface charge on the outermost layer was found to be more dependent on the properties of the adsorbed polymer than of the substrate. An additional benefit is that the polyelectrolytes can bridge over underlying defects. The conformation of a given polymer at the surface is then more dependent on the chosen polyelectrolytes and the adsorption conditions than the changes on the surface of the substrate [4]. Numerous studies have shown experimental evidence of a linear increase of film thickness with the number of deposited layers independent of the nature of the initial substrate [12-17].

The most obvious property of an individual layer is its thickness, which depends on the nature of underlying surface and on the deposition conditions. Parameters with

respect to the underlying substrate are important, such as the density of charged groups and the surface roughness. Meanwhile, polyelectrolyte concentration, adsorption time, pH and solvent composition are also essential control parameters in the adsorption process. The deposition is highly reproducible if these parameters are maintained strictly constant. When polyanion and polycation pair adsorptions are repeated consecutively, each polyanion adsorbs onto polycation-coated surface and vice versa. After a few layers, the structure and properties of each layer are governed by the polyanion or polyantion layer as well as the deposition conditions. The influence of the substrate is typically lost after a few layer-by-layer deposition cycles.

2.2.3 Advantages of Layer-by-Layer Assembly

Compared to other similar surface modification techniques, the process of creating multilayer thin films by layer-by-layer adsorption has several advantages: (1) the film architecture is almost completely determined by the deposition technique; (2) a wide variety of different materials can be used to create the multilayer thin films, and hence creating truly multi-composite multilayer films [4]. The original work was done by Keller et al., who incorporated clay particles with silica microspheres using alternating sequential adsorption [18]. Some functional particles and macroscopic systems have been incorporated into the films in past few years. For example, Schmitt et al. used Au nanoparticles to create conducting films [19, 20]. Current examples of multi-composite films include structures that contain proteins, clay platelets, metals and gold colloids [4, 21-23].

Although electrostatic self-assembly has become widely used in recent years, certain details of the process are still not clearly understood. For example, the existence of a minimum time needed to complete the deposition process has not been explained. The purpose of the intermediate washing and drying steps are also not well defined. Quantitative evaluation of the assembly process will be necessary to make electrostatic self-assembly a practical method [24]. Electrostatic self-assembly is also influenced by a variety of factors that can be difficult to control such as shielding effects, charge transfer interactions, and hydrogen bonding [25]. All these factors can influence film thickness, surface properties, and so on. The behavior of highly charged, strong polyelectrolyte chains attract more interest in fundamental understanding of layer-by-layer adsorption, which can be shielded by altering ionic strength. In weak polyelectrolytes such as polyacids or polybases, shielding and surface charge density affects layer thickness and stability by varying pH. Consequently, the relative amount of charge along backbone has also been affected. Surface charge, interpenetration between layers and layer thickness can be dramatically changed by varying pH for the polycation and polyanion [26, 27]. No single theory has been developed to completely describe the deposition process. However, a variety of studies have been conducted that have helped to clarify many aspects of the electrostatic self-assembly method [28, 29].

Layer-by-layer self-assembly is a very general method by using adsorption from solution to create multi-component nanolayer films on solid substrates [4]. The

multilayer films created by using this process are made up of a number of layers, and each layer has its own individual structure and properties. The multilayer films can then be tailored to serve specific purposes [11]. Biological compounds, conducting polymers, light emitting polymers, and dyes can be manipulated by self-assembled nanolayers onto a suitable substrate [27, 29].

Due to the nature of easy preparation and versatility, self-assembled ultra-thin films are widely applied. Self-assembled films can function as barriers, with controllable levels of permeability, for gases, liquids, covalent molecules, ions and electrons. These properties have been used for the construction of insulators, passivators, sensors and modified electrodes. Self-assembled nanolayers are also suitable for the construction of devices based on molecular recognition. Molecules or nanoparticles within a self-assembled layer can be aligned spontaneously, or by changing the temperature, pressure and pH, or by applying an electric or magnetic field. These characteristics permit the formation of superlattices with the desired architecture and allow the production of a number of photonic, electronic, magnetic and non-linear optical devices. The layer-by-layer self-assembly of insulators, conductors, and magnetic, ferroelectric and semiconductor nanoparticule films allow the construction of molecularly controlled heterostructures. Control of the sizes and interparticle distances of the monodispersed nanoparticles within the self-assembled film can also be used in optical applications [30-33]. Self-assembled nanolayers have been used to create polymer light emitting diode devices with improved performance

compared to traditional devices [34]. Controlling the various solution parameters such as surface charge and pair combinations has opened the possibility of creating new light sensitive materials and optical devices [35].

In addition to the applications and advantages listed above, the self-healing capability of electrostatic self-assembled nanolayers provides an increased tolerance to defects. This self-healing ability sets the electrostatic method apart from other selforganization techniques [10]. The electrostatic method can be used on substrates with non-uniform surfaces and compensates for defects caused during the adsorption process. It also allows the use of nanoparticles which might not necessarily provide smooth layers [24, 36]. The self-healing process is simply a result of the adsorption of multiple layers. As layers are added, defects are covered up or filled [37].

2.3 Survey of Substrates Used

Nanolayer films have been produced by electrostatic self-assembly on a number of different substrates including glass, quartz, mica, and silicone [10, 16]. Gold and silver have also been used as base substrates [38-42]. Meanwhile, nanolayer thin films have been successfully built on both hydrophilic (fluorine, glass, and silicon) and hydrophobic (silanized glass) substrates by this technique [43]. Due to different analysis techniques, the choice of substrates has often been determined by their convenience. UV-VIS spectroscopy and optical microscopy are used to analyze glass and quartz [10]. Ellipsometric studies were used to study silicon wafers [18, 43]. The smooth surfaces of substrates such as quartz, silica and glass also make them well

suited for X-ray reflectivity analyzes [16, 17]. Specially, Quartz Crystal Microbalance can study the ultrathin films on gold and silica sensors by the oscillation of resonator.

2.3.1 Influence of Substrate Characteristics

Each of the different types of substrates has different physical property in regards to their topology, smoothness and roughness. However, due to the characteristics of the layer-by-layer deposition technique, the adsorption mostly depends on the surface charge distribution of the substrate [44].

The deposition of a film depends on the used polyelectrolytes and the adsorption conditions. Therefore, the amount of polyelectrolyte adsorbed during the first few deposition steps depend on the substrate and that substrate's surface charge [45- 49]. For the first five deposition steps, the amount of adsorbed polymer normally increases before reaching a more constant level [14, 31]. The surface charge of the substrate determines how long it takes to reach a constant level. However, as long as the polyelectrolytes create an electrostatic equilibrium, constant growth is eventually reached despite the substrate characteristics [37, 46, 50].

Previous research has shown the influence of surface charge on the deposited layers on different layers [51]. In the research of Fou and Rubner, they used microscopic glass slides with hydrophilic, hydrophobic, negatively charged, and positively charged surfaces as substrates. The surface charge of the substrates was found to have a great influence on the deposition time, layer thickness, and layer uniformity. While previous research has clearly shown that the substrate's surface

charge has an great influence on adsorption of ionic polymer, the characteristics of the substrate structure itself have very little effect on the adsorption of the individual layer. The electrostatic self-assembly process allows various substrates of different sizes and shapes to be coated with polyelectrolyte films [44].

2.3.2 Polymers as Substrates for Layer-by-Layer Deposition

Since it was thought that the layer-by-layer assembly process required flat clean surfaces, much of the early work involving the process used inorganic substrates such as quartz and silicone [16, 22, 25]. Later work began looking at the electrostatic deposition of nanolayers on polymer films and other organic materials as substrates [52, 53]. Further reports has looked at using a number of different polymer films as substrates for the deposition process, including poly (propylene), poly(isobutylene), poly(styrene), poly(methylmethacrylate), poly(ethyleneterephthalate), poly-(phenyleneoxide), and poly (etherimide) [45].

Delcorte and others looked at the deposition of polyelectrolyte layers onto polymer films [45]. Surface analysis techniques showed that alternate polyelectrolyte thin films could be built up on polymer substrates. The series of polymer were tested included poly (propylene), poly (isobutylene), poly (styrene), poly (etherimide), poly (ethyleneterephthalate) (PET), poly (phenyleneoxide), and poly (methylmethacrylate). Semi-crystalline PET films were found to be the best substrate for supporting multilayers. Results of the study stated that polymer substrates containing carbonyl groups and/or benzene rings performed better than the other substrate choices.

Particular interest to the textile industry, PET film was used as a substrate for the nanolayers self-assembly. AS we known, PET can be surface modified by a variety of techniques including plasma, corona discharge, ion beam, laser treatment, photo-initiated graft polymerization, saponification, aminolysis, reduction, and entrapment of poly (ethylene oxide). Neutral PET can react with polyamines to incorporate amine functionality that can support positive charge (PET-NH_3^+) in nonbasic solution. On the other hand, the surface can be readily hydrolyzed to introduce carboxylic acid functionality that can support negative charge (PET-CO_2^-) in sufficiently basic solution. Figure 2.2 shows the method how to prepare the PET substrate for layer-by-layer disposition [54].

Chen and McCarthy conducted a study involving the modification of PET with layer-by-layer deposition in 1997. Poly (sodium styrenesulfonate) and poly (allylamine hydrochloride) were used as polyelectrolytes for surface modification. These particular polyelectrolytes were used because of their extensive use in previous studies on self-assembled nanolayers [53]. The techniques of contact angle analysis and X-ray photoelectron spectroscopy were used to analyze and prove effectively in indicating the structure of the outermost layers, the individual layer thicknesses, and the overall multilayer thicknesses [54].

Through X-ray photoelectron spectroscopy and contact angle analysis, the layers were stratified and the wet ability of the multilayer assemblies could be determined by the identity of the outermost polyelectrolyte layer. The individual polymer layers were

extremely thin (2-6 Å). The thickness was affected by the substrate surface properties and it was confirmed that the thickness of each layer could be controlled by the ionic strength of the polyelectrolyte solutions. The stoichiometry of the deposition process (ammonium ion: sulfonate ion ratio) was also affected by the substrate and solution ionic strength. This indicated that the layer-by-layer deposition process was quite forgiving and could be done under a variety of conditions. Multilayer assemblies had good mechanical properties via peel tests. No failures were observed in the multilayers. In addition, Decher et al. has been demonstrated that manganese chloride added to PAH and PSS solutions would increase the thickness of the layers by screening charge-charge repulsions during adsorption [4.31]. This opinion has also been proved by Wei Chen et al.. In their work, sodium chloride added to PAH/PSS system had the same function. These experiments indicated that layer-by-layer deposition was a viable tool for polymer surface modification and that PET fibers/fabrics could eventually be used as a base substrate for the electrostatic self-assembly process [54].

2.4 Survey of Polyelectrolytes Used

A large number of polyelectrolytes have been used to create a variety of nanostructured thin film coatings on the substrates [37-40]. One of the most studied and well understood systems is the poly (allylamine hydrochloride) (PAH) and poly (styrene sulfonate) (PSS) system [32, 35, 41-44]. A number of more complex, functionalized polyelectrolytes have also been used based on their ability to form

structured coatings and enable secondary chemical modifications. One of the greatest advantages of the layer-by-layer deposition technique is that almost any polyelectrolyte can be used as long as the appropriate oppositely charged partner polyelectrolyte is chosen [27].

The properties of polyelectrolyte films can be controlled by changing characteristics of the solution such as the pH level. Different pH leads to different charge density of polyelectrolyte. PSS and PAH are examples of polyelectrolytes that are often deposited at pH values less than 7.0. Recent studies have looked at multilayers composed of weak polyelectrolytes. The charge density of these polyelectrolytes can be controlled by adjusting the pH values of the solutions [45]. Weak polyelectrolytes such as PAH allow for a more precise control over the physical characteristics of the multilayers. Weak polyelectrolytes can be deposited with a high percentage of the chains making loops and tails under pH conditions of incomplete charge. If using strong polyelectrolytes, they often deposit as molecularly thin layers (about 5 Å). However, when using weak polyelectrolyte solutions of PAA/PAH, layer thicknesses have reached greater than 80 Å. The thickness of the nanolayers are also depends on operational factors such as concentration, adsorption time, ionic strength, temperature, rinsing time, dipping speed, and drying time [21]. For a given pair of strongly dissociated polycations and polyanions, the concentration of salt in the deposition solution appears to exert the strongest influence on the adsorption process and the thickness of each polymer layer [33].

The group of Serizawa focused on the research of electrostatic adsorption of polystyrene particles onto an ultrathin polymer film. The ultrathin thin films are prepared by alternate adsorption using both cationic PAH solution and anionic PSS solution containing suitable concentrations of sodium chloride [59]. They quantitatively analyzed the electrostatic adsorption of anionically polystyrene particles on the surface by quartz crystal microbalance (QCM) and scanning electron microscopy (SEM) techniques. They studied the effect of the charge density of the particle surface on electrostatic adsorption onto the film surface, and the effect of the film's surface charge on particle adsorption. QCM was used to calculate the mass of the particles adsorption according to the frequency shift.

Natural polyelectrolytes can also be applied in layer-by-layer electrostatic self-assembly to create multilayer thin films, such as nucleic acids, proteins, and polysaccharides [46-48]. Studies involving these polyelectrolytes focus on the biological function of films and their ability to simulate biological processes. And the main advantage of using this method is that the assembly of proteins via layer-by-layer deposition has no chemical modification and in theory normal protein behavior should be maintained [49, 50].

2.5 Applications of Layer-by-Layer Films

Currently, polymeric nanolayer films are used to modify the surface properties of materials in electronic products, machinery tools, and medical supplies. These polyelectrolyte based films are capable of self-organization [21]. Self-assembled films

can be the barriers to hinder permeability for gases, liquids, covalent molecules, ions, and electrons with controllable levels [35, 51]. Due to these properties, they have been used for the construction of insulators, passivators, sensors, and modified electrodes. Self-assembled nanolayers are also suitable for the construction of devices based on molecular recognition [52, 53]. Molecules or nanoparticles within a self-assembled layer can be aligned spontaneously, or by the application of an electric or magnetic field. They can be also aligned by changing the temperature, pressure or pH. Due to these characteristics super lattices with the desired architecture can be formatted, and the production of a number of photonic, electronic, magnetic, and nonlinear optical devices is permitted [52]. The layer-by-layer self-assembly of insulators, conductors, and magnetic, ferroelectric and semiconductor films also constructs molecularly controlled heterostructures [55-58].

2.6 Self-assembled Nanolayers on Textiles

Layer-by-layer deposition technique has been used to improve the properties in many materials. Recently, the group of Juan P. Hinestroza did a lot research of LbL deposition process in textile and natural fibers. Because of the chemical heterogeneity of natural fibers' surface as well as their iruntreated shape, they present many challenges in this field. In order to use LbL deposition on textile materials, it may be necessary to modify the surface of the given substrate to provide an adequate number of surface reaction groups. Recent research has demonstrated that self-assembled nanolayers of polyelectrolytes can be deposited over cationic cotton fibers and

indicated the thickness of nanolayers. This opens a number of possibilities for a novel fully conformal surface modification technique.

2.7 Ionic Cotton

2.7.1 Cellulose and its chemistry

The chemical structure of its molecules and their structural and morphological arrangements in the fibrous form should be best known when discussing chemical and physical properties of cotton cellulose. Cotton grows as a natural fiber from the surface of the cotton plant seeds with impurities of wax, protein, etc. When these impurities are removed through scouring and bleaching processes, cotton is almost 99% pure cellulose [60]. Cellulose is a linear condensation polymer consisting of D-anhydroglucopyranose units often called anhydroglucose joined together by β- 1, 4-glucosidic bonds. Its repeat unit is the anhydrobeta- cellobiose. Figure 2.3 shows the chemical structure of cellulose polymer. The number of repeat units bound together gives the degree of polymerization, which is between 1000 and 15000 in native cotton [61]. There are three hydroxyl groups in each anhydroglucose unit, one primary and two secondary. These hydroxyl groups strongly influence the chemical reactivity of cellulose. The primary hydroxyl group is the most reactive because its greater acidity compared to the secondary hydroxyl groups forming ionized cellulosate which is a good nucleophile for attack on moieties like vinyl group (Michael addition), or for nucleophilic substitution [62]. These hydroxyl groups serve as principal sites for reactions like etherification and esterification and are responsible for dyeing and

finishing applications.

Approximately 65 to 70% of natural cotton cellulose is crystalline, and the rest is amorphous [63]. Inter-chain hydrogen bonds hold polymeric chains in place [64]. The hydrogen bonding is more prominent in crystalline areas than in the amorphous regions. The molecules are parallel and loosely packed in the crystalline areas. The hydroxyl groups of cellulose served as adsorption sites for water molecules, when cotton adsorbed moisture, hydrogen bonding increases. Therefore, cotton shows improved strength as its moisture content increases [64].

2.7.2 Carboxymethylation of cotton cellulose

Cellulose can be made with negatively charged via various routes, such as treated with chloroacetic acid, chlorosulphonic acid, or sodium, 4-(4, 6-dichloro-1, 3, 5-triazinylamino)- benzenesulfonate [65, 66]. The product of the carboxymethylation of cotton cellulose is carboxymethylcellulose (CMC), anionic cellulose [67]. It is also termed as cellulose glycolate and cellulose glycolic acid, which is formed by the treatment of cellulose with chloroacetic acid and sodium hydroxide. The chemical structure of CMC is shown in Figure 2.4.

Different degrees of substitution depend on different steps of treatment [67]. The substitution is at the 6-O- position predominantly on the cellulose molecules followed by 2-O, 2, 6- di-O, 3- O, 2, 3- di-O and then 2, 3, 6- tri-O positions. The reaction proceeds unevenly with areas of high and low substitutions [68].

At low degree of carboxymethylation, CMC molecules are extended and its

structure looks like a rod. As the degree of carboxymethylation increases, the molecules overlap and form coils. This is influenced by the degree of substitution and average chain length.

This two-step method is used to get carboxymethylated cellulose in previous work [65, 69]. In step 1, fabric samples were soaked in 20% NaOH for 10min, padded to 100% wet pick-up and dried at 45 °C for 12 min. The sample looked yellow and was completely dry. In step 2, mono chloroacetic acid was neutralized by the weak base sodium carbonate. The samples from step 1 were soaked in the aqueous sodium chloroacetate solution of the specified concentration for 5 min, padded to 100% wet pick-up, cured at 85 °C for 30 min, washed with water, acidified with 2 g/L acetic acid, washed with water again and dried in air.

2.7.3 Cationization of cotton cellulose by CHTAC

Cellulose can be cationized by 3- chloro-2-hydroxypropyl trimethyl ammonium chloride 6, [70-72] which is commercially available as a 69% aqueous solution under the name of CR-2000 from Dow chemical. Reaction of cellulose with CHTAC depends on time, temperature and pH. The sodium hydroxide acts as a base catalyst. In the present of sodium hydroxide, CHTAC forms 2, 3- epoxypropyl trimethyl ammonium chloride, (an epoxy intermediate). It can react with cellulose. But the epoxy intermediate starts hydrolyzing when it is formed. Because the hydrolyzed product does not react with cellulose, the cellulose should be treated immediately when the CHTAC with alkali solution is made. Reaction of cellulose with CHTAC

and alkali to form cationic cellulose is showed in Figure 2.6 [73].

The cationization has been tried by several methods [70]: pad- batch, pad-steam, exhaust, and pad-dry cure. In the pad-batch process fabric is padded through the sodium hydroxide-CHTAC solution and batched at room temperature for 24 hours. In the exhaust method, fabric is treated for 90 min at 75°C. Different solvents such as water, acetone, ethanol, isopropanol and methanol have been tried. Acetone gave the best reaction efficiency. In the pad-steam method, fabric is padded through the mixture and steamed at 100°C for 30 min. The pad-dry cure method involves padding the fabric in the mixture of NaOH and CHTAC solution and drying and curing at different temperatures for different times. NaOH to CHTAC mole ratios were varied. The highest cationization was achieved by drying at 35°C for 5 min followed by curing at 110°C for 5 min. All these methods produced different reaction efficiencies. The exhaustion method gave 10% fixations; pad-batch gave 25% substitution, whereas pad-dry15 cure gave 85%. The reaction efficiency went down with increase in CHTAC concentration. The NaOH: CHTAC mole ratio of 1.8 or slight more was found the best for the reaction in our previous tests [65].

2.8 Analysis Methods

2.8.1 X-ray Photoelectron Spectroscopy

X-ray Photoelectron Spectroscopy (XPS) is a surface chemical analysis technique, and also known as electron spectroscopy for chemistry analysis (ESCA). It is a quantitative method in measuring the empirical formula, chemical state and

electronic state of the elements in the surface. A beam of X-rays irradiates a material, while simultaneously measuring the kinetic energy (KE) and number of electrons that emit from the top 1 to 10 nm of the material being analyzed, and then XPS spectra are obtained. Figure shows the principle of XPS. In order to count the number of electrons at each KE value, with the minimum of error, XPS must be operated under UHV conditions [74].

Because the energy of a particular X-ray wavelength is a known quantity, we can determine the electron binding energy (BE) of each of the emitted electrons by using an equation below:

$$E_{binding} = E_{photon} - E_{kinetic} - \Phi$$

$E_{binding}$ is the energy of the electron emitted from one electron configuration within the atom, E_{photon} is the energy of the X-ray photons being used, $E_{kinetic}$ is the kinetic energy of the emitted electron as measured by the instrument and Φ is the work function of the spectrometer [75].

A XPS spectrum is a plot of the binding energy (BE) of the electrons detected (X-axis) versus the number of electrons detected (Y-axis). A characteristic set of XPS peaks at characteristic binding energy (BE) values can directly identify each element that exist in or on the surface of the material being analyzed. These characteristic peaks correspond to the electron configuration of the electrons within the atoms, such as 1s, 2s, 2p and so on.

XPS detects all elements with an atomic number (Z) from 3 to 103, which

means that it cannot detect hydrogen or helium. This technique is routinely used to analyze inorganic compounds, metal alloys, semiconductors, polymers, etc.

An XPS system mainly includes these components: a source of X-rays, an ultra-high vacuum (UHV) stainless steel chamber with UHV pumps, an electron collection lens, an electron energy analyzer, Mu-metal magnetic field shielding, an electron detector system, a moderate vacuum sample introduction chamber, sample mounts, a sample stage and a set of stage manipulators.

Figure 2.8 provides a schematic of how XPS system works. A source of X-rays illuminates an area of a sample causing electrons to eject with a range of energies and directions. And then these electrons pass through the transfer lenses. An electron collection lens used for collecting a proportion of these emitted electrons defined by those rays that can transfer through the apertures and focus on the analyzer entrance slit. Electrons of a specific initial kinetic energy are measured by setting voltages for the lens system. The electrons of the required initial energy retard their velocity so that their kinetic energy after passing through the transfer lenses matches the pass energy of the hemispherical analyzer. Magnetic field shielding is always an electrostatic field within the hemispherical analyzer (HSA), which are established to only allow electrons of a given energy (pass energy) to arrive at the detectors. An ultra-high vacuum condition should be offered by a set of UHV system in order to prevent arcing and high voltage breakdown and eliminate adsorption of contaminants on the surface.

XPS is a useful technique which chemically analyses the top layers of a solid material. It not only determines the surface elements, but also the chemical state and atomic concentration (directly from the areas of the peaks). XPS can be used for organic and inorganic materials. Samples can be conductors, semiconductors or non-conductors.

2.8.2 Transmission Electron Microscopy

Transmission electron microscopy (TEM) is a microscopy technique whereby a beam of electrons is transmitted through an ultra thin specimen. An imaging is formed by the electrons interacting with the specimen as they pass through, which is magnified and focused by an objective lens and onto an imaging device.

The transmission electron microscope operates on the same basic principles as the light microscope but uses electrons instead of light. The wavelength of light limits the objects are observed with a light microscope. TEM use electrons as light resource and their much lower wavelength make it possible to get a resolution a thousand times better than with a light microscope.

The source at the top of the microscope emits the electrons that travel through vacuum in the column of the microscope. Instead of glass lenses focusing the light in the light microscope, the TEM uses electromagnetic lenses to focus the electrons into a very thin beam. The electron beam then travels through the specimen that be studied. Depending on the density of the material present, some of the electrons are scattered and disappear from the beam. At the bottom of the microscope the unscattered

electrons hit an imagine device, which is usually a fluorescent screen. The imagine device gives rise to a "shadow image" of the specimen with its different parts displayed in varied darkness according to their density. The image can be studied directly by the operator or photographed with a camera. Figure 2.9 provides a schematic of how the TEM system used for this research works.

2.8.3 Streaming current tests

The streaming current technique (SC) is a sensitive method to characterize the surface charge of colloidal materials and polymer in solution, which is important in the fields of colloid and interface science. Most common streaming current analyses are based on the two following principles: First, it is assumed that most of the titratable charge is on colloidal or polymeric materials that are small enough to pass through the filtering process that is typically used as preparative step for the experiments; second, the emphasis is on measuring a titration endpoint, rather than quantifying the absolute values of the streaming current signals from the instrument. Such titration end point can be easily identified when the streaming current signal reaches a zero value. Furthermore, in the case of fibrous materials, it is assumed that the amount of colloidal charge in the dissolved and colloidal phase is large relative to the charge at the fiber surface.

Figure2.10 shows the most essential mechanical parts of a streaming current device [78]. A non-conducting piston moves up and down with a frequency of about four cycles per second. The piston diameter is about 1-1.5cm and the distance of

travel is about 0.5cm. The piston reciprocates within a cylinder. The piston and cylinder are made from PTFE, because it has such little affinity for most soluble polymers. Since the PTFE surface does not have very much of their "own" charge relative to other materials, it makes it possible to attribute most of the signal to the effects of adsorbed materials. There are two electrodes spaced at different positions of the cylinder wall. When a sample to be tested is in a narrow annulus between the piston and cylinder, the piston's motion causes the loosely adsorbed materials to be displaced rapidly up and down through the annulus. The signal generated by an SC device is due to the ionic double layers at the surface of the piston and cylinder. It can be assumed that the probe surfaces are charged and the counter-ions lie outside of the probe surface. The reciprocating flow sweeps these ions up and down, creating an electrical current or voltage that can be measured by the two electrodes. This is the signal that is recorded and used as indicator of the end point in the titration protocol to determine the charge.

2.8.4 Quartz crystal microbalance

The quartz crystal microbalance (QCM) technique allows the measurement of the gain (or reduction) of mass at the surface of a quartz resonator by monitoring its change in frequency with time. The QCM can be used under vacuum, in gas phase and in liquid environments.

A piezoelectric resonator (quartz) undergoes electric polarization due to applied mechanical stresses (piezoelectricity). A QCM crystal consists of a thin quartz disc

sandwiched between a pair of electrodes (typically gold) (Figure2.11). Due to the piezoelectric properties of quartz, it is possible to excite the crystal to oscillate when an AC voltage is applied across its electrodes. The principle of the QCM technique is the converse effect: the crystal is made to oscillate by applying an AC voltage over the electrodes. The resonance frequency, Δf changes in QCM measurements and such shifts are then related to the gain (or release) of mass.

Quartz Crystal Microbalance with Dissipation monitoring (QCM-D) collects both the dissipation and the resonance frequency of a quartz crystal. Dissipation refers to the frictional and viscoelastic energy losses due to changes in the sensing surface. The frequency is measured intermittently, while the oscillator or sensor is driven to resonate, and D is measured during periods when the driving field is disconnected. The dissipation is a parameter quantifying the damping in the system, and is related to the sample's viscoelastic properties. In the case of adsorbed layers, for example, it is related t the rigidity (or softness) of the film.

Overall, the QCM technology can be used to characterize the formation of thin films and/or changes at the interface with nanoscale resolution. Typical applications of quartz include interfacial phenomena involving proteins, surfactants, polymers and cells.

When any material is adsorbed onto the crystal, it can be treated as an equivalent mass change of the crystal itself. The increase in mass, Δm, induces a proportional

shift in frequency, Δf. A linear relationship between Δm and Δf can be described by the Sauerbrey equation [11].

$$\Delta m = \frac{-\rho_q t_q \Delta f}{f_0 n} = \frac{-\rho_q v_q \Delta f}{2 f_0^2 n} = -\frac{C \Delta f}{n} \quad (1)$$

In equation (1), ρ_q and υ_q are the specific density and the shear wave velocity in quartz, respectively, t_q is the thickness of the quartz crystal, and f_0 is the fundamental resonance frequency (when n =1). This relation is valid provided the following conditions are fulfilled: (i) The adsorbed mass is distributed evenly over the resonator, (ii) Δm is much smaller than the mass of the crystal itself (<1%), and (iii) the adsorbed mass is rigidly attached, with no slip or inelastic deformation due to the oscillatory motion which means no change in energy dissipation.

In measurements in the liquid phase, the QCM-D provides valuable information about reactions and conditions at the liquid-solid interface. In many applications, such as thick deposited polymeric films, electrochemically created polymeric films, biomacromolecular films, composites comprised of proteins and nucleic acids, and biosensors, the systems may not behave as an elastic body (on the QCM sensor surface). In these cases, the Sauerbrey equation may not apply, and it is difficult if not impossible to extract the corresponding changes in mass.

In such situations, the energy dissipation becomes an important variable that can be used for a more accurate characterization of viscoelastic films. The dissipation is proportional to the power dissipation in the oscillatory system, which as stated before

is related to the rigidity of the adsorbed layer. The relation between the dissipation and energy dissipated and stored can be stated as follows:

$$D = \frac{E_{\text{dissipated}}}{2\pi E_{\text{stored}}} \tag{2}$$

Where $E_{\text{dissipated}}$ is the value of energy dissipation and E_{stored} is the value of storage during one oscillation in the oscillating system. Hence, slip and viscous losses make the measured changes in D. For QCM-D measurements in liquids, the major contribution to D comes from frictional (viscous) losses within the liquid contacting the crystal. According to Stockbridge, the shift in the dissipation factor in a liquid environment is

$$\Delta D = \frac{1}{\rho_q t_q} = \sqrt{\frac{\rho_l \eta_l}{2\pi f}} \tag{3}$$

Here, η_l is the viscosity and ρ_l is the density of the fluid; t and ρ are the thickness and the density of the quartz plate, respectively [12]. If the adsorbed film slips on the electrode, frictional energy is created that increases the dissipation. Furthermore, when the film is viscous, energy is also dissipated because the oscillatory motion induced in the film (internal friction in the film). A rigid adsorbed layer gives no change in dissipation [13]. Generally, soft adsorption layers dissipate more energy and thus are of higher dissipation value. From this point of view, dissipation value is an indicator of the conformation of the adsorbed layers.

In liquid, an adsorbed layer may consist of a considerably high amount of water (coupled water), which is also sensed as a mass uptake by the QCM. By measuring simultaneously the shift in frequency and the respective dissipation at various overtones it becomes possible to determine whether the adsorbed film is rigid or water-rich (soft), which is not possible by looking only at the frequency response.

The top diagram In Figure 2.12 illustrates how the frequency of the oscillating sensor crystal (gold-coated quartz, for example) changes when the mass is increased by addition of a molecular layer. Here antibodies (green) are added to a layer of protein (red). The bottom of the same figure illustrates the difference in dissipation signal generated by rigid (red) and soft (green) molecular layers on the sensor crystal. This procedure can be repeated over 200 times per second, which gives QCM-D unmatched sensitivity and high resolution.

In summary, QCM-D is a surface-sensitive technique that allows the measurement of structural and viscoelastic properties as well as changes of adsorbed mass changes in situ and in real time with molecular or nano-scale sensitivity.

2.9 Reference

1. Huang, J.G., Ichinose, I. & Kunitake, T. Biomolecular modification of hierarchical cellulose fibers through titania nanocoating. *Angew Chem Int Edit* **45**: 2883-2886 (2006).

2. Tomasino, C., *Chemistry and Technology of Fabric Preparation and Finishing*. (North Carolina State University, Raleigh, NC; 1992).

3. Hudson, P.B., Clapp, A.C. & Kness, D. Joseph's Introductory Textile Science, Edn. 6th. (Harcourt Brace Jovanovich College Publishers, New York; 1993).

4. Decher G., Fuzzy Nanoassemblies: toward layered polymeric multicomposites. *Science,* **277**:1232–1237 (1997).

5. Paula T. Hammond. Recent explorations in electrostatic multilayer thin film assembly. *Current Opinion in Colloid & Interface Science,* **4**: 430-442 (2000).

6. Lvov, Y., G. Decher, and M. H., Assembly, Structural Characterization, and Thermal Behavior of Layer-by-Layer Deposited Ultrathin Films of Poly(vinyl sulfate) and Poly(allylamine). *Langmuir*, **9**: p. 481-486 (1993).

7. Lvov, Y., G. Decher, and G. Sukhorukov, Assembly of Thin Films by Means of Successive Deposition of Alternate Layers of DNA and Poly(allylamine). *Macromolecules*, **26**: p. 5396-5399 (1993).

8. Lvov, Y., F. Essler, and G. Decher, Combination of Polycation/Polyanion Self-Assembly and Langmuir-Blodgett Transfer for the Construction of Superlattice Films. *J Phys Chem*, **97**: p. 13773-13777 (1993).

9. Lvov, Y., et al., Assembly of Polyelectrolyte Molecular Films onto Plasma-Treated Glass. *J Phys Chem*, **97**: p. 12835-12841 (1993).

10. Bertrand, P., et al., Ultrathin Polymer Coatings by Complexation of Polyelectrolytes at Interfaces: Suitable Materials, Structure, and Properties. *Macromol Rapid Commun*, **21**: p. 319-348 (2000).

11. Decher G. Polyelectrolyte multilayers, an overview In: Decher G, Schlenoff J (eds) Multilayer thin flims. *Wiley-VCH, Newyork*, pp 1–46 (2003).

12. Chen, W. and T. McCarthy, Layer-by-Layer Deposition: A Tool for Polymer Surface Modification. *Macromolecules*, **30**: p. 78-86 (1997).

13. Cooper, T.M., A.L. Campbell, and R.L. Crane, Formation of Polypeptide-Dye Multilayers by an Electrostatic Self-Assembly Technique. *Langmuir*, **11**(7): p. 2713-2718 (1995).

14. Dubas, S. and J. Schlenoff, Factors Controlling the Growth of Polyelectrolyte Multilayers. *Macromolecules*, **32**: p. 8153-8160 (1999).

15. Hoogeveen, N.G., et al., Formation and stability of multilayers of poly-electrolytes. *Langmuir*, **12**(15): p. 3675-3681 (1996).

16. Losche, M., et al., Detailed Structure of Molecularly Thin Polyelectrolyte Multilayer Films on Solid Substrates as Revealed by Neutron Reflectometry. *Macromolecules*, **31**: p. 8893-8906 (1998).

17. Schmitt, J., et al., Internal Structure of Layer-by-Layer Adsorbed Polyelectrolyte Films: A Neutron and X-ray Reflectivity Study. *Macromolecules*, **26**: p. 7058-7063 (1993).

18. Keller, S.W., H. Kim, and T.E. Mallouk, Layer-by-Layer Assembly of Intercalation Compounds and Heterostructures on Surfaces: Toward Molecular "Beaker" Epitaxy. *Journal of the American Chemical Society*, **116**: p. 8817-8818 (1994).

19. Schmitt J, Decher G, Dressick WJ et al, Metal nanoparticle/polymer superlattice films: fabrication and control of layer structure. *Adv Mater* 9:61 (1997).

20. Liu YJ, Wang YX, Claus RO, Layer-by-layer ionic self-assembly of Au colloids into multilayer thin-films with bulk metal conductivity. *Chem Phys Lett* **298**:315-319 (1998).

21. Feldheim, D.L., et al., Electron Transfer in Self-Assembled Inorganic Polyelectrolyte/Metal Nanoparticle Heterostructures. *Journal of the American Chemical Society*, **118**: p. 7640-7641 (1996).

22. Lvov, Y., et al., Assembly of Multicomponent Protein Films by Means of Electrostatic Layer-by-Layer Adsorption. *Journal of the American Chemical Society*, **117**: p. 6117-6123 (1995).

23. Lvov, Y., et al., Formation of ultrathin multilayer and hydrated gel from montmorillonite and linear polycations. *Langmuir*, **12**(12): p. 3038-3044 (1996).

24. Lvov, Y., et al., A Careful Examination of the Adsorption Step in the Alternate Layer-by-Layer Assembly of Linear Polyanion and Polycation. *Coll Surf A*, **146**: p. 337-346 (1999).

25. Delcorte, A., et al., TOF-SIMS Study of Alternate Polyelectrolyte Thin Films: Chemical Surface Characterization and Molecular Secondary Ions Sampling Depth. *Surface Science*, **366**: p. 149-165 (1996).

26. Shiratori S, Rubner MF, pH Dependent thickness behavior of sequentially adsorbed layers of weak polyelectrolytes. *Macromolecules*, **33**: 4213-4219 (2000).

27. Yoo D, Shiratori SS, Rubner MF, Controlling bilayer composition and surface wettability of sequentially adsorbed multilayers of weak polyelectrolytes. *Macromolecules*, **31**:4309-4318 (1998).

28. Ninham, B.W., K. Kurihara, and O.I. Vinogradova, Hydrophobicity, Specific Ion Adsorption and Reactivity. *Coll Surf A*, **123-124**: p. 7-12 (1997).

29. Kotov, N., Layer-by-Layer Self-Assembly: The Contribution of Hydrophobic Interactions. *Nanostruc Mat*, **12**: p. 789-796 (1999).

30. Advincula, R., E. Fells, and M. Park, Molecularly Ordered Low Molecular Weight Azobenzene Dyes and Polycation Alternate Multilayer Films: Aggregation, Layer Order, and Photoalignment. *Chem Mater*, **13**: p. 2870-2878 (2001).

31. Decher, G., Y. Lvov, and J. Schmitt, Proof of Multilayer Structural Organization in Self-assembled Polycation-Polyanion Molecular Films. *Thin Solid Films* **244**: p. 772-777 (1994).

32. Fendler, J., Preparation and Utilization of Self-assembled Ultrathin Films Composed of Polyelectrolytes, Nanoparticles and Nanoplatelets. *CCACAA*, **71**: p. 1127-1137 (1998).

33. Kato, N., et al., Thin Multilayer Films of Weak Polyelectrolytes on Colloid Particles. *Macromolecules*, **35**: p. 9780-9787 (2002).

34. Advincula, R., Supramolecular Strategies Using the Layer-by-Layer Sequential Assembly Technique: Applications for PLED and LC Display Devices and Biosensors. *IEICE Trans Electron*, **E83-C**: p. 1104-1111 (2000).

35. Advincula, R., et al., Photo-induced Alignment of Polymer Ultrathin Films Fabricated by Alternate Self-assembly Solution Adsorption of Polyelectrolytes and Small Azo Dye Chromophores. *ACS Polymer Preprints*, **Spring**: p. 1-2 (1999).

36. Lvov, Y., et al., Thin Film Nanofabrication via Layer-by-Layer Adsorption of Tubule Halloysite, Spherical Silica, Proteins, and Polycations. *Coll Surf A*, **198-**

200: p. 375-382 (2002).

37. Kleinfield, E. and G. Ferguson, Healing of Defects in the Stepwise Formation of Polymer/Silicate Multilayer Films. *Chem Mater*, **8**: p. 1575-1578 (1996).

38. Caruso, F., et al., Ultrathin Multilayer Polyelectrolyte Films on Gold: Construction and Thickness Determination. *Langmuir*, **13**: p. 3422-3426 (1997).

39. Cassagneau, T. and J. Fendler, Preparation and Layer-by-Layer Self-Assembly of Silver Nanoparticles Capped by Graphite Oxide Nanosheets. *J Phys Chem B* **103**: p. 1789-1793 (1999).

40. Artyukhin, A.B., et al., Layer-by-layer electrostatic self-assembly of polyelectrolyte nanoshells on individual carbon nanotube templates. *Langmuir*, **20**(4): p. 1442-1448 (2004).

41. Caruso, F., et al., Quartz Crystal Microbalance and Surface Plasmon Resonance Study of Surfactant Adsorption onto Gold and Chromium Oxide Surfaces. *Langmuir*, **11**: p. 1546-1552 (1995).

42. Lu, C.H., et al., Au nanoparticle micropatterns prepared from self-assembled films. *Langmuir*, **20**(3): p. 974-977 (2004).

43. GirardEgrot, A.P., R.M. Morelis, and P.R. Coulet, Direct influence of the interaction between the first layer and a hydrophilic substrate on the transition from Y- to Z-type transfer during deposition of phospholipid Langmuir-Blodgett films. *Langmuir*, **12**(3): p. 778-783 (1996).

44. Sano, M., Y. Lvov, and T. Kunitake, Formation of Ultrathin Polymer Layers on Solid Substrates by Means of Polymerization-induced Epitaxy and Alternate Adsorption. *Ann Rev Mat Sci*, **26**: p. 153-187 (1996).

45. Delcorte, A., et al., Adsorption of polyelectrolyte multilayers on polymer surfaces. *Langmuir*, **13**(19): p. 5125-5136 (1997).

46. Lutt, M., M.R. Fitzsimmons, and D. Li, X-ray Reflectivity Study of Self-Assembled Thin Films of Macrocycles and Macromolecules. *Journal of Physical Chemistry B*, **102**: p. 400-405 (1998).

47. Bergbreiter, D.E., J.G. Franchina, and K. Kabza, Hyperbranched grafting on oxidized polyethylene surfaces. *Macromolecules,* **32**(15): p. 4993-4998 (1999).

48. Schlenoff, J.B., H. Ly, and M. Li, Charge and mass balance in polyelectrolyte multilayers. *Journal of the American Chemical Society*, **120**(30): p. 7626-7634 (1998).

49. Ferreira, M., J.H. Cheung, and M.F. Rubner, Molecular Self-Assembly Of Conjugated Polyions - A New Process For Fabricating Multilayer Thin-Film Heterostructures. *Thin Solid Films*, **244**(1-2): p. 806-809 (1994).

50. Decher, G., et al., New Nanocomposite Films For Biosensors, Layer-By-Layer Adsorbed Films Of Polyelectrolytes, Proteins or Biosensors & Bioelectronics, **9**(9-10): p. 677-684 (1994).

51. Fou, A.C. and M. Rubner, Molecular-Level Processing of Conjugated Polymers. 2. Layer-by-Layer Manipulation of In-Situ Polymerized Conducting Polymers. *Macromolecules*, **28**: p. 7115-7120 (1995).

52. Brynda, E. and M. Houska, Multiple alternating molecular layers of albumin and heparin on solid surfaces. *Journal of Colloid and Interface Science*, **183**(1): p. 18-25 (1996).

53. Godinez, L.A., et al., Multilayer self-assembly of amphiphilic cyclodextrin hosts on bare and modified gold substrates: Controlling aggregation via surface modification. *Langmuir*,. **14**(1): p. 137-144 (1998).

54. Wei Chen, Thomas J. McCarthy, Layer-by-layer deposition: a tool for polymer surface modification. *Macromolecules* **30**:78-86 (1997).

55. Hammond, P.T. and G.M. Whitesides, Formation of Polymer Microstructures By Selective Deposition of Polyion Multilayers Using Patterned Self-Assembled Monolayers as A Template. *Macromolecules*, **28**(22): p. 7569-7571 (1995).

56. Advincula, R. and W. Knoll, Supramolecular thin films via the Langmuir-Blodgett-Kuhn (LBK) technique. Colloids and Surfaces A-Physicochemical and Engineering Aspects, **123**: p. 443-455 (1997).

57. Advincula, R., et al., In situ investigations of polymer self-assembly solution adsorption by surface plasmon spectroscopy. *Langmuir*, **12**(15): p. 3536-3540 (1996).

58. Janos H. Fendler, Preparation and Utilization of Self-assembled Ultrathin Films Composed of Polyelectrolytes, Nanoparticles and Nanoplatelets, *CCACAA* **71** (4) 1127-1137 (1998).

59. Takeshi Serizawa, Satoko Kamimura, Mitsuru Akashi, Electrostatic adsorption of polystyrene particles with different surface charge onto the surface of an ultrathin polymer film. *Colloids and Surfaces A: Physicochemical and Engineering Aspects* **164**: 237–245 (2000).

60. Hebeish, A. & El Rafie, M.H. and El Sisy F. Combined desizing, scouring and bleaching of starch-sized cotton fabric. *Cellulose Chemistry and Technology* **21**, 147-148 (1987).

61. Islomov, S., Bobodzhanov, P. K., Marupov, R. M. & Likhtenshtein, G.I. and Zhbankov, R.G. Study of the structure of cotton cellulose during biosynthesis by the spin-label method. *Cellulose Chemistry and Technology* **20**, 277-287 (1986).

62. Nevell, T. P. & Zeronian, S. H. *Cellulose chemistry and its applications* (Ellis Harwood Limited, Chichester, England, 1985).

63. Hatch, K. L. *Textile Science* 162-171 (West Publishing Co., St. Paul, MN, (1993).

64. Venkataraman, A. & Subramanian, D.R. and Jacob S. Effect of low-concentration alkalion modified and decrystallized cotton cellulose structures. *Cellulose Chemistry and Technology* **21**, 475-482 (1987).

65. Thomason, S. M.S. Thesis. *Optimization of ionic crosslinking* (North Carolina State University, Raleigh, NC, 2006).

66. Butnaru, R. & Muresanu, A. and Mitu S. Influence of crease resist finish treatments upon the comfort indices in cotton-type textiles. *Cellulose Chemistry and Technology* **20**, 349-355 (1986).

67. Ibrahim, N.A. and El Alfy, EA. Concurrent dyeing and finishing II. Combined dyeing and easy-care finishing of aminized cotton with acid dyestuffs and N-methylol compounds. *Cellulose Chemistry and Technology* **21**, 507-512 (1987).

68. Vaidya, A.A. and Trivedi, S.S. *Textile auxiliaries and finishing Chemicals* 90-100 (R. C. Vora for Ahmedabad Textile Industry's Research Association, Ahmedabad, India, 1975).

69. Bilgen, M. M.S. Thesis *Wrinkle recovery for cellulose fabric by means of ionic crosslinking* (North Carolina State University, Raleigh, NC, 2005).

70. Hashem, M. & Hauser, P. and Smith, B. Reaction efficiency for cellulose cationization using 3-Chloro-2-hydroxypropyl trimethyl ammonium chloride. *Textile Research Journal* **73**, 1017-1023 (2003).

71. Kittinaovarut, S. Acrylic and citric acid in nonformaldehyde durable press finishing on cotton fabric. *AATCC Review,* **3**, 62-64 (2003).

72. Shore John, e. *Colorants and auxiliaries organic chemistry and application properties* 664-666 (Hampshire: Hobbs the Printers, Hampshire, 2002).

73. Hauser PJ, Tabba AR. Improving the environmental and economic aspects of cellulose dyeing using a cationised cellulose. *Color Technol* **117**:282–288 (2001).

74. Watts, John F., Wolstenholme, John. *An Instruction to Surface Analysis By XPS and AES*, Chichester, West Sussex, England, New York John Wiley & Sons, Ltd. (UK), (2003).

75. Briggs, David. Surface *analysis of polymers by XPS and static SIMS*, Cambridge, U.K, New York: Cambridge University Press, (1998).

76. http://en.wikipedia.org/wiki/Transmission_electron_microscopy

77. http://www.accuratedetection.com/products/streaming.html

78. Junlong, Song. Ph.D. Thesis *Adsorption of Amphoteric and Nonionic Polymers on Model Thin Films* (North Carolina State University, Raleigh, NC, 2008)

79. http://www.q-sense.com/dbfiles/QCM-D%20technology%20note.pdf

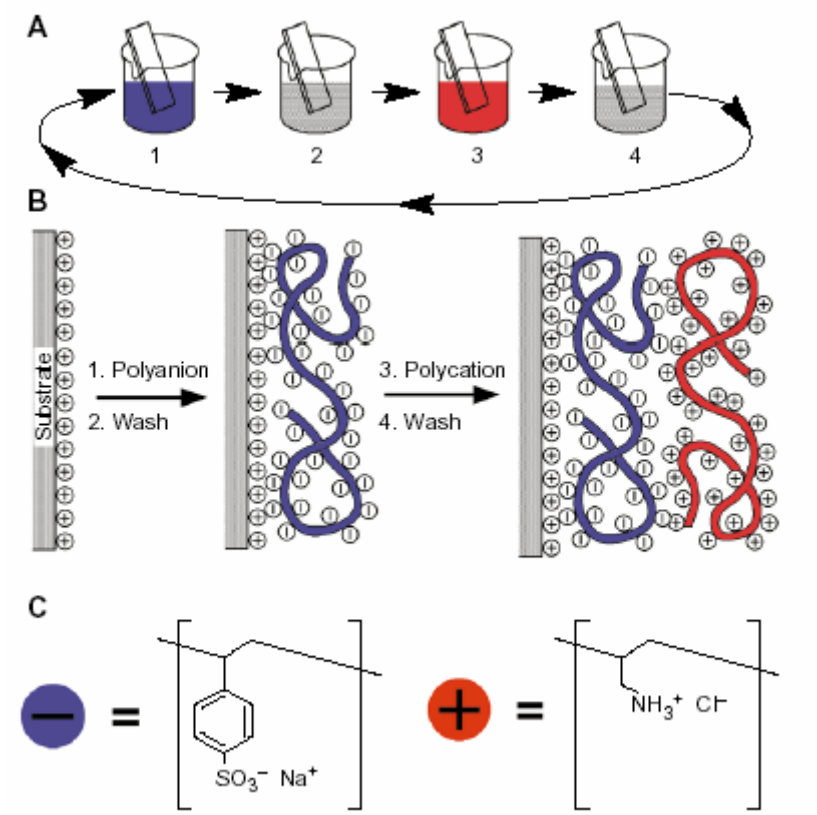

Figure 2.1. "Schematic of the layer-by-layer deposition process using the poly (allylamine hydrochloride) and poly (styrene sulfonate) system. First, the cotton undergoes a cationic surface treatment. The polyelectrolytes are then alternately deposited onto the surface of the fabric. Water rinses separate the polyelectrolyte deposition steps to remove loosely adhered molecules. (A) Schematic of the film deposition process (B) Molecular representation of layer creation (C) Two typical polyelectrolytes: poly (styrene sulfonate) and poly (allylamine hydrochloride)." [11]

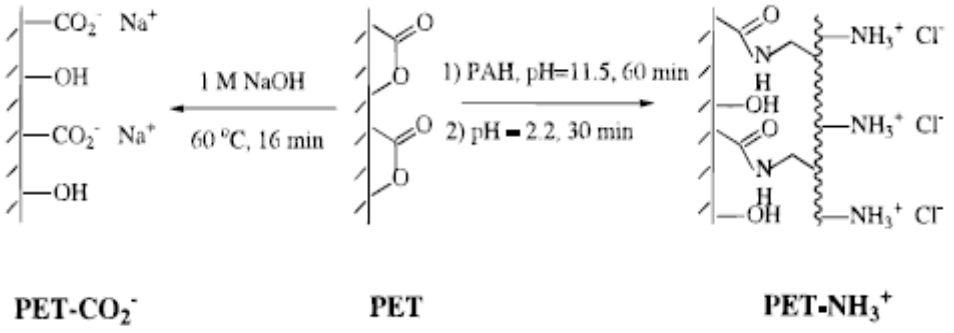

Figure 2.2. Preparation of PET substrate for layer-by-layer deposition [12]

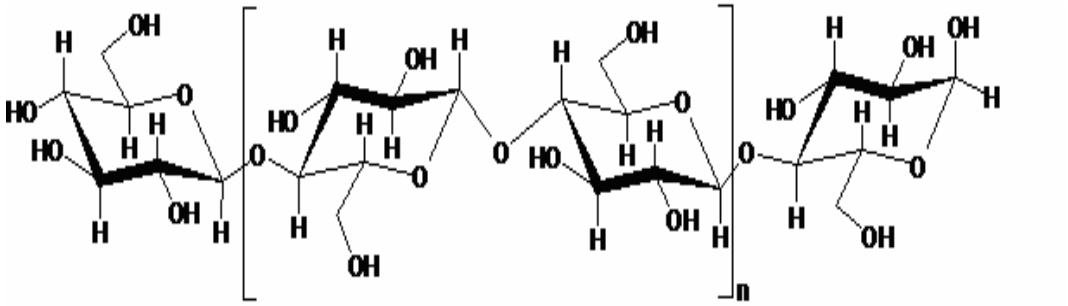

Figure 2.3. Cellulose polymer chain [60]

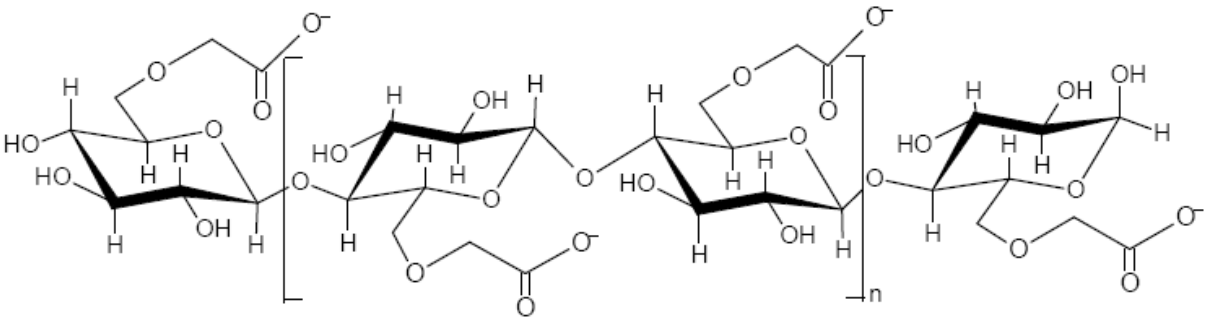

Figure 2.4. Chemical structure of carboxymethyl cellulose [65]

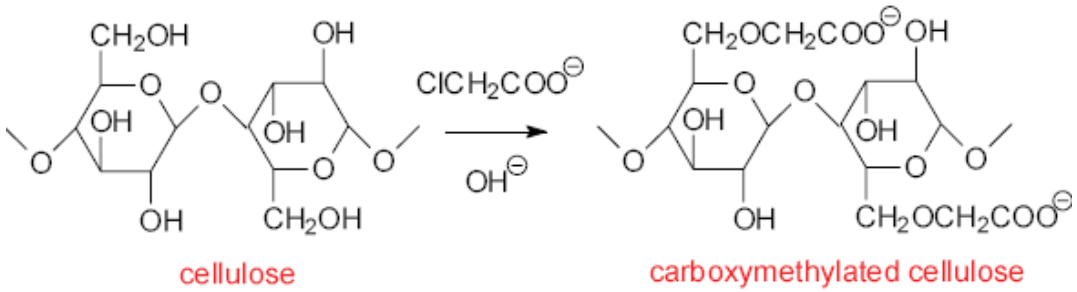

Figure 2.5. Reaction of cellulose with chloroacetic acid and alkali to form carboxymethylated cellulose [65]

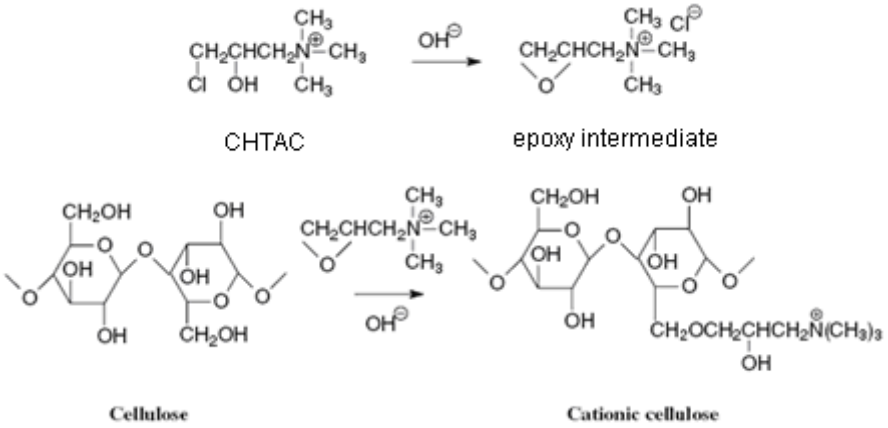

Figure 2.6. (Top) Reaction of 3-chloro-2-hydroxypropyltrimethyl ammonium chloride (CHTAC) with alkali to form 2, 3- epoxypropyltrimethyl ammonium chloride (epoxy intermediate). (Bottom) Reaction of epoxy intermediate and the hydroxyl groups in cellulose creating cationic cellulose. [70]

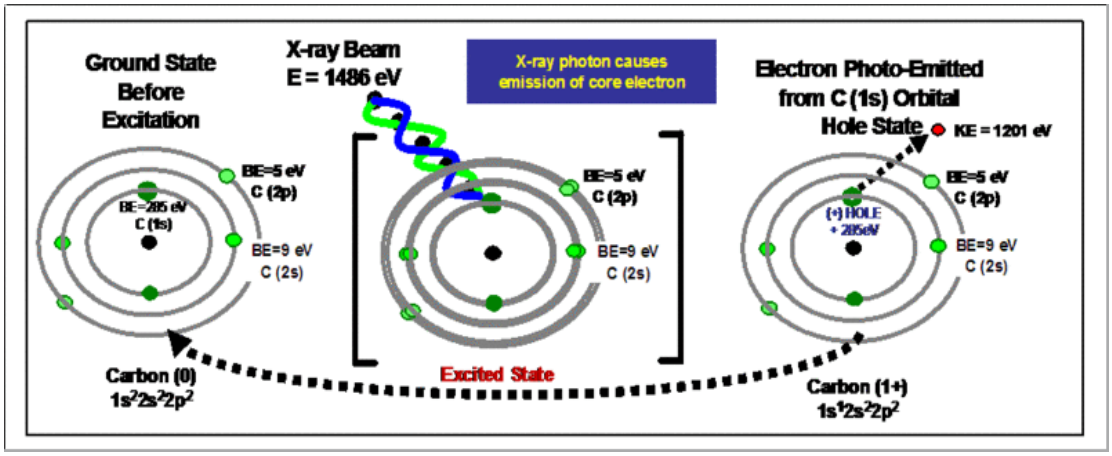

Figure 2.7. The principle of X-ray Photoelectron Spectroscopy [75]

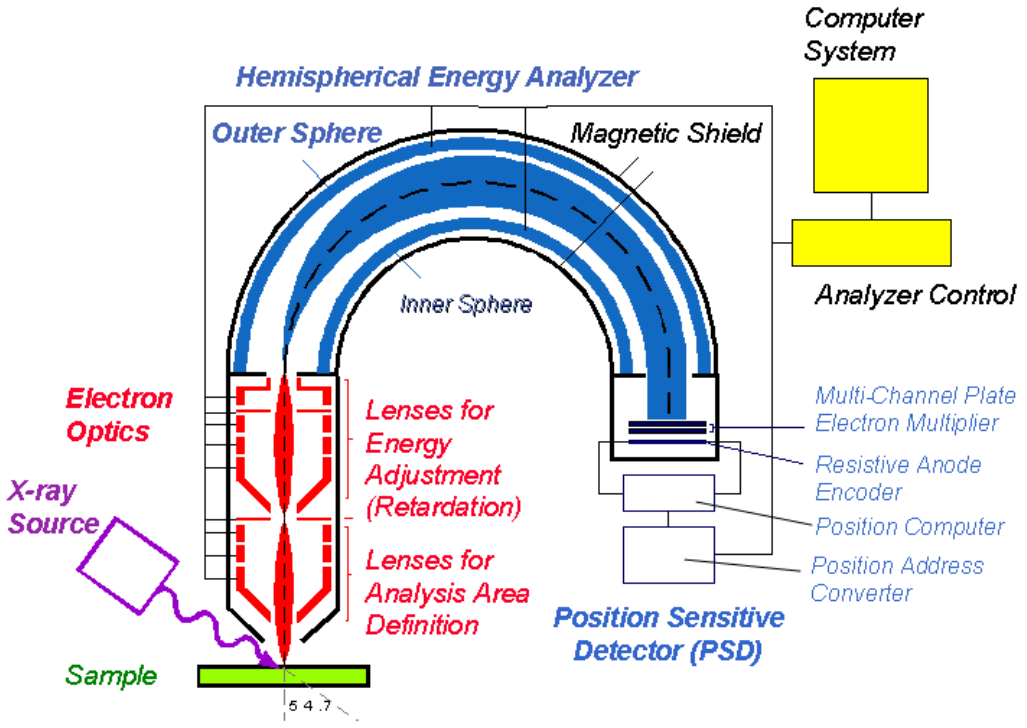

Figure 2.8. Optical schematic of XPS

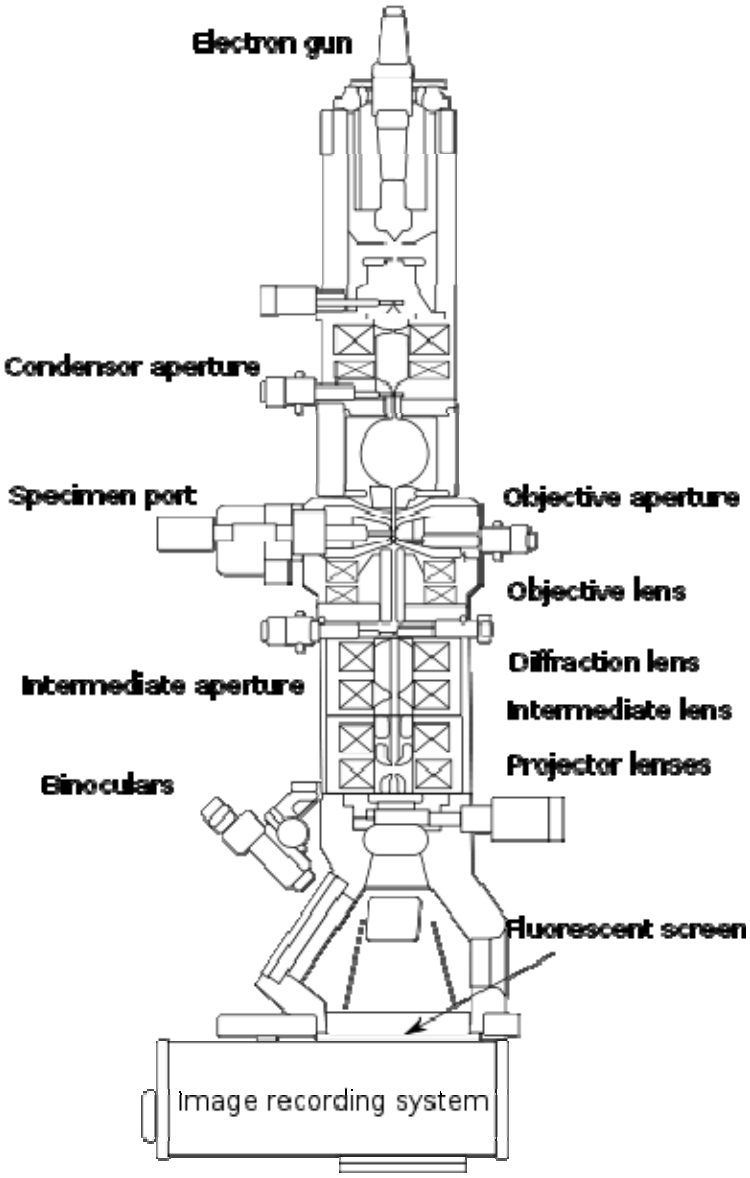

Figure 2.9. The schematic of TEM system. [76]

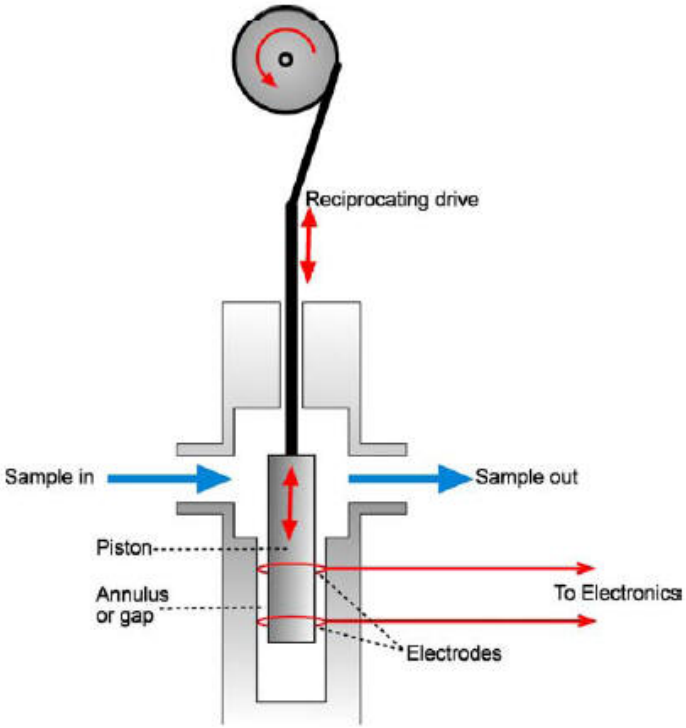

Figure 2.10. Schematic diagram of streaming current device [77]

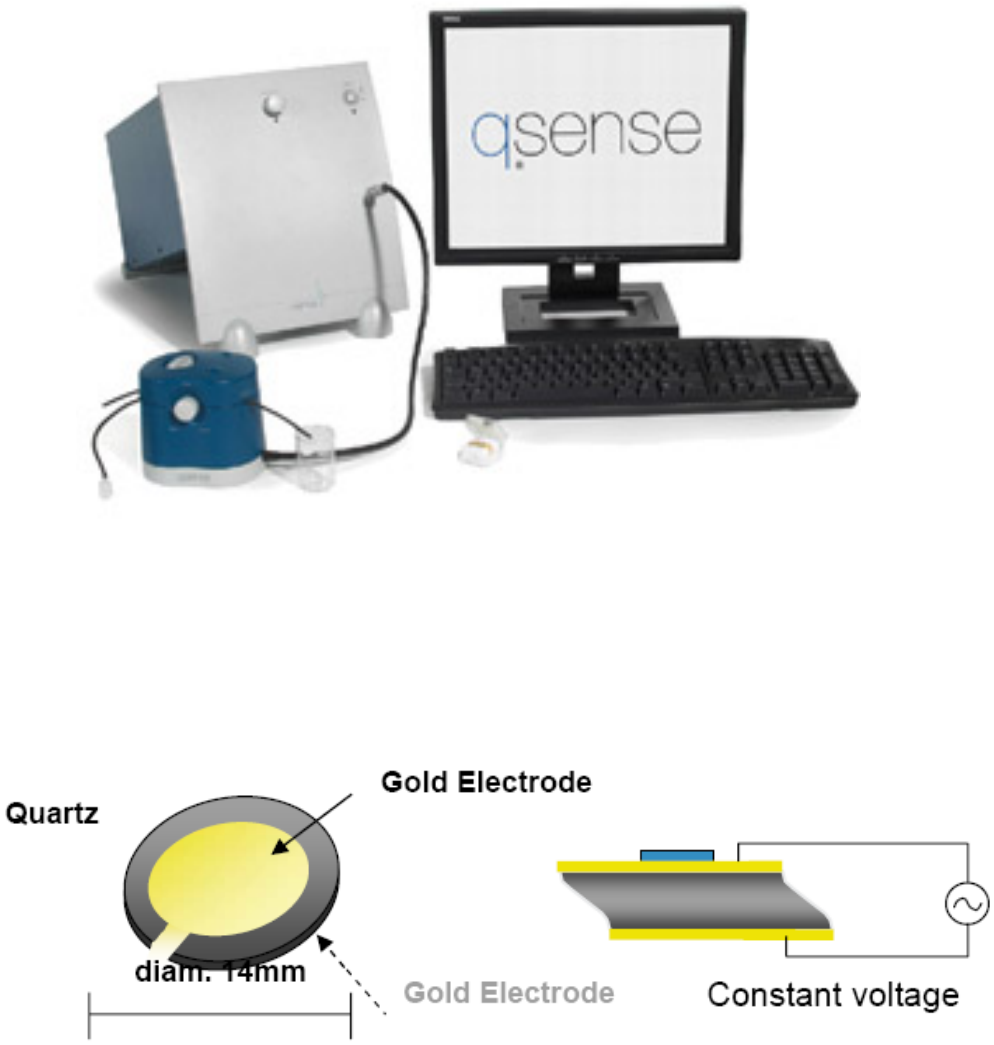

Figure 2.11. The schematic of QCM-D300 system and QCM sensor [78]

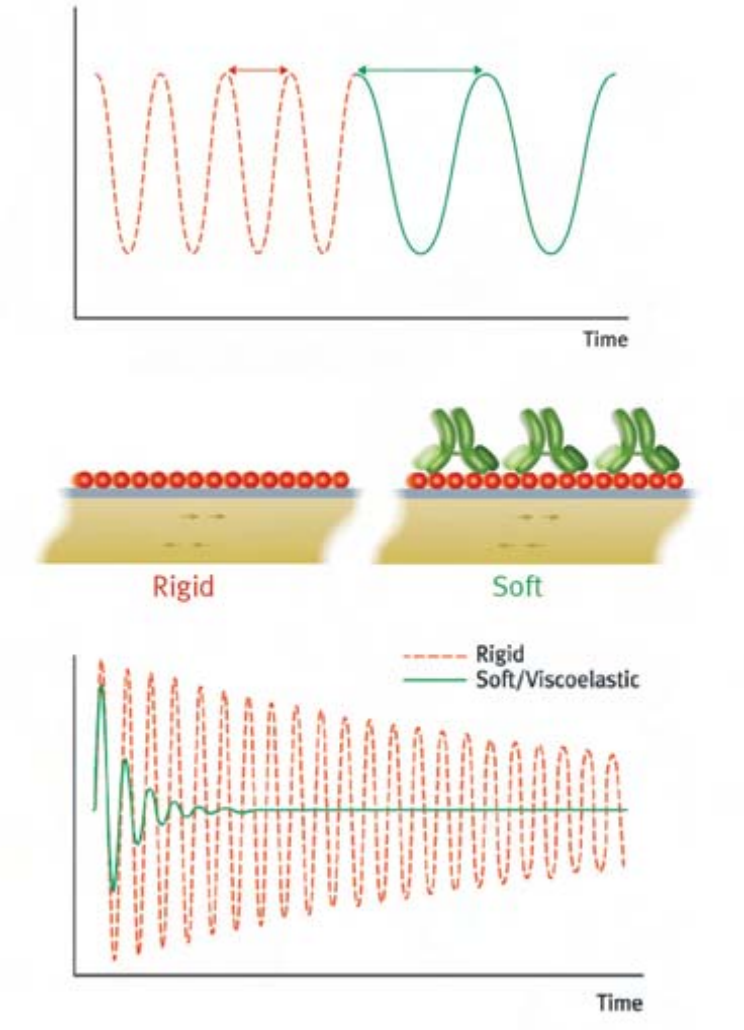

Figure 2.12. "The top is how the frequency of the oscillating quartz crystal changes with the mass on the sensor. The bottom is the dissipation for a soft (green) and rigid (red) film when the driving voltage is turned off." [79]

CHAPTER 3: CHARGE DISTRIBUTION OF CATIONIC COTTON FROM STREAMING CURRENT MEASUREMENTS

3.1 Introduction

In this research, a non-polymeric cationic reactant, 2, 3-epoxypropyltrimethyl ammonium chloride (EPTAC), was used to modify cotton fabric. EPTAC was formed by the reaction of 3-chloro-2-hydroxypropyltrimethylammonium chloride with sodium hydroxide. Earlier work has shown that EPTAC can provide cationized cotton with greatly enhanced affinity for anionic dyes [1-3]. Due to the quaternary amino groups introduced to cotton by EPTAC, positive charges are always present in the fiber, and the fabric can react with anionic dyes at any pH.

The relative amount of positive charges in cationic cotton can be quantified by determining the difference in the percentage of nitrogen present in treated and untreated cotton fabrics [4]. The surface charge is an important variable since adsorbed nanolayers self-assemble on the surface of fibers driven by electrostatic integrations. The layer-by-layer adsorption is not only affected by the total charge of the substrates but also by the charge distribution. In order to obtain more detailed information on the charge distribution on cationic cotton surfaces, the streaming current (SC) method was used. SC tests are commonly used to carry out titrations to determine the so-called cationic demand. In this chapter, the total charge of cationic cotton after two different treatments was determined by analysis of atomic (C, H, N, S)

content. Meanwhile, the surface charge of two control cottons were determined by streaming current tests.

3.1.1 Theoretical background

The theory of streaming current can assume one-to-one pairing of charged groups formed by complexes or other structure between oppositely charged polyelectrolytes in solution. Two mechanisms for complex formation have been proposed. These are so-called ‘‘ladder’’ and the ‘‘scrambled egg’’ models of polyelectrolyte complexation [5]. The ladder model assumes that the two polyelectrolytes can fasten together in a cooperative fashion because they have sufficient flexibility and appropriate charge densities [6, 7]. For much lower molecular mass polyelectrolytes, an adaptation of the ladder model appears to successfully explain the behavior of a ‘‘host’’ and a ‘‘guest’’ polyelectrolytes zipping together spontaneously [8, 9]. However, when carrying out titrations or other complexation reactions between polyelectrolytes both having relatively high molecular masses the ladder model may not be suitable. Due to high molecular mass, the polyelectrolyte chains will tangle themselves preventing the formation of highly untreated “ladders”. Thus, a “scrambled egg’’ model is expected to be a better description under the limiting conditions of high molecular mass, concentration, and/or flow where the rate of irreversible collisions between macromolecules is high relative to their rate of conformational adjustment [10].

The driving force for formation of polyelectrolyte complexes has been described

in two ways; the first one is the attraction of oppositely charged groups [6, 8, 9]; the second is an increase in entropy when polyelectrolyte complexation results in release of counter-ions [6]. These two phenomena can be considered as complementary. Possibly with incomplete pairing of charged groups, entropy considerations alone would lead one to expect iruntreated structures. But it is clear that electrostatic reactions will tend to drive the system to arrange itself so that as high a fraction as possible of the charged groups on the respective polyelectrolytes are paired up with their opposite charges. In the case of linear polyelectrolytes of similar charge densities, it is clear that such rearrangement ought to yield 1:1 stoichiometry. Previous studies have demonstrated 1:1 stoichiometry over a wide range of charge densities and charge density ratios, especially when the complexation occurs in the absence of added low mass ions, i.e., salts [11, 12].

The present experimental work was limited to linear, high-mass polyelectrolytes of high charge density. These conditions were selected to avoid complications related to non-stoichiometric complexation: First the two polyelectrolytes should not differ greatly in molecular mass so that there are no stable nonstoichiometric complexes existing in solution [5, 13]. In addition, without sharply contrasting charge densities and unbranched molecular structures there is little chance of producing stoichiometric polyelectrolyte interactions [14]. Therefore in this research, in order to get 1:1 complexation stoichiometry and avoid undesirable interactions, an excess of an anionic polymer (PVSK, the potassium salt of poly-vinylsulfonic acid) was first added

to the cationic cotton, to neutralize the surface charge and leave an excess negative charges. A cationic polymer (poly-diallyldimethyl ammonium chloride, poly-DADMAC) was then used as titrant. The molecular mass of PVSK was chosen to be similar to that of poly-DADMAC, and no additional salt was added.

3.1.2 Qualitative titration models

Previous researchers attempted to explain why titrations between a highly charged, linear, high-mass poly-acid and a corresponding poly-base depended on the order of addition by proposing two idealized, qualitative models. These models will be used to calculate and explain the experimental results shown later. In each case we are interested in the relative amounts of charged groups in the two polyelectrolytes that are present in the mixture when the titration has been carried out to a SC endpoint of zero.

The idealized models are intended to cover the most likely explanation for titration results. Also, the two models may not be mutually exclusive. Figure3.1 illustrates a ‘‘segment entrapment’’ model. According to this model, poly-ions from the sample solution fasten to titrant macro-ions with opposite charges. The titrant polyelectrolyte is surrounded by the sample’s charge group, which emphasizes initial collisions that occur relatively early in a titration. The word ‘‘titrant’’ here refers to whichever of the poly-ions is gradually added to a solution of the oppositely charged polyelectrolyte [15].

For the sake of simplicity in this model it is assumed that complexation begins

at the periphery of the titrant molecule, forming a layer of complexed units surrounding the core of the titrant molecule. Non-complexed segments of the titrant molecule are protected within the complexed layer and become isolated. As suggested by Michaels et al. [11], some ionic groups are inaccessible for reaction due to a tightly coiled conformation, which is possibly caused by the presence of salt. Under conditions where the segment entrapment model is valid, the model implies deviations from 1:1 stoichiometry. Specifically, in this case, the amount of titrant needed to fully titrate the sample will appear ‘‘inefficient’’ from we expect from 1:1 stoichiometry. Therefore the amount of the titrant added in the sample solution cannot be used to calculate the charge density of the polyelectrolyte with opposite charges.

Though the segment entrapment model remains to be proven, possible theoretical justifications can be given. The model requires, first of all, that rates of molecular collisions be fast relative to the rates of molecular conformations, factors that can be estimated based on concentrations, molecule sizes, and conditions of flow [16]. A second requirement of the model is that complexation is an essentially irreversible process. It is reasonable to assume that the polyelectrolytes can remain ‘‘stuck’’ in the kind of non-equilibrium situation envisioned in figure3.1. Evidence of such irreversibility has been observed in some other aspects of high-mass polyelectrolyte behavior, including adsorption onto oppositely charged surfaces and formation of polymer bridges [17, 18]

Figure 3.2 shows the ‘surface excess’ model that is used to explain non-

stoichiometric endpoints of SC titrations. Three assumptions are made for this model: 1) global 1:1 stoichiometry of complexation during the titration, including the core regions for each polyelectrolyte; 2) Any excessive amount of polyelectrolytes at different part of the titration will stabilize the charge of the resulting complexes; and 3) the tails and loops of the titrant expands outward from the surface of the remaining complexes at the end of titration [19, 20].

This model was justified from two aspects provided the continuous adsorption of titrant onto the surfaces of polyelectrolyte complexes extends beyond the 1:1 stoichiometric endpoint. Studies by both single layer [21-23] and multilayers [24, 25] show continuous adsorption onto polyelectrolyte surfaces, which are a consistent with the model prediction.

In many respects, the two competing models just described are similar, but there are some key differences. For interactions between linear, high-charge polyelectrolytes of similar molecular mass, both models agree with respect to the following qualitative predictions: (a) compared with 1:1 stoichiometry, more titrant should be required to reach an endpoint; (b) the effects ought to be approximately symmetrical, depending on which of two polyelectrolytes is used as the titrant; and (c) increasing electrical conductivity will lead to deviations increasing from 1:1 stoichiometry due to denser molecular conformations of the individual poly-ions before they interact [26,27]. On one hand, a less extended average conformation is expected to make titrant molecules easier to surround and entrap. On the other hand,

higher amounts of titrant molecules should be present in a stabilizing layer of a charge-stabilized complex. The latter explanation has been used by others to give the reason why adsorbed amounts of polyelectrolytes onto surfaces of opposite charge are often increased by intermediate levels of salt [28, 29]. The two idealized models suggest contrasting behavior in certain other respects. The segment entrapment model ought to depend on the concentrations of both polyelectrolytes during the titration because the rates of collisions affect the interaction. The surface-excess model of charge-stabilized polyelectrolyte complexes implies that at the SC endpoint at moderately high salt concentrations it should be possible to measure zeta potentials of such complexes that match the charge of the titrant.

These two models explain why deviations from 1:1 stoichiometry increase with increasing salt concentration, and different adding sequence of titrant will lead to the shift of end-point. In order to minimize errors, any sample with high conductivity should be diluted with distilled water to bring the electrical conductivity below about 1000μS/cm. In this study, the titration was assumed to yield 1:1 stoichiometry, and the surface charge of cationic cotton was calculated according to this assumption.

3.2 Experimental

3.2.1 Materials and Chemicals

The materials and chemicals used for this research were all commercially available and are shown in Table 3.1 along with their descriptions and manufacturers.

Experiments were conducted in solutions prepared from deionized water. The

abbreviation PVSK stands for potassium salt of poly-vinylsulfonic acid. PVSK was prepared fresh from a master batch of dry power and the solutions were completely used within 2 months. The abbreviation poly-DADMAC stands for poly-diallyldimethyl ammonium chloride. The samples of PVSK and Poly-DADMAC used in this study had nominal molecular masses of 170kDa and 400-500kDa, respectively. The polyelectrolytes were used without further purification. The chemical structures of PVSK and poly-DADMAC are showed in figure 3.3.

3.2.2 Cationic Cotton Preparation

Cationic cotton was prepared by using CR-2000, 3-chloro-2-hydroxypropyl trimethyl ammonium chloride (CHTAC), 69% solution, to insert a cationic group into the cotton fiber. The cationization mechanism is described in Figure2.6, 2, 3-epoxypropyltrimethyl ammonium chloride (EPTMAC) was prepared in aqueous solution by reacting 3-chloro-2-hydroxypropyltrimethyl ammonium chloride (CHTAC) with alkali (50% NaOH in water). EPTAC reacted with the hydroxyl groups of cotton creating cationic charges on the surface of the sample. The mixture of CR-2000 and sodium hydroxide was pad applied on the cotton specimens at 100% wet pick-up. Two reagent concentrations of 188 g/L and 376 g/L were applied to the cotton, respectively. The ratio of CR-2000 and sodium hydroxide is 1:1.8, which was found optimal in previous reports [30]. The samples were dried at 45°C and cured at 115°C for 10 minutes. The cured fabrics were washed with cold water, neutralized with dilute acetic acid (2g/L), washed with cold water again, centrifuged and air-dried.

Finally the specimens were cut into one inch squares and random samples were cut into very tiny pieces as samples to be used in streaming current measurements.

3.2.3 Carbon, Hydrogen, Nitrogen and Sulfur Elemental (CHNS) Analysis

The percent of nitrogen present in quaternary ammonium compound in the cationic cotton was used as an indicator to estimate the amount of CHTAC reacted with cotton. This nitrogen analysis was accomplished using a Perkin-Elmer PE 2400 CHN Elemental analyzer (manufactured by Perkin-Elmer Corporation, Norwalk, CT, USA). Soybean leaves were used to calibrate the instrument. Internal standards, NBS 1572-citrus leaves and NBS 1564-wheat flour were used to ensure proper functioning of the equipment. The sample analyzer is based on the classical methods of Pregal and Dumas [31]. The samples were combusted in a pure oxygen environment resulting in the formation of combustion gases. These gases were passed through a separation zone and a thermal conductivity detector column to separate the combustion gas mixture and to measure the amount of nitrogen content in an automated fashion.

3.2.4 Streaming Current (SC) Tests

An ECA2000P instrument (Chemtrac Systems, Inc.) was used in the experiments. A common industrial test involves gradual addition of a polyelectrolyte solution to the sample. The titration endpoint usually is identified with the point at which the signal equals zero.

The procedure for testing cationic cotton is summarized as follows. Cationic cotton sample was cut into very tiny pieces (1mm×1mm) and about 0.25 g of the

fibers was mixed with 50 ml deionized water. PVSK (0.003N) was added to make the solution be negative and then stirred for 20 minutes, the mixture was then filtrated to yield 10 ml of sample. The device was cleaned to prevent any effect from previous samples or titrations. 5ml volume of diluted sample was placed in the device. The apparatus was equilibrated with a preliminary aliquot of the current sample. A fresh aliquot (5ml) was added, the initial signal determined from the meter output. The initial sign of charge indicated by the streaming current detector was noted. When the initial sign was negative, then the sample was titrated with a suitably dilute solution of a high-charge cationic titrant, Poly-DADMAC (0.002N) of opposite charges. Due to the charge density of the sample being relatively low, poly-DADMAC was added very gradually, usually in 0.1ml or 0.2 ml increments. Titration was continued until the meter output passed from negative to positive. The endpoint of the titration was found from a curve of the amount of titrant added vs. the streaming signal. The amount of titrant added to neutralize the sample was therefore be determined by the endpoint.

3.3 Results and Discussion

3.3.1 Nitrogen Tests

The untreated cellulosic fabric had an atom nitrogen content of about 0.02% due to the naturally occurring impurities such as proteins, minerals, pectin and waxes. As expected, the treatment of cotton with CHTAC changed this %N content. However, the nitrogen content of fabric was not significantly changed by carboxymethylation treatment. Therefore nitrogen tests were only useful to measure the total charge of

cationic cotton. The CHNS test provided nitrogen contents as percent values from which the mmol N/100g of fabric were calculated. For example, 0.10 % nitrogen content can be expressed in mmol of N/100g as shown below, which for this example means there were 7.14 mmol quaternary ammonium compounds in 100g cationic cotton:

$$mmol\ of\ N/100g = \%N \times 1000/14 = 0.1 \times 1000/14 = 7.14$$

This method was used to determine the total charge of cationic cotton. The amount of quaternary ammonium compounds can be regarded as the total positive charges in cationic cotton. In these experiments, five squares (5×5 cm) randomly cut from the cationic cotton specimens (8 x 12 inch) were chosen in order to get average values and standard deviations.

Table 3.2 gives the total charge of cationic cotton after different treatments and five repetitions. From these results, cotton treated with 376g/L concentration had more positive charges than cotton treated with 188g/L concentration. As expected, higher chemical concentration led to higher cationization. The standard deviations are quite low compared to the average values; the five separate determinations yield similar values which mean that the cotton fabrics equally reacted with the cationic chemicals. In summary, the cationic treatment process used in this research provided repeatable results.

The results proved the difference in total positive charges between the cationic cotton samples treated with two different concentrations of the cationic reactant.

Although the total charge of cationic cotton with the 376g/L treatment was higher than that treated with the 188g/L concentration, the relative increments were not linearly-related. As the concentration of cationic reactant increases, the total charge of the cotton also increase, but the increase in charges is not proportional to the increase the cationic reactant. There are two reasons that can explain this result. The first one is that two reactions happened when the cellulose was cationized by EPTAC. EPTAC not only reacts with the hydroxyl groups of cellulose but also with water. With the cationic reactant concentration increasing, the cotton cationization reaction rate increases, but the rate of hydrolysis reaction also increases. Therefore, adding excess of cationic reactant in the treatment may not be useful to increase the total charge. Another reason is that when there are more positive charges in the cotton fiber, it becomes difficult for positive groups of the cationic reactant to access the cotton due to the electrostatic repulsions. Therefore increasing the cationic chemical concentration can produce more positive groups in cotton, but to a limited extent.

3.3.2 Streaming Current (SC) Tests

The first area of concern were the baseline tests of streaming current output due to a possible influence of the initial apparent charge of the plastic surfaces within the sensing areas of the SC apparatus. Though the PTFE or other hard plastics used in fabrication of SC devices are usually described as “uncharged’’ and oleophilic, experience suggests that these surfaces develop a negative surface charge when exposed to water.

To summarize the baseline tests from previous reports [32], the plastic probe surfaces behaved as if they had a weakly negative surface charge. However, the amount of cationic polyelectrolyte needed to neutralize the charges of the bare surfaces of the apparatus, in the absence of anionic polyelectrolyte, were too small to account for the observed shifts in apparent stoichiometry of the complexation interactions, as sensed by the SC tests.

For the reasons explained in previous chapters, the streaming current is affected by excess electrolyte conductivities, above ca. 1000μS/cm. Figure3.4 illustrates the kind of contrasting results that can be obtained. The "ideal" curve corresponds to a solution of ionic polymer and other materials to the conductivity of tap water. The "high salt" curve corresponds to the same in the presence of enough salt such as NaCl or $CaCl_2$ to give a conductivity of 3000μS/cm. The reasons to explain why it becomes difficult or impossible to observe good endpoints at higher conductivity levels include the following: (1) the absolute magnitude of the SC signal is decreased; (2) the salt ions are expected to inhibit adsorption of polyelectrolytes onto the plastic; and (3) the phase of the SC signal may be shifted so that it does not match the phase of the motion of the piston [15]. Higher levels of conductivity progressively reduce the signal and further reduce the tendency of polyelectrolytes to adsorb onto the PTFE surface.

The following factors appear to contribute to the problems observed in the case of SC titrations, discussed before: the increase of salt ions leads to decrease the

tendency for certain charged materials to adsorb onto the surfaces of SC components; decrease tendency for polymer titrants to form strong enough complexes with ionic materials in the sample; and an overall decrease in the electrical signal with increasing electrical conductivity of the solution [14]. Therefore excellent results are expected in most cases if the conductivity is below 1000μS/cm. In our experiments, the polyelectrolytes were prepared using deionized water, which produced as solution conductivity small enough to avoid artifacts in the determination of the endpoint.

Through the curve of SC meter output with the titrant added, the endpoint of titration can be evaluated. Figure3.5 shows the curve for a positive titrant, poly-DADMAC that is added, thereby changing the SC meter output from negative to positive. When the output is zero, the amount of titrant at the endpoint is determined.

The SC meter output of the filtrated sample which came from the solution composed of cationic cotton fibers and added anionic polyelectrolyte PVSK, was negative. Theoretically, the amount of poly-DADMAC added in the solution should depend on the excess PVSK. The charges of poly-DADMAC added to the solution to reach the end point should equal the charges of PVSK minus the charges of cationic cotton. The surface charge of cationic cotton can therefore be calculated from the amount of titrant added at the endpoint.

Pieces of cationic cotton fiber (0.2622 g of the188g/L cationic cotton) were mixed with 50 ml deionized water and 10 ml PVSK (0.003N) was added. At this point, the solution had net negative charges. The mixture was filtered and 10ml removed to

use as a sample for test in the SC. The dosage amount of titrant poly-DADMAC (0.002N) neutralizing the solution was 0.38 ml, as seen in Figure3.5.

Equation:

Positive Charges of poly-DADMAC = Negative Charges of PVSK – Surface charge of Cationic Cotton

$2mol/L \times 0.38 \times 10^{-3}\ L = (3mmol/L \times 0.01L - X) \times 1/6$

$X = 25.44 \times 10^{-3} mmol$

$25.44 \times 10^{-3} / 0.2622g$ = Surface charge of 188g/L Cationic Cotton/100g

Surface charge of 188g/L Cationic Cotton = 9.8 mmol/100g

From the results in the Table 3.3, 188g/L or 376g/L cationic cotton samples showed similar surface charge in five separate evaluations. The standard deviations are very small, and each test result was very close to the average value, which means that the SC tests are repeatable. In addition, positive charges inserted by the cationic treatment are uniformly distributed on the fiber surface because the samples used in five tests were cut randomly from different places in a large cationic treated cotton specimen. The surface charge of cationic cotton from the 376g/L treatment was found to be twice that from the 188g/L treatment. As seen in Figure 3.6, surface charge was more sensitive to an increase in the cationic treatment than total charge. Let's assume the quantity of cationic chemical reacted with cotton is Q; the quantity reacted with internal fiber is Qi; and the quantity reacted on the fiber surface is Qs. When the cationic chemical quantity is increased to 2Q, the quantity reacted with the fiber

surface Qs' almost equals to 2Qs, and the quantity reacted with the internal fiber Qi' is more than Qi, but less than 2Qi. Through these results, we find the surface of the cotton fiber that reacted with 188g/L reactant was not completely covered. There remain are some places to react with cationic agent on the fiber surface. As the treatment concentration increase, the surface charge increase. Due to the cationic groups on the surface are less than positive charges in the internal fiber, it is easy for cationic chemical to react on the surface. However, the positive groups are difficult to access in the fiber because the electrostatic repulsion.

Table 3.4 gives the each value of cationic agent reacted with interior cotton or surface. Here the amount of charges indentifies the quantity of reacted cationic chemicals. For cationic cotton, Qi' equal 1.272Qi and Qs' equal 1.694 Qs. Surface and inner charges increase due to the increase in cationic reactant. The surface charge has increased more than the inner charges because when the cationic reactant concentration increases, the electrostatic repulsion in the fiber is greater than that on the surface. This electronic repellent prevents reaction between the cationic groups and the hydroxyl groups.

Surface charge is shown in Figures 3.7 and 3.8, to be only a little part of the total charge, regardless of cationic chemical concentration. This may be caused by twists in the polymer chain, only few cationic groups are available outside, this the "entrapment" model is capable to explain it. Titrant poly-ion begins to only neutralize outside charge groups, and uncomplexed segments are coiled inside. When the

negative polyelectrolyte is added, the outside positive charges are neutralized, but the internal part, within the polymer, would be expected to remain positive in charge.

The other reason to explain the ratio of surface charge to total charge is less than 20% may be due to the cationic cotton fiber has some pores; therefore, they act as if they are dead-ended cylinders, having one end open to the aqueous solution. In low conductivity, the characteristic sizes of pores in the fiber seem to be sufficient small so that polyelectrolytes of high molecular mass will have difficulty in getting inside. The negative titrant PVSK cannot neutralize positive charges in the pores of fiber. Thus the amount of added PVSK decreases, and accordingly decreases the surface charge determined by SC technique. In addition, the cotton has some crystal and amorphous regions, the charges in the crystal regions can't be measured by streaming current method.

3.4 Conclusion

In this phase of the research, the total and surface charge of cationic cotton were determined by CHNS and streaming current tests. According to the difference of nitrogen content, loads of 376g/L reactant yield cationic cotton with more positive charges than that for 188g/L cationic cotton. However, increasing the concentration of cationic chemical (CR-2000) in the treatment may not be the best way to increasing the total charge of the cotton. Reactant concentration larger than 376g/L did not produce an obvious effect on the increase of the total charge. Through streaming current tests, surface charge of cationic cotton by two treatments was found to be only

a small portion of the total charge. Compared to total charge, the surface charge were more sensitive to the cationic chemical concentration. Five observations from random samples gave the similar results. The cationic treatment was shown to be feasible and to yield uniform charge distribution.

3.5 Reference

1. Hauser, P. J., *AATCC Review*, Vol.2, No. **5**, 36-39 (2002).

2. Hauser, P. J., *Textile Chemist and Colorist & American Dyestuff Reporter*, Vol. 32, No. **6**, 44-48 (2000).

3. Hauser, P. J., and A. H. Tabba, *Coloration Technology*, vol.117, No. **5**, May, pp282-288 (2001).

4. Thomason, S. M.S. Thesis. *Optimization of ionic crosslinking* (North Carolina State University, Raleigh, NC, 2006)

5. A.S. Michaels, Polyelectrolyte complexes, *Ind. Eng. Chem*.**57** (10) 32-40 (1965).

6. S.H. Tse, The effects of ionic spacing and degree of polymerization on the stoichiometry of polyelectrolyte interactions in dilute aqueous solutions, Ph.D. Diss., Inst. Paper Chem., Appleton, WI, (1979).

7. W. Argu¨elles-Monal, M. Ga´rciga, C. Peniche-Covas, Study of the stoichiometric polyelectrolyte complex between chitosan and carboxymethyl cellulose, *Polym. Bull.* **23** pp: 307-313 (1990).

8. V.A. Kabanov, A.B. Zezin, Soluble interpolymeric complexes as a new class of synthetic polyelectrolytes, *Pure Appl. Chem*. **56** (3) pp: 343-354 (1984).

9. B. Philippe, H. Dautzenberg, K.-J. Linow, J. Ko¨ tz, W. Dawydoff, Polyelectrolyte complexes /recent developments and open problems, *Prog. Polym. Sci.* **14** (1) pp: 91-172 (1989).

10. A. Swerin, L. .O¨ dberg, Some aspects of retention aids, in: C.F. Baker (Ed.), The Fundamentals of Papermaking Materials, vol. **1**, PIRA, Leatherhead, UK, pp. 265-351 (1997).

11. A.S. Michaels, L. Mir, N.S. Schneider, A conductometric study of polycation_/polyanion reactions in dilute aqueous solution, *J. Phys. Chem.* **69** (5) 1447-1455 (1965).

12. S. Dragan, M. Cristea, Polyelectrolyte complexes IV. Interpolyelectrolyte complexes between some polycations with N, N-dimethyl-2-hydroxyl prolyleneammonium chloride units and poly(sodium styrenesulfonate) in dilute aqueous solution, *Polymer* **43** (1) 55-62 (2002).

13. S. Dragan, M. Cristea, Influence of low-molecular-weight salts on the formation of polyelectrolyte complexes based on polycations with quaternary ammonium salt groups in the main chain and poly(sodium acrylate), *Eur. Polym. J.* **37** 1571-1575 (2001).

14. M. Mo¨ ller, E. Nordmeier, Polyelectrolyte complexes formed by poly(diallyl-N,N-dimethylammoniumchloride) and oligo(dextransulphate), *Eur. Polym. J.* **38** (3) 445-450 (2002).

15. J. Chen, J.A. Heitmann, M.A. Hubbe, Dependency of polyelectrolyte complex stoichiometry on the order of addition. 1. Effect of salt concentration during streaming current titrations with strong polyacid and poly-base, *Colloids Surf.* A **223** pp: 215–230 (2003).

16. A. Swerin, L. .O¨ dberg, Some aspects of retention aids, in: C.F. Baker (Ed.), The Fundamentals of Papermaking Materials, vol. 1, PIRA, Leatherhead, UK, pp: 265-351 (1997).

17. M.D. Sikora, R.A. Stratton, Shear stability of flocculated colloids, *Tappi* **63** (11) pp: 97-101 (1981).

18. H. Tanaka, A. Swerin, L. .O¨ dberg, Transfer of cationic retention aid from fibers to fine particles and cleavage of polymer chains under wet-end papermaking conditions, *Tappi J*. **76** (5) 157-163 (1993).

19. H. Dautzenberg, N. Karibyants, Polyelectrolyte complex formation in highly aggregating systems. Effect of salt: response to subsequent addition of NaCl, Macromol. *Chem. Phys*. **200** pp: 118-125 (1999).

20. H.-M. Buchhammer, G. Petzold, K. Lunkwitz, Nanoparticles based on polyelectrolyte complexes: effect of structure and net charge on the sorption capability for solved organic molecules, *Colloid Polym. Sci.* **278** pp: 841-847 (2000).

21. O.J. Rojas, M. Ernstsson, R.D. Neuman, P.M. Claesson, X-ray photoelectron spectroscopy in the study of polyelectron adsorption on mica and cellulose, *J. Phys. Chem.* B **104** (43) 10032-10042 (2000).

22. M.A. Hubbe, T.L. Jackson, M. Zhang, Fiber surface saturation as a strategy to optimize dual-polymer dry strength treatment, *Tappi*, vol.**2** pp: 7-12 (2003).

23. S.T. Dubas, J.B. Schlenoff, Factors controlling the growth of polyelectrolyte multilayers, *Macromolecules*, **32** pp: 8153-8160 (1999).

24. Decher, M. Eckle, J. Schmitt, B. Struth, Layer-by-layer assembled multi-composite films, Curr. Opin. *Colloid Interf. Sci*. **3** pp: 32-39 (1998).

25. F. Caruso, H. Lichtenfeld, E. Donath, H. Mo¨hwald, investigation of electrostatic interactions in polyelectrolyte multilayer films: Binding of anionic fluorescent probes to layers assembled onto colloids, *Macromolecules* **32** pp: 2317-/2328 (1999).

26. M. Beer, M. Schmidt, M. Muthukumar, The electrostatic xpansion of linear polyelectrolytes: effects of gegenions, co-ions, and hydrophobicity, *Macromolecules* **30** (26) 8375_/8385 (1997).

27. J.Yang, D.Sohn, N.-J.Kim, Conformations of anionic and cationic poly-electrolytes in various salt solutions, *Polymer* (Korea) **23** (5) 708_/716 (1999).

28. T. Lindstro¨m, L. Wagberg, Effects of pH and electrolyte concentration on the adsorption of cationic polyacrylamides on cellulose, *Tappi J.* **66** (6) 83_/85 (1983).

29. H.G.M. Van de Steeg, M.A. Cohen Stuart, A. de Keiser, B.H. Bijsterbosch, Polyelectrolyte adsorption: a subtle balance of forces, *Langmuir* **8** 2538_/2546 (1992).

30. Mohamed Hashem, Peter Hauser, and Brent Smith, Reaction Efficiency for Cellulose Cationization Using 3-Chloro-2-Hydroxypropyl Trimethyl Ammonium Chloride, *Textile Research Journal*, Vol. **73**, No. 11, 1017-1023 (2003)

31. Kiran Kumar Goli, M.S. Thesis. *Use of Modified Cellulose for the Improvement of Water Repellency* (North Carolina State University, Raleigh, NC, 2008)

32. Hauser, P. J., *AATCC Review*, Vol.2, No. **5**, 36-39 (2002).

33. http://water.me.vccs.edu/concepts/scm.html

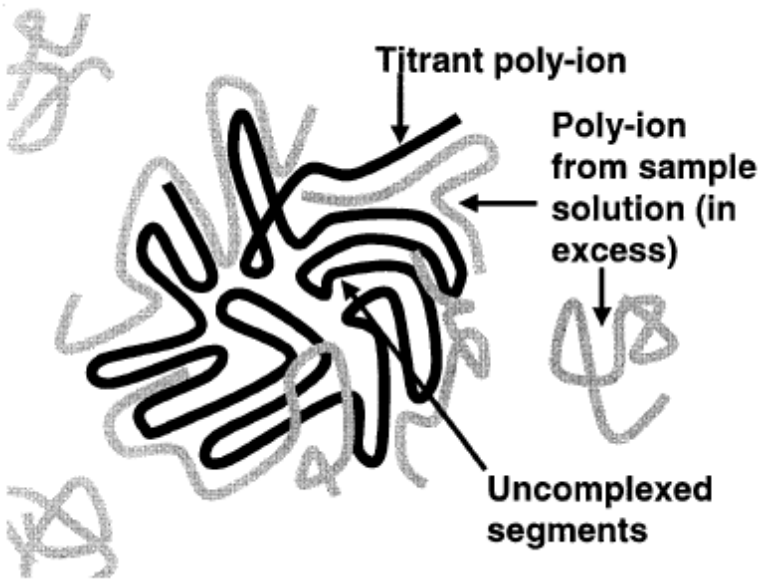

Figure 3.1. ""Entrapment" model, in which the addition of titrant is assumed to cause segments of an oppositely charged polyelectrolyte to become isolated, protected from further complexation or equilibration." [15]

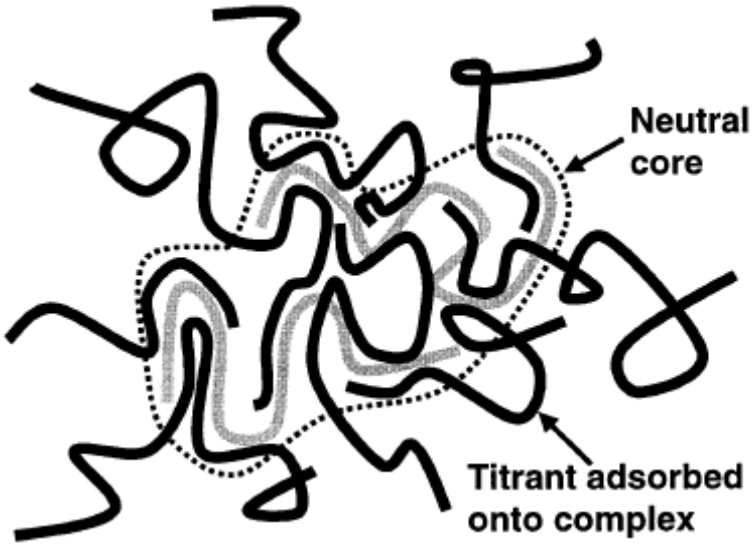

Figure 3.2. ""Surface excess" model in which polyelectrolyte complexes in the solution phase are assumed to have a near-neutral core, loops and tails of the titrant extending from their surface."[15]

Table 3.1. Test materials and chemicals

Name or Group	Description	Manufacturer
Cotton Fabric	Standardized TIC-400 woven cotton fabrics	Textile Innovators, Inc.
Cationic Agent	CR-2000, 3-chloro-2-hydroxypropyl trimethyl ammonium chloride (CHTAC), 69% solution	Dow Chemical
Base	Sodium hydroxide, 50% w/w aqueous solution	Fisher Scientific
Negative Titrant	PVSK	Aldrich Co.
Positive Titrant	Poly-DADMAC	Aldrich Co.

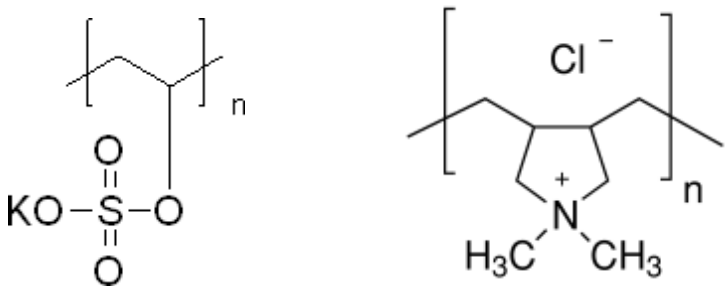

Figure 3.3. The chemical structure of PVSK (left) and poly-DADMAC (right)

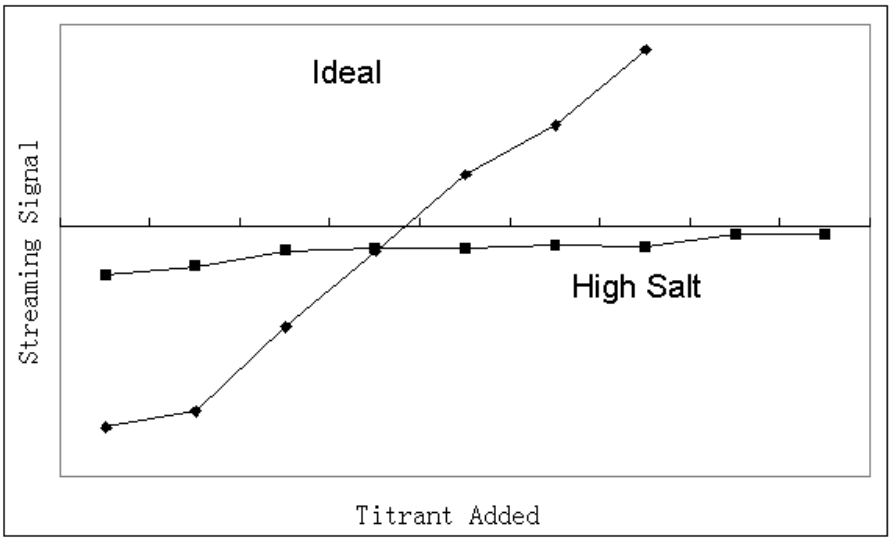

Figure 3.4. Lack of SC endpoint at high salt concentration. The "ideal" curve corresponds to a solution of anionic polymers and other materials at the conductivity of deionized water. The "high salt" curve corresponds to the same solution in the presence of enough NaCl to give a conductivity of 3000µS/cm.

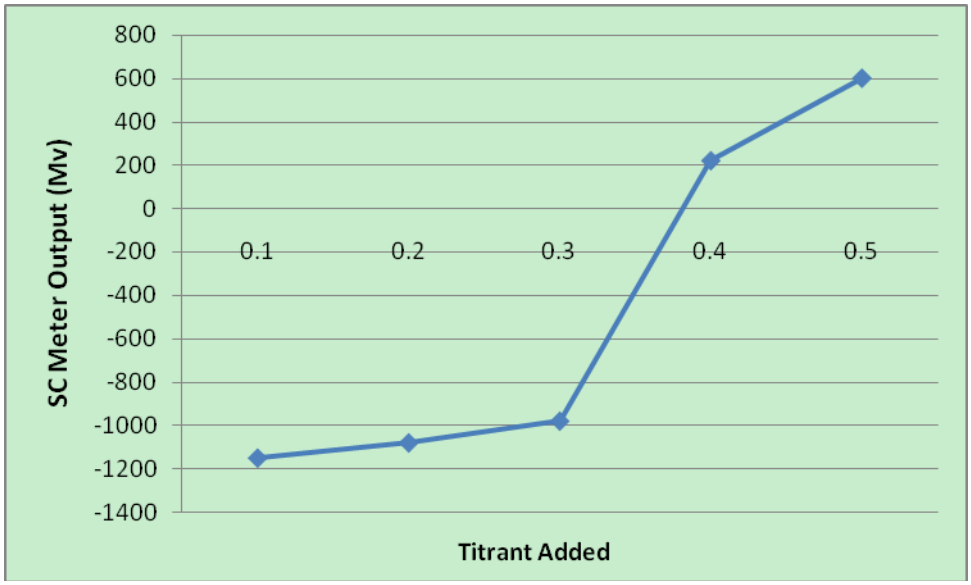

Figure 3.5. The curve of SC Meter output with the titrant added. The curve corresponds to a solution of the sample titrated by poly-DADMAC at neutral condition. Each time the additive amount is 0.1ml.

Table 3.2. Total charge of cationic cotton with different concentration treatment

Times	188g/L Treatment (mmol/100g)	376g/L treatment (mmol/100g)
1	60.9	80.9
2	61.2	81.2
3	56.5	76.5
4	58.6	78.6
5	58.3	78.3
Mean	**59.1**	**79.1**
STDEV	1.96	1.96

Table 3.3 Surface charge of cationic cotton with different concentration treatment by SC tests

Times	188g/L Treatment (mmol/100g)	376g/L treatment (mmol/100g)
1	9.8	16.1
2	9.1	14.9
3	8.7	15.6
4	9.5	15.7
5	9.3	16.3
Mean	**9.28**	**15.72**
STDEV	0.41	0.54

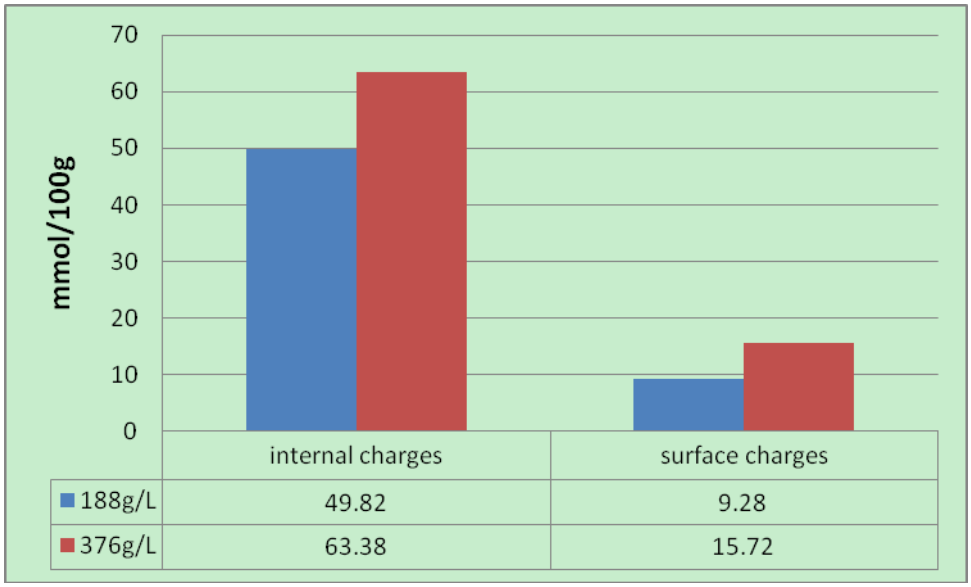

Figure 3.6. Average value of cationic cotton's surface and internal charge by different treatment

Table 3.4 The different cationic reactant quantity reacts with the internal fiber or surface

	Cationic Cotton
Qi	49.82
Qi’	63.38
Qs	9.28
Qs’	15.72
Qi’/Qi	1.272
Qs’/Qs	1.694

Qi: for 188g/L treatment, the quantity of reacted cationic reactants in the internal fiber;

Qi’: for 376g/L treatment, the quantity of reacted cationic reactants in the internal fiber;

Qs: for 188g/L treatment, the quantity of reacted cationic reactants on the fiber surface;

Qs’: for 376g/L treatment, the quantity of reacted cationic reactants on the fiber surface;

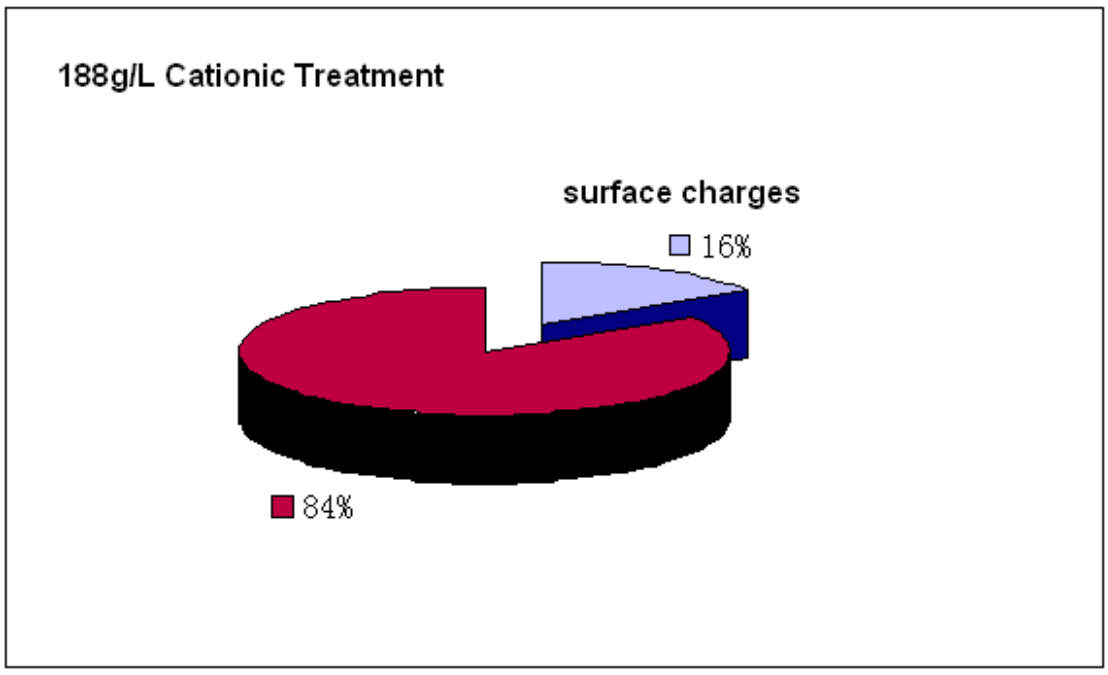

Figure 3.7. Cationic cotton treated by 188g/L concentration: the ratio of surface charge to total charge.

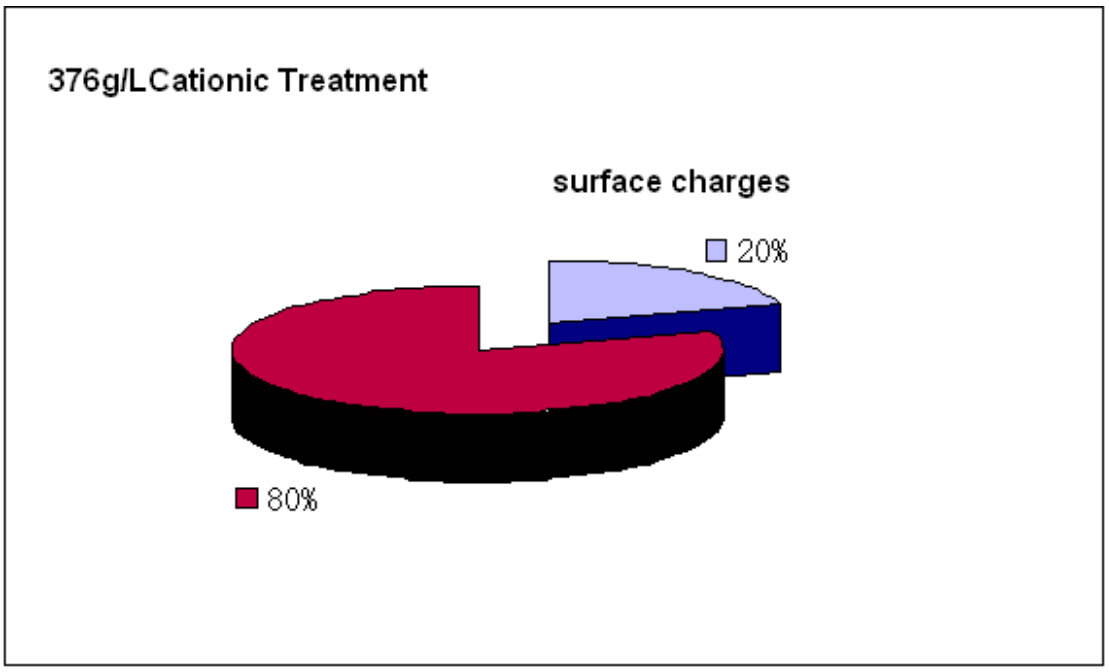

Figure 3.8. Cationic cotton treated by 376g/L concentration: the ratio of surface charge to total charge.

CHAPTER 4: CHARGE DISTRIBUTION OF ANIONIC COTTON FROM STREAMING CURRENT TESTS

4.1 Introduction

Anionic cotton is formed from the carboxymethylation reaction throughout the cotton fiber cross section [1]. Carboxymethylation of cotton fiber proceeds initially at accessible hydroxyl groups and subsequently with slow penetration into the ordered regions. Compared to the crystalline regions, carboxymethylation proceeds very easily in the amorphous regions. At the early stages of the reaction the distribution of the carboxymethyl groups is very uneven [1]. With reaction time, the reactants penetrate to the more highly ordered regions resulting in more complete and even distribution of carboxymethyl groups [2].

In the carboxymethylation reaction, the cellulosic fabric is soaked in sodium hydroxide and then padded followed by drying. In the process, the hydrogen of the primary hydroxyl groups is removed leaving negatively charged oxygen. After this step, the cellulose becomes soda cellulose, which has the reactive sites for sodium chloroacetate to react. Treatment with sodium chloroacetate is done either by soaking and padding or by direct padding through chloroacetate solution followed by drying. The dried samples are cured and washed. Otherwise, the cellulosic fabric can be soaked and padded through the mixture of sodium chloroacetate solution prepared by neutralizing mono chloroacetic acid with a weak base like sodium carbonate, ammonium carbonate, etc. The mono chloroacetic acid flakes are dissolved in

deionized water. Solution concentrations up to 9.0 M have been prepared and neutralized using the weak base. Carbon dioxide is evolved in the reaction as mono chloroacetic acid is neutralized. This solution is used to pad the cotton followed by further treatment at various conditions. The hydroxyl groups on the cellulose chains are replaced by the stable ether linkages forming anionic cellulose as shown in Figure 4.1 [2-5].

The relative amount of total negative charges of anionic cotton can be found by acid-base titration explained in other reports [6]. In addition, as discussed in chapter 3, the surface charge of anionic cotton by two treatments was determined by streaming current tests. In this chapter, the total and surface charges on anionic cotton from two levels of treatment are compared, and the charge distributions determined.

4.2 Experimental

4.2.1 Materials and Chemicals

The materials and chemicals used in this research were all commercially available and are shown in Table 4.1, along with their descriptions and manufacturers.

Experiments were conducted in solutions prepared from deionized water. The titrant agents are anionic PVSK and cationic poly-DADMAC, which were also used in chapter 3.

4.2.2 Anionic Cotton Preparation

This two-step method for carboxymethylated cellulose was based on previous work [2, 3]. In step 1, fabric samples were soaked in 20% NaOH for 10min, padded to

100% wet pick-up and dried at 45 °C for 12 min. The samples were yellow and completely dry. In step 2, mono chloroacetic acid was neutralized by the weak base sodium carbonate. The samples from step 1 were soaked in the aqueous sodium chloroacetate solution of the specified concentration for 5 min, padded to 100% wet pick-up, cured at 85 °C for 30 min, washed with water, acidified with 2 g/L acetic acid, washed with water and dried in air.

4.2.3 Total charge Titration

The anionic content of the carboxymethylated samples was quantitatively determined by acid base titration and reported as mmol/100 g fabric. The method was adopted from previous work [6]. Small pieces (2.5cm × 2.5cm) were cut from different parts of the treated sample. These pieces were further cut into smaller pieces (3mm × 3mm). They were then soaked in 0.5% hydrochloric acid overnight. The sample pieces were then filtered off, washed several times with deionized water until the washed water showed no presence of chloride by the silver nitrate drop test, then dried at 105°C for 3 hours. They were then weighed accurately to 0.25 g and soaked overnight at room temperature in 25 ml of 0.05N NaOH. The blank was kept without any fabric sample in it. The next day, the blank was first titrated with 0.05N aqueous HCl using phenolphthalein indicator. At the endpoint the volume of HCl spent was recorded as V_{blank}. The procedure was repeated for the soaked sample and the reading was noted as V_{sample}.

Negative groups of the anionic cotton were reacted with hydrochloric acid. After reaction, the fibers were filtered and washed until no hydrochloric acid left, which can be proved by the silver nitrate drop test. The amount of sodium hydroxide was added to neutralize the filter fibers and an excess part was left to be titrated by hydrochloric acid. V_{blank} is the amount of HCl to neutralize NaOH without fibers. V_{sample} is the amount of HCl to neutralize left part NaOH. Therefore, the difference between V_{blank} and V_{sample} caused by the amount of negative groups in anionic cotton can determine total negative charges of anionic cotton by the following equation.

Equation:

$$mmol\ of\ carboxymethyl\ content/100g = 100\times(V_{blank} - V_{sample})\times N_{HCl}/0.25$$

Where, N_{HCl} = 0.05N, the normality of the titrant HCl solution.

For example, if V_{blank} is 14ml and V_{sample} is 10ml, and then mmol of carboxymethyl content/100g is equal to 80mmol/100g.

This method was used to determine the total negative charges of the anionic cotton.

4.2.4 Streaming Current (SC) Tests

The same ECA2000P instrument (Chemtrac Systems, Inc.) used earlier was used in these experiments. The procedure for testing anionic cotton is summarized as follows [7]. Anionic cotton sample was cut into very tiny pieces, and about 0.25g of anionic cotton fibers was mixed with 50ml deionized water, when the fibers were cut from 95g/L anionic cotton, poly-DADMAC (0.002N) was added to make the solution

be positive and after, stirring for 20 minutes, the mixture was then filtrated to yield 10ml of sample. The SC device was cleaned to remove any residual sample from previous titrations. 5 ml of diluted sample was placed in the device. The apparatus was equilibrated with a preliminary aliquot of the sample to be tested. A fresh aliquot was added, and the initial signal was recorded from the meter output. Note the initial sign of charge indicated by the streaming current detector. When the initial sign is positive, sample was titrated with a suitably dilute solution of high-charge anionic titrant PVSK (0.0025N). The addition rate of PVSK was equivalent to small amounts added each 10 seconds or so, with the aim of completing each titration in about 60 to 120 seconds. Titration was continued until the meter output changed from positive to negative. The endpoint of titration was obtained from curve of amount of titrant added vs. the streaming signal. The amount of titrant added to neutralize the sample was used to determine the endpoint.

4.3 Results and Discussion

4.3.1 Total charge

Table4.2 shows the total charge of anionic cotton by different treatments in five repetitions. Form these results, the cotton treated by 190g/L concentration of CAA caused a little rise in total negative charges compare to the cotton treated at a concentration of 95g/L. As the same in the chapter 3, higher chemical concentration leads to higher anionization. The standard deviation is quite low compare to the average value; the five separate determinations yield parallel values, which states that

the cotton fabrics are equally reacted with the anionic chemicals. the anionic treatment procedure is reproducible.

These values proved the difference of total negative charges between the anionic cotton samples by two concentration treatments. Although the total charge of anionic cotton with the 190g/L treatment is higher than that treated with the 95g/L concentration, it is not twice as high. As the concentration of anionic reactant increases, the total charge of the cotton also increase, but the increase in charges is not proportional to the increase the anionic reactant. For instance, the biggest difference of total charge of anionic cotton by 190g/L treatment and 95g/L treatment is about 25mmol/100g. Therefore, above 95g/L concentration, only increasing the anionic agent's concentration at the same condition can not directly obtain more negative charges on the cotton. The reasons explained for this result are the same as discussed in chapter 3. First, increase anionic reactant leads to increase hydrolysis reaction speed. Second, the electrostatic repulsion increase due to more negative groups, which makes the anionic reactant hardly access to the cotton.

Contrasting the total charge of cationic cotton, the anionic cotton has more total charge after treatment, because the fiber without any anionic treatment still has some negative charges when it is in aqueous solution, due to the carboxyl groups. After the anionic treatment, more negative charges should be getting on the cotton.

4.3.2 Streaming Current (SC) Tests

As mentioned in the chapter 3, the endpoint of titration can be evaluated by the

curve of SC-meter output vs. the titrant added. Figure 4.2 shows the SC signal changes from positive to negative with the negative titrant PVSK adding. The amount of titrant at the endpoint is determined when the output goes to zero

In the blended solution, which is composed of anionic cotton and added cationic polyelectrolyte poly-DADMAC, the charges of poly-DADMAC minus the charges of anionic cotton should theoretically equal to the charges of PVSK. The surface charge of anionic cotton can therefore be calculated from the amount of titrant added in the sample solution at the endpoint.

0.2535g cut anionic cotton fiber (95g/L) pieces were mixed with 50ml deionized water, and then 20 ml poly-DADMAC (0.002N) was added. Analogous to the streaming current experiments of cationic cotton, positive polyelectrolyte poly-DADMAC should be mixed with the anionic sample. Because anionic cotton cellulose has more negative charges than untreated cotton, it is assumed that there are more negative charges on the fiber surface. To make sure that all negative charges on the anionic fiber's surface were neutralized, 20ml poly-DADMAC was added. The mixture was filtered, and10ml removed to use as a sample for test in the SC. The output of the sample used in the test should be positive. With negative titrant PVSK added, the SC output value changed from positive to negative. According to the end-point, the dosage of added PVSK (0.0025N) to neutralize the positive sample is 0.29 ml (This is evaluated from the curve SC Meter output vs. the amount of titrant added in figure4.2).

Equation:

Negative Charges of PVSK = Positive Charges of poly-DADMAC – Surface charge of Anionic Cotton

$2.5\text{mmol/L}\times 0.29\times 10^{-3}\text{ L} = (2\text{mmol/L}\times 0.02\text{L} - X)\times 1/7$

$X = 34.93\times 10^{-3}\text{mmol}$

$34.93\times 10^{-3}/0.2535\text{g}$ = Surface charge of Anionic Cotton/100g

Surface charge of Anionic Cotton = 13.8 mmol/100g

From the results in the table 4.3, 95g/L or 190g/L anionic cotton samples showed similar surface charge in five separate evaluations. The standard deviations are very small, and each test result is very close to the average value, which means the anionic treatment is repeatable and negative charges are uniform onto the surface even though these samples were cut from different places in a large anionic treated cotton specimen. The surface charge of anionic cotton from 190g/L treatment was less than twice that of the 95g/L treatment. An increase of anionic agent concentration does not proportionately increase negative charges on the cotton surface. As discussed in the chapter 3, let the amount of anionic agent reacted with cotton be Q, the quantity reacted with inner fiber be Qi, and the quantity reacted on the fiber surface be Qs. When the anionic agent quantity is increased to 2Q, the quantity reacted with the fiber surface Qs' is more than Qs, but less than 2Qs, which means that the surface of the cotton fiber that reacted with 95g/L CAA was not completely covered. There remain are some places to react with anionic agent on the fiber surface.

Table 4.4 gives the each value of anionic agent reacted with cotton interior or surface. Here the amount of charges indentifies the quantity of anionic reactant. For anionic cotton, Qi' equal 1.232Qi and Qs' equal 1.336 Qs. Surface and inner charges increase due to the increase in anionic reactant. The surface charge has increased more than the inner charges because when the anionic reactant concentration increases, the electrostatic repulsion in the fiber is greater than that on the surface. This electronic repellent force retards the anionic groups reacting with hydroxyl groups. For cationic cotton, Qi' equal 1.272Qi and Qs' equal 1.694Qs. Increasing the cationic reactant concentration has a greater effect of the amount of charges increase than the anionic reactant. This is because anionic cotton has more total charge both in the fiber and on the surface, than cationic cotton. Therefore less anionic reactant reacts with cotton when its concentration increases due to more electrostatic repulsion.

In Figures 4.5 and 4.6, no matter what anionic chemical concentration is, the surface charge was only a small part of the total charge. This could be due to the same reason as discussed before. That is that the polymer chains are twisted with only a few internal anionic groups have reacted with the cationic polyelectrolyte. When the negative polyelectrolyte is added, the outside negative charges are neutralized, but the internal part, within the polymer, would be expected to remain negative in charge. The other reason might be due to the fact that the anionic cotton fiber has pores that act as if they are dead-ended cylinders, having one end open to the aqueous solution. In low conductivity, the characteristic sizes of pores in the fiber seem to be sufficient

small so that polyelectrolytes of big mass will have difficulty to get into them. But in acid base titration, the titrant is low-mass ions, which easy penetrate into the pores of the fibers, and all charges of treated fibers are neutralized.

Figures 4.4 and 4.5 show that for anionic cotton cellulose treated with two concentrations of reactant, the ratios of surface charge to the total charge are almost the same value, about 20%. 190g/L anionic cotton has a higher ratio of surface charge to the total charge than the 95g/L anionic cotton. From these pie charts, no matter what concentration treatments were applied, and no matter what kind of ionic treatments were applied, the ratios of surface charge over total charge are almost constant. Increasing the anionic agents doesn't increase the ratio of surface charge over the total charge. That means the anionization process of cotton occurred evenly through the fiber. The treatments only give the fiber anionic charges, but do not change its physical structures. When the concentration of the anionic reagents is increased, it is more difficult for them to react with hydroxyl groups inside the fiber than with hydroxyl groups on the fiber surface. Due to this reason, the ratio of surface charge over total charge has increases slightly as anionic reactant concentration increases.

4.4 Conclusion

According to the acid base titration, 190g/L anionic cotton has more negative charges than 95g/L anionic cotton. Because cellulose has negative charges when in the aqueous dispersions, the process to make it further anionic makes cotton more

negatively charged as compared to the initial charges in the cationic sample. However, changing the CAA concentration in the anionic treatments was not very effective in increasing the total charge of cotton cellulose.

Through streaming current tests, surface charge of cotton fiber treated with two concentrations of anionic reagent were found, only a small percentage of total charge was contribution from the surface. Five repetitions from random samples gave similar SC results. The anionic treatment was found to be reproducible and the reaction was evenly occurred in the fiber. In all samples, the ratio of surface charge to total charge was similar. Neither concentration of reactant nor type of ionization was found to affect the ratio of surface to total charge.

4.5 Reference

1. Ibarra, L. and Alzorriz, M. Vulcanization of carboxylated nitrile rubber (XNBR) by amixed zinc peroxide–sulphur system, *Polymer International* **49**, 115-121 (2000).

2. Bilgen, M. M.S. Thesis *Wrinkle recovery for cellulose fabric by means of ionic crosslinking* (North Carolina State University, Raleigh, NC, 2005).

3. Thomason, S. M.S. Thesis *Optimization of ionic crosslinking* (North Carolina State University, Raleigh, NC, 2006).

4. Hashem, M. & Hauser, P. and Smith, B. Wrinkle recovery for cellulosic fabric by means of ionic crosslinking, *Textile Research Journal* **73**, 762-766 (2003).

5. Borsa, J. & Ravichandran, V. and Obendorf, S. K. Distribution of carboxyl groups in the carboxymethylated cotton fibers, *Journal of Applied Polymer Science* **72**, 203-207 (1999).

6. Pruthesh Hariharrao Vargantwar, Thesis *Preparation of ionic cellulose for wrinkle resistant fabrics* (North Carolina State University, Raleigh, NC, 2007).

7. Martin A. Hubbe, Accurate charge-related measurements of samples from the wet-end: Testing at low electrical conductivity, *Paper Technology* HEADING 1-6 (2008).

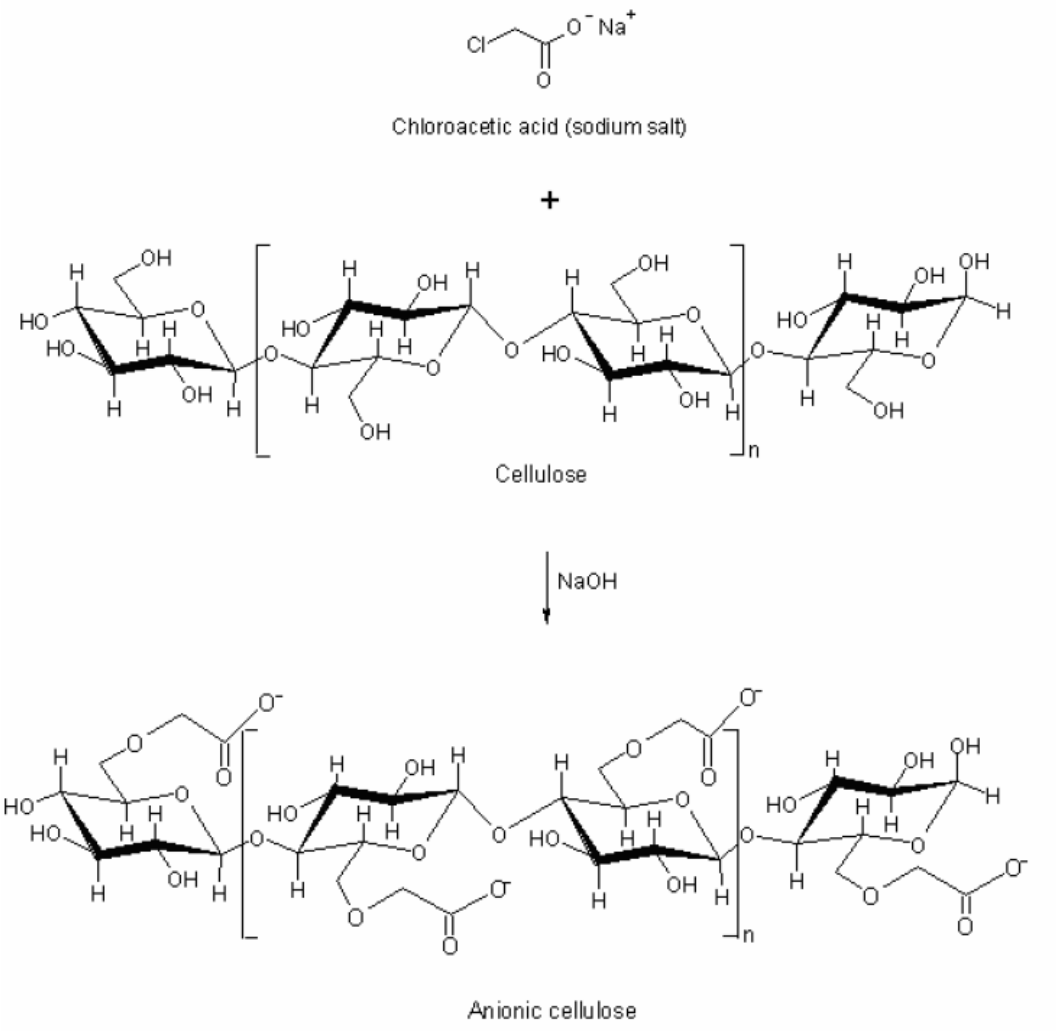

Figure 4.1. Carboxymethylation reaction of cotton with chloroacetic acid and sodium hydroxide [4]

Table 4.1 Test materials and chemicals.

Name or Group	Description	Manufacturer
Cotton Fabric	Standardized TIC-400 woven cotton fabrics	Textile Innovators, Inc.
Base	Sodium hydroxide, 50% w/w aqueous solution	Fisher Scientific
Anionic Agent	Mono chloroacetic acid, 99%	Acros Organics
Negative Titrant	PVSK	Aldrich Co.
Positive Titrant	Poly-DADMAC	Aldrich Co.

Table 4.2 Total charge of anionic cotton with different concentration treatment

Times	95g/L Treatment (mmol/100g)	190g/L Treatment (mmol/100g)
1	85.6	100.1
2	83.7	107.5
3	79.5	104.3
4	84.3	99.7
5	77.9	102.6
Mean	**82.2**	**102.84**
STDEV	3.31	3.21

Table 4.3 Surface charge of anionic cotton with different concentration treatment by SC tests

Times	95g/L Treatment (mmol/100g)	190g/L treatment (mmol/100g)
1	13.8	19.7
2	15.1	20.2
3	15.7	20.8
4	14.5	20.6
5	16.3	19.4
Mean	**15.08**	**20.14**
STDEV	0.98	0.59

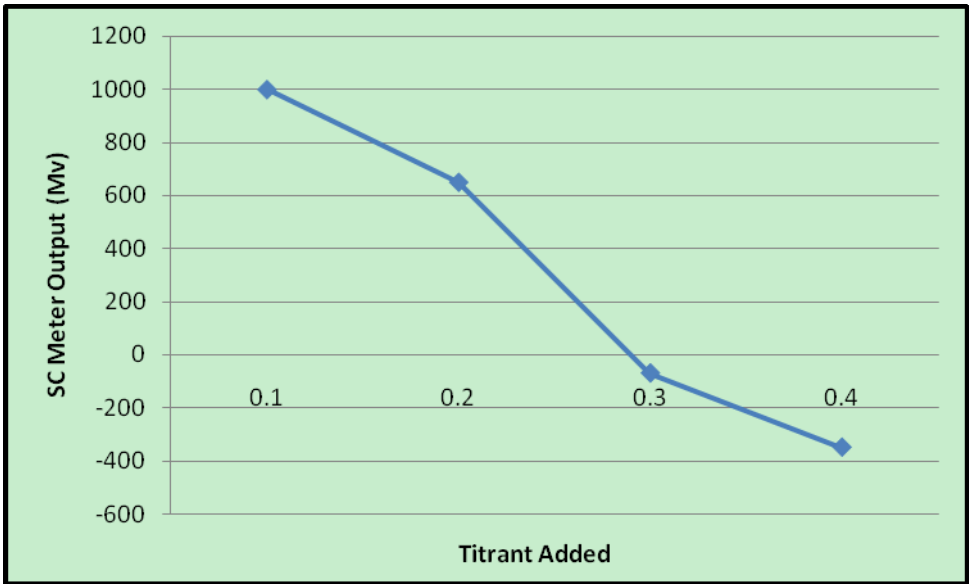

Figure 4.2. The curve of SC Meter output vs. the amount of titrant added. The curve corresponds to a solution of the sample titrated by PVSK at neutral condition. Each time the additive amount is 0.1ml.

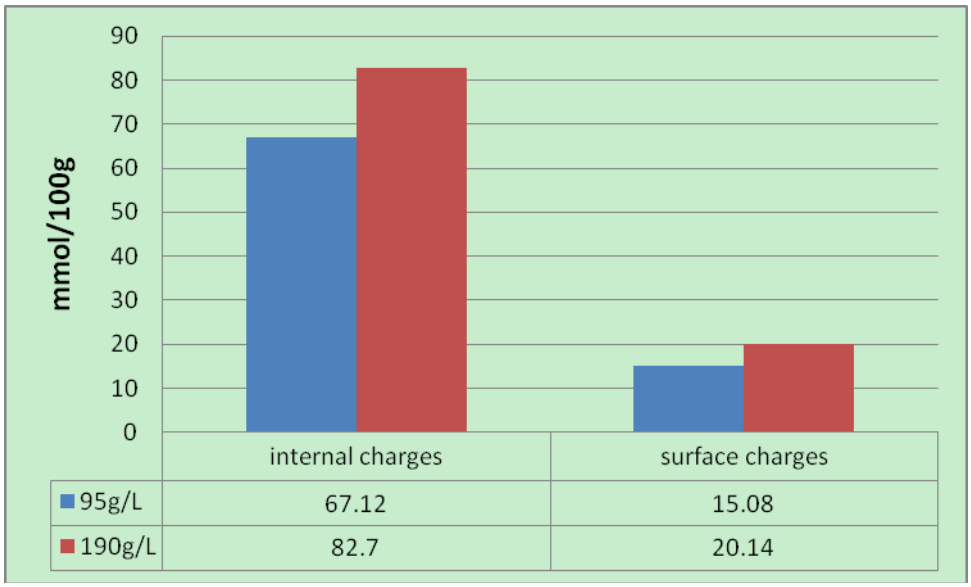

Figure 4.3. Average value of surface and internal charge of the anionic cotton by different treatment

Table 4.4 The different anionic reactant quality reacts with the fiber inner or surface

	Anionic Cotton
Qi	67.12
Qi’	82.7
Qs	15.08
Qs’	20.14
Qi’/Qi	1.232
Qs’/Qs	1.336

Qi: for 95g/L treatment, the quantity of reacted anionic reactant in the internal fiber;

Qi’: for 190g/L treatment, the quantity of reacted anionic reactant in the internal fiber;

Qs: for 95g/L treatment, the quantity of reacted anionic reactant on the fiber surface;

Qs’:for 190g/L treatment, the quantity of reacted anionic reactant on the fiber surface;

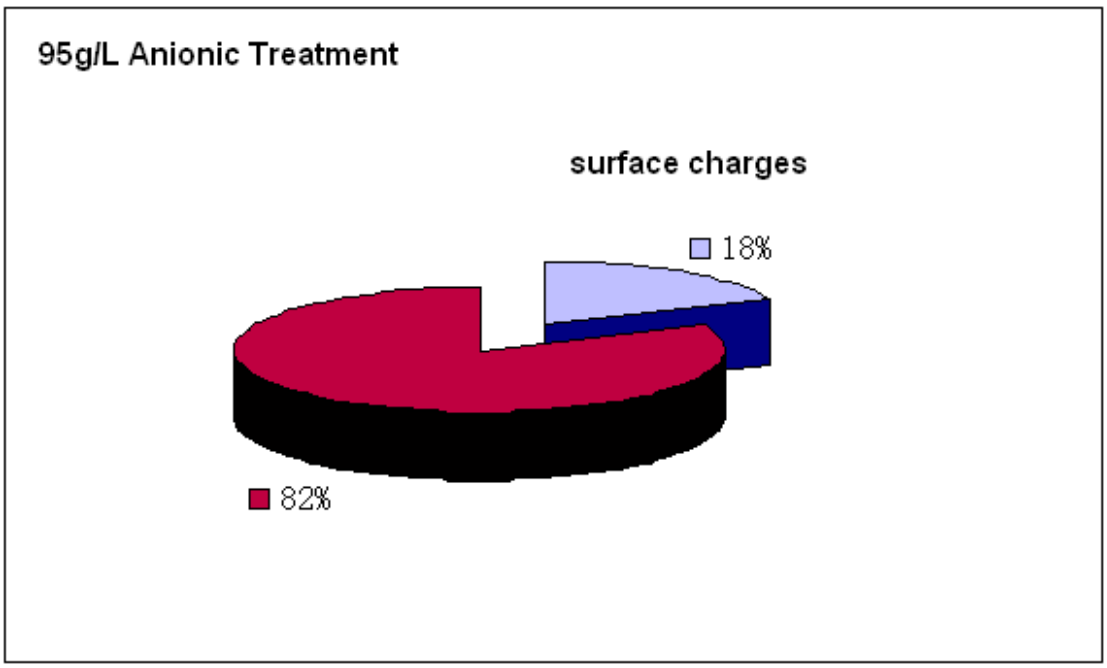

Figure 4.4. Anionic cotton by 95g/L treatment: the ratio of surface charge to total charge.

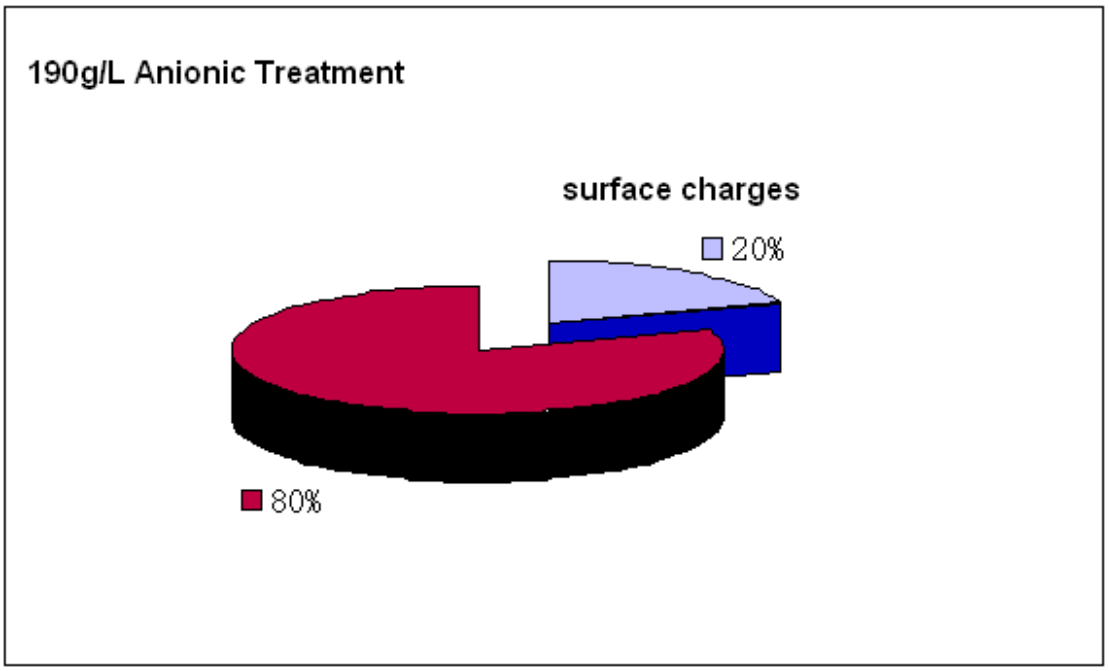

Figure 4.5. Anionic cotton by 190g/L treatment: the ratio of surface charge to total charge.

CHAPTER 5: CHARGE DISTRIBUTION OF IONIC COTTON FROM STREAMING POTENTIAL TESTS

5.1 Instruction

The streaming potential (SP) method is another way to determine the charged nature of fiber surfaces. This is a “direct” and “quick” method to evaluate the charge density on a solid when the electrostatic forces are exerted at the outside surfaces of the fibers of interest [1-3].

The principle of SP is similar to that of streaming current (SC) test but instead of measuring the current generated by the streaming phenomena, in the SP measurement the potential gradient generated by fluid flow through a fiber network (pad) is determined. More specifically, instead of the reciprocating plastic surface in SC equipment (usually PTFE), in the SP instrument the liquid flows through a pad of fiber from the sample itself by a pressure gradient. As in the case of the SC tests described, the flowing liquid causes counter-ions to move down-stream relative to the fiber surface. The resulting voltage is measured between electrode probes on both surfaces of the fiber pad. This voltage is then compared with the voltage when the applied pressure is zero. The raw value of the SP test equals the potential in the presence of flow through the pad subtracting the reference measurement. SP is related to the zeta potential by factors that include the electrical conductivity, fluid viscosity, and the structure of the fiber pad. The value of SP test under given conductivity and pressure conditions can be used to determine how strongly the sample will interact

with anionic or cationic additives [4-9].

In this chapter, fiber-pad SP tests were used to determine the zeta potential of cotton fiber surfaces. Compared to the SC tests, SP tests have some advantages. First, the signals of fiber-pad SP tests originate directly from the cotton fiber surface of interest, not from an arbitrary plastic surface. Second, it is not necessary to wait 5-20 seconds for an additive or titrant to equilibrate with plastic surface like in the SC equipment. Mixing and adsorption can happen within a second in a stirring fiber suspension. Figure 5.1 gives a schematic illustration of the essential parts of the fiber-pad SP device [10]. Such device uses vacuum to draw a fiber suspension from a beaker toward a small screen. If we assume that a negative charged polymer will be retained with very high efficiency on the cationic fiber surfaces with positive groups, fiber-pad SP tests can be used to verify that the fibers have positive charges before being reacted with the selected anionic polyelectrolyte. In addition, by knowing the amount of polyelectrolyte added in the sample, the charge density of fiber surface can be determined from the titration endpoint. The goal of this chapter is to determine the average charge density on the ionic cotton surface from fiber-pad SP tests.

Cotton used in the fiber-pad SP tests was cut into tiny fibers. The fiber structure is a porous medium, though which water can flow around or through. Due to the porous nature of cellulosic fibers, the results of SP tests can be also sensitive to the charge condition of sub-microscopic pore surfaces, not just the outside surfaces of fibers [11, 12]. Figure 5.2 illustrates this phenomenon.

However, since the typical pores in the cell walls of fibers are extremely small [13-15], it is not reasonable to expect a large amount of polyelectrolytes to diffuse into those pores during the relatively brief contact times typically provided. Consequently, the real requirement of researchers is a way to carry out SP tests so that they can detect information just related to the outer surfaces. Such method was shown in recent work [11, 12]. If the aqueous solution in a fiber suspension is filtered off and replaced by deionized water, it turns out that the electrostatic potential due to the outer surface of fibers can be measured. Here outer surface doesn't include the pores in the cell walls of fibers.

The reason why this approach works is due to the characteristic distance of counter-ions from charged surfaces, such as the "double layer thickness". For example, the effective double layer thickness can be about 1-4 nm under typical aqueous conditions found in fiber systems, which is much smaller than the diameter of a typical pore in a water-swollen cell wall. That means the unmodified fiber stock samples taken process suspensions and tested by SP will be attributed to a combination of effects, including those from the interior and exterior of the fibers [16-18].

By contrast, if the same tests are done in deionized water, with the electrical conductivity below 10 μS/cm, there won't be sufficient space within the small pores for double layers to develop fully, and therefore contribute little to the observed electro-kinetic effects. For this reason, only the outer surfaces of the fibers, the parts of interest, will contribute to the measured results in the absence of salt ions.

In summary, a modest effort to replace the liquid phase of a sample with deionized water can pay off, giving a much better SP data [11]. As mentioned in chapter 3, both SP and SC tests

should be done in solutions of low electrical conductivity without salt additive.

5.2 Experimental

5.2.1 Materials and Chemicals

The materials and chemicals used for this research were all commercially available. They are shown in Table 5.1 along with their descriptions and manufacturers.

5.2.2 Ionic Cotton Preparation

The same ionic cotton specimens (prepared in chapter 3 and 4) were used in this chapter.

5.2.3 Fiber-pad Streaming Potential (SP) Tests

The procedure of SP is based on an assumption that the purpose of the fiber-pad SP tests is to evaluate the nature of charges on the outer surface of the fibers. The SP tests were conducted with deionized water and carried out with the SP device. Untreated, cationic and anionic cotton were cut in very tiny fibers. Samples (pH~7) of the cut fibers (about 0.25g for each) on an oven-dry basis were blended in 50 ml deionized water for a few minutes. Flow of a fiber suspension towards a screen caused gradual build-up of a fiber pad. Streaming potentials were determined with a pressure differential of 207 kPa across the fiber pad. The streaming potential of untreated cotton fiber solution was measured without titrant additive. Poly-DADMAC (0.002N) was used as a titrant with positive charges in anionic cotton tests; PVSK (0.003N) was used as a titrant with negative charges in cationic cotton tests.

5.3 Results and Discussion

5.3.1 Surface charge of treated anionic cotton

As shown in Figure5.3, initial addition of 10 ml poly-DADMAC to anionic cotton (95g/L) fiber suspension caused an immediate rise in streaming potential to less negative or more positive values. Thereafter, the streaming potential began to decay back in the direction of its initial state prior to adding poly-DADMAC. The obvious rise in this Figure is due to the positive charges of cationic titrant, which affects the potential of the anionic cotton fiber solution. As titration with highly charged cationic polymers was carried out, the decay of streaming potential values with time was consistent with diffusion of polyelectrolyte into the anionic solution as the cationic polymer was gradually adsorbed onto the anionic fiber surface. A second, equal dosage of poly-DADMAC was added after an elapsed time of 12 minutes. It immediately reversed the streaming potential to positive; but later the value of streaming potential decayed again, resulting in a near-zero streaming potential after an additional 8 minutes of continual stirring. Based on that a total of 20 ml poly-DADMAC was added in the anionic sample (95g/L) to reach the endpoint, the surface charge of anionic cotton fiber (95g/L) was calculated by the following equation.

Positive Charges of poly-DADMAC = Surface charge of Anionic Cotton

$2\text{mmol/L} \times 20 \times 10^{-3}\text{L} = 40 \times 10^{-3}\text{mmol}$

$40 \times 10^{-3}/0.2675\text{g}$ = Surface charge of Anionic Cotton/100g

Surface charge of Anionic Cotton = 14.95 mmol/100g

Here, 20 ml titrant poly-DADMAC (0.002N) was added to neutralize the

solution of anionic cotton fibers (95g/L). However in four other tests, every initial quantity of cationic poly-DADMAC additive to the solution may be slightly different. The titration endpoint was reached for all the tests in spite of the different additive quantity every time, which affected the entire time of SP test and the total amount added to neutralize the negative charges on the surface of anionic cotton fibers. Five anionic samples used in the experiment were randomly cut from a large anionic cotton specimen treated at a reagent concentration of 95g/L.

Like the titration process in anionic samples (95g/L), 10ml poly-DADMAC was added to anionic cotton (190g/L) fiber suspensions at first, and caused an immediate rise in streaming potential to less negative values (shown in Figure 5.4). The streaming potential began to decay back afterwards in the direction of its initial state prior to the addition of cationic polyelectrolyte. A second, equal dosage of poly-DADMAC, added after an elapsed time of 12 minutes, raised the streaming potential to zero; however the streaming potential decayed to negative again later. Compared to the amount of cationic titrant to neutralize the anionic cotton (95g/L) fiber suspensions, more cationic titrant was needed for neutralization in the 190g/L anionic cotton fiber suspension. Therefore another equal dosage of poly-DADMAC was added at the 20^{th} minute, the streaming potential was reversed from negative to positive after decay, resulting in a near-zero streaming potential after an additional 8 minutes of continual stirring. At the endpoint, a total of 30 ml poly-DADMAC was added in the 190g/L anionic cotton fiber suspension. The surface charge can be

calculated by using the same method from the previous example.

Equation:

Positive Charges of poly-DADMAC = Surface charge of Anionic Cotton

$2mmol/L \times 30 \times 10^{-3}L = 60 \times 10^{-3}mmol$

$60 \times 10^{-3}/0.2675g$ = Surface charge of Anionic Cotton/100g

Surface charge of Anionic Cotton = 22.43mmol/100g

The amount of cationic titrant poly-DADMAC (0.002N) to neutralize the anionic solution of cotton (190g/L) fibers was 30 ml. As mentioned before, in four other tests every initial quantity of cationic poly-DADMAC added to the solution was different. However, the titration endpoint was reached for all the tests in spite of the different addition of cationic poly-DADMAC. Five anionic samples were randomly cut from a large anionic cotton specimen treated at a reagent concentration of 190g/L.

Figure 5.5 shows that the streaming potentials of anionic cotton fibers with two treatments were negative. The suspension of anionic cotton fiber (190g/L) had a much higher potential than anionic cotton fiber (95g/L). The potential of untreated cotton is -28mV, while the potentials of anionic cotton fibers with two treatments were -163 and -254mV respectively. The higher concentration of anionic reactant led to higher streaming potential of anionic cotton fibers. These observations indicate that the untreated cotton fibers had a negative charge in aqueous condition, and that carboxymethylation produced further negative charges on the surface of cotton fibers. The streaming potential of anionic cotton from 190g/L treatment was less than twice

the value corresponding to the 95g/L treatment. An increase of anionic agent concentration did not proportionately increase the streaming potential of anionic cotton fiber suspension.

The same procedures of SP tests were applied to measure the surface charge of anionic cotton in five different samples. For each experimental run, the dosage of poly-DADMAC varied. The SP output changed from negative to positive by adding cationic titrant several times, which depends on its initial quantity of addition. The results of negative charges on the cotton fiber surface by five separate evaluations are showed in Table 5.2. The standard deviations were very small. The results for each test results were very close to the average value, which means that SP tests were reproducible.

5.3.2 Surface charge of cationic cotton

Because the concentration of PVSK was larger than poly-DADMAC, and since the absolute charges of anionic cotton are greater than those of cationic cotton, the amount of PVSK added to reach the titration's endpoint was smaller. As shown in Figure 5.6, the initial 5 ml PVSK added to cationic cotton (188g/L) fibers suspension caused an immediate drop in streaming potential to less positive values. After that, the streaming potential began to rise back in the direction of its initial state prior to adding anionic PVSK. There is an obvious drop in Figure 5.6, because the negative charges of anionic titrant reduced the potential of the cationic cotton fiber suspension. Due to the reaction with the highly charged anionic polymers, the rise of streaming potential with time was consistent with the diffusion of the polyelectrolyte into the cationic solution. A second, equal

dosage of PVSK was added after an elapsed time of 12 minutes. It initially reversed the streaming potential to negative, but the value rose again afterwards, resulting in a near-zero streaming potential after an additional 8 minutes of continual stirring. Based on the amount of PVSK addition, the surface charge of cationic cotton was calculated by the following equation.

Equation:

Negative Charges of PVSK = Surface charge of cationic Cotton

$3mmol/L \times 10 \times 10^{-3}L = 30 \times 10^{-3}mmol$

$30 \times 10^{-3}/0.2675g$ = Surface charge of Cationic Cotton/100g

Surface charge of Cationic Cotton = 11.21mmol/100g

10 ml titrant PVSK (0.003N) was used to neutralize the cationic cotton (188g/L) fiber solution. In four other tests, every initial quantity of anionic PVSK added in the solution was different; however, the titration endpoint was reached for all the tests in spite of the different quantities, which affected the entire time of SP test and the total amount to neutralize the positive charges on the surface of cationic cotton fiber. Five cationic samples used in the experiment were randomly cut from a large cationic cotton specimen (188g/L). Similar results were obtained in the case of five cationic samples.

For the 376g/L cationic cotton fiber suspensions (Figure 5.7), initial addition of 5 ml PVSK caused an immediate drop in streaming potential to less positive values. Thereafter, the streaming potential began to rise back in the direction of its initial state prior to the addition of PVSK. Because the negative charges of PVSK would decrease

the potential of the cationic solution, there was an obvious drop in the figure. With diffusion of the polyelectrolyte into the cationic solution, the streaming potential values increased with time. After an elapsed time of 12 minutes, a second equal dosage of PVSK was added. The streaming potential was reversed to near zero, but later rose again. The positive charges on the surface of 376g/L cationic cotton fibers needs more anionic titrant to neutralize than 188g/L cationic cotton. Therefore, another equal amount of PVSK was added at the 20^{th} minute, which then reversed the streaming potential to negative (near zero) after an additional 8 minutes of continual stirring. According to the dosage of PVSK used in the 376g/L cationic cotton fiber suspension, their surface charge can be calculated by the following equation.

Equation:

Negative Charges of PVSK = Surface charge of cationic Cotton

$3\text{mmol/L} \times 15 \times 10^{-3}\text{L} = 45 \times 10^{-3}\text{mmol}$

$45 \times 10^{-3}/0.2675\text{g}$ = Surface charge of Cationic Cotton/100g

Surface charge of Cationic Cotton =16.82 mmol/100g

Where, 15 ml anionic titrant PVSK (0.003N) was added to neutralize the solution of 376g/L cationic cotton fiber.

Figure 5.6 and 5.7 show the potentials of two cationic cotton fibers suspensions are positive. In Figure 5.8, the streaming potentials of cationic cotton fibers with two treatments are 89 and 157 mV, respectively. The solution of cationic cotton fiber with 376g/L treatment has much higher potential than that with 188g/L treatment, which

means higher cationic reactant concentration leads to higher streaming potential. Due to the -28mV potential of untreated cotton fibers, the positive streaming potentials of cationic cotton prove that cationization produces positive charges on the surface of cotton fibers. The increment in streaming potential of cationic cotton sample is almost proportional to the cationic reactant concentration, while the similar trend was missing for the anionic cotton sample. The different observations are attributed to that anionic cotton has more charges than cationic cotton, Therefore the electrostatic repulsionof anionic cotton is greater than that of cationic cotton. Although anionic reactant concentration increases, the negative charges in it are more difficult to reach the surface of anionic cotton, which induces only partially reaction.

The same procedure of SP tests was applied to measure the surface charge of cationic cotton (376g/L) five times. The titration endpoint was reached for all the tests. The results of positive charges on the cotton fibers surface by five separate evaluations are shown in Table 5.3. The standard deviations are very small, and the results for every test were very close to the average value, which further supported the fact that SP tests are reliable. In addition, the cationic treatment was repeatable and positive charges were uniformly distributed on the fiber surface.

Figure 5.9 shows the differences of positive and negative charges on cationic and anionic cotton surface, respectively. For cotton, more negative charges are produced by anionic treatment than positive charges by cationic treatment, of which the reason has been discussed in the chapter 3 and 4. Similar results have been

obtained in this chapter. A doubled cationic reactant concentration (376g/L) resulted in the positive charges on the cotton surface more than 1.5 times of 188g/L concentration, while the same increment of anionic reagent concentration has little effect on the amount of negative charges on the cotton surface. Consequently, the surface charge is more sensitive to the change of cationic reactant concentration.

5.3.3 Comparison of the results by SC and SP

The surface charge of anionic cotton in two treatments was determined by two measurements: SC and SP tests. Streaming current (SC) tests measure the surface charge of ionic cotton by the titration of filtered solution, which composed of ionic cotton fibers and polyelectrolytes with counter-ions; while SP tests measure the surface charge directly by the titration of the ionic cotton fibers suspension. The first titration takes place in the ionic solution and the second one on the ionic fiber surface. SC method is mostly used for cationic or anionic demand titration endpoint determination, while the fiber-pad SP method is for the estimation of the zeta potential of fiber surfaces, depending on the sequence and levels of chemical treatments. A comparison between these two methods is made based on the experimental results.

As showed in figure 5.10 and 5.11, there is only a small difference between the surface charge by two methods, with value by SP higher than SC. Such difference is due to the pores in the cotton fiber. When the titrant with positive charges is added to the anionic solution, it only reacts with the charges outside. As increasing the mixing time, some titrant molecules diffuse into

the pore, and react with the charges inside. For example in 190g/L anionic fiber solution, the stirring time of SP was longer than SC, which means the poly-DADMAC macromolecule had more chances to diffuse into the pores and reacted with negative charges, therefore the surface charge of 190g/L anionic cotton measured by SP test was a little higher than SC tests. However, because of the similar stirring time for 95g/L anionic samples in both tests, the results of 95g/L anionic cotton by two methods had almost the same value. For cationic cotton, the charges of cotton fibers surfaces with 188g/L and 376g/L treatment tested by SP were a little higher than the results by SC. Such difference is due to that SP tests the fiber surface potential directly, while in SC test the endpoint is determined by neutralizing the partly filtered solution, from the mixture of cut ionic fibers and titrant. However, the differences of surface charge between SC and SP are very small. Both of them are reliable to measure the surface charge of fiber.

5.4 Conclusions

Surface charges of anionic and cationic cotton were determined by fiber-pad SP tests. The results of their surface charge obtained by the SP technique were similar to those obtained by the SC technique. The absolute amount of surface negative charges in anionic cotton was larger than the positive charges in cationic cotton. The surface charge measured after cationic treatment was more sensitive to the variation of reactant concentration compared to those measured after anionic treatment.

5.5 Reference

1. Hubbe, M. A., and Wang, F., “Charge-Related Measurements – A Reappraisal. Part2: Fiber-pad Streaming Potential,” Paper Technol. 45 (9): 27-34 (2004).

2. Hubbe, M. A., "Selecting Lab Tests to Predict Effectiveness of Retention and Drainage Aid Programs," Paper Technol. 44 (8): 20-34 (2003).

3. Davison, R. W., and Cates, R. E., “Electrokinetic Effects in Papermaking Systems: Theory and Practice,” Paper Technol. Ind. 16 (4): 107-144 (1975).

4. Goring, D. A. I., and Mason, S. G., “Electrokinetic Properties of Cellulose Fibers,” Can. J. Res. B28 (6): 307-322; 323-338 (1950).

5. Penniman, J. G., “Comparison of Pulp Pad Streaming Potential Measurement and Mobility Measurement,” Tappi J. 75 (8): 111-115 (1992).

6. Nazir, B. A., “An On-line Streaming Potential Meter (SPM) – Wet-End Applications,” Paper Technol. Ind. 35 (3): 28-35 (1994).

7. Sanders, N. D., and Schaeffer, J. H., “Comparing Papermaking Wet-End Charge-Measuring Techniques in Kraft and Ground wood Systems,” TAPPI J. 78 (11): 142-150 (1995).

8. Miyanishi, T., and Shigeru, M., “Optimizing Flocculation and Drainage for Microparticle Systems by Controlling Zeta Potential,” Tappi J. 80 (1): 262-270 (1997).

9. Hubbe, M. A., Rojas, O. J., Lucia, L. A., and Jung, T. M. “Consequences of the Nanoporosity of Cellulosic Fibers on their Streaming Potential and their Interactions with Cationic Polyelectrolytes,” Cellulose 14 (6), 655-671(2007).

10. Nazir, B. A., “An On-line Streaming Potential Meter (SPM) – Wet-End Applications,” Paper Technol. Ind. 35 (3): 28-35 (1994).

11. Hubbe, M. A., Rojas, O. J., Lee, S. Y., Park, S., and Wang, Y, “Distinctive Electrokinetic Behavior of Nanoporous Silica Particles Treated with Cationic Polyelectrolyte,” Colloids and Surfaces A 292 (2), 271-278 (2007).

12. Hubbe, M. A. “Sensing the Electrokinetic Potential of Cellulosic FiberSurfaces,” BioResources 1(1), 93-125 (2006).

13. Stone, J. E., and Scallan, A. M. “A Structural Model for the Cell Wall of Water-Swollen Wood Pulp Fibers Based on their Accessibility to Macromolecules,” Cellulose Chem. Technol. 2 (3): 343-358 (1968).

14. Berthold, J., and Salmén, L. “Effects of Mechanical and Chemical Treatments on the Pore-Size Distribution in Wood Pulps Examined by Inverse Size-Exclusion Chromatography (ISEC),” J. Pulp Paper Sci. 23(6), J245-253 (1997).

15. Alince, B., and van de Ven, T. G. M. (1997). “Porosity of Swollen Pulp Fibers Evaluated by Polymer Adsorption,” in C. F. Baker, ed., The Fundamentals of Papermaking Materials, Pira Intl., Leatherhead, Surrey, UK, 771-788.

16. Sack, W., Storbeck, W., and Winiker, R., “Ten Years of Research Experience with Continuous Zeta Potential Measurements for Paper Machine Process Control,” Wochbl. Papierfabr. 121 (19): 803-805 (1993).

17. Hand, V., Koethe, J., Kuchibhotla, S., and Scott, W., “An Evaluation of Two Pad-Forming Paper Stock Charge Analyzers,” Papermakers Conf. Proc., TAPPI Press, Atlanta, 1993, 591-598.

18. van de Ven, T. G. M., “Effect of FiberConductivity on Zeta Potential Measurements of Pulp Fibers,” J. Pulp Paper Sci. 25 (7): 243-245 (1999).

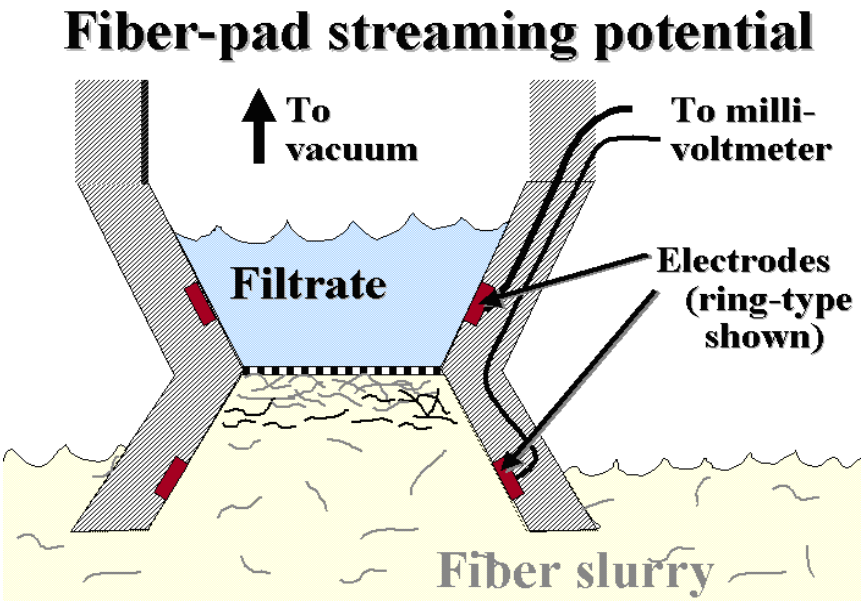

Figure 5.1. Fiber-pad streaming potential [10]

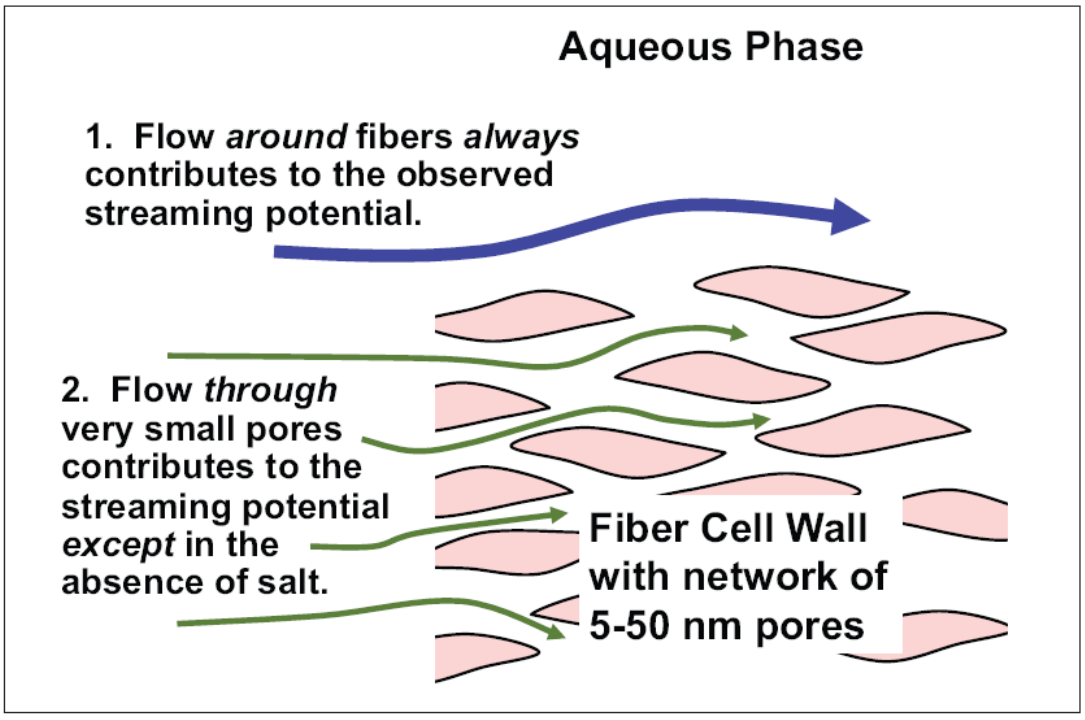

Figure 5.2. "Just like a sponge, water can flow around a fiber and it can flow through it. That means that results of SP tests can be sensitive to the charged condition of sub-microscopic pore surfaces, not just the outsides of fibers." [12]

Table 5.1. Test materials and chemicals

Name or Group	**Description**	**Manufacturer**
Cotton Fabric	Standardized TIC-400 woven cotton fabrics	Textile Innovators, Inc.
Cationic Agent	CR-2000, 3-chloro-2-hydroxypropyl trimethyl ammonium chloride (CHTAC), 69% solution	Dow Chemical
Anionic Agent	Mono chloroacetic acid, 99%	Acros Organics
Base	Sodium hydroxide, 50% w/w aqueous solution	Fisher Scientific
Negative Titrant	PVSK	Aldrich Co.
Positive Titrant	Poly-DADMAC	Aldrich Co.

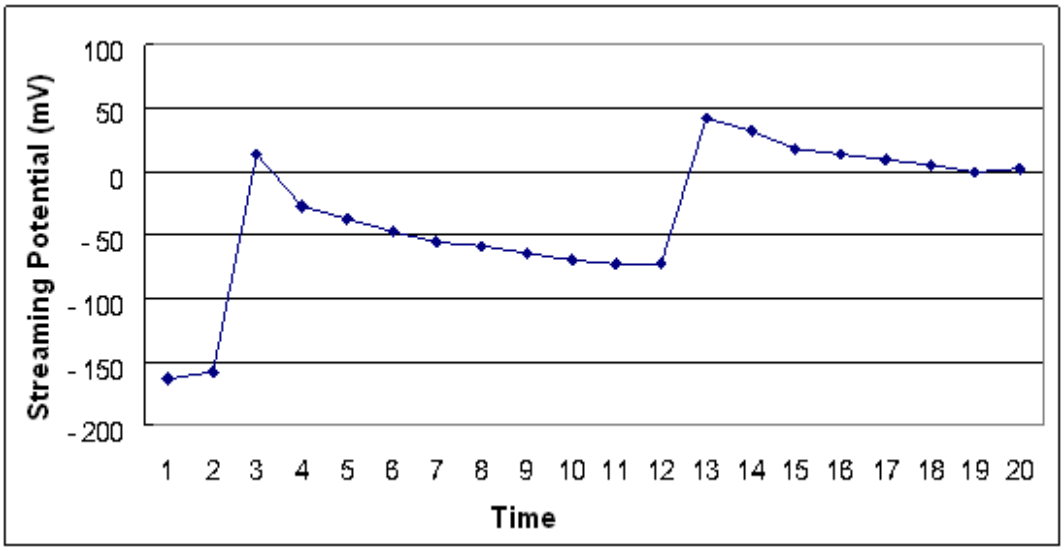

Figure 5.3. Decay of streaming potential with time when adding poly-DADMAC in the 95g/L anionic sample at the second and 12th min.

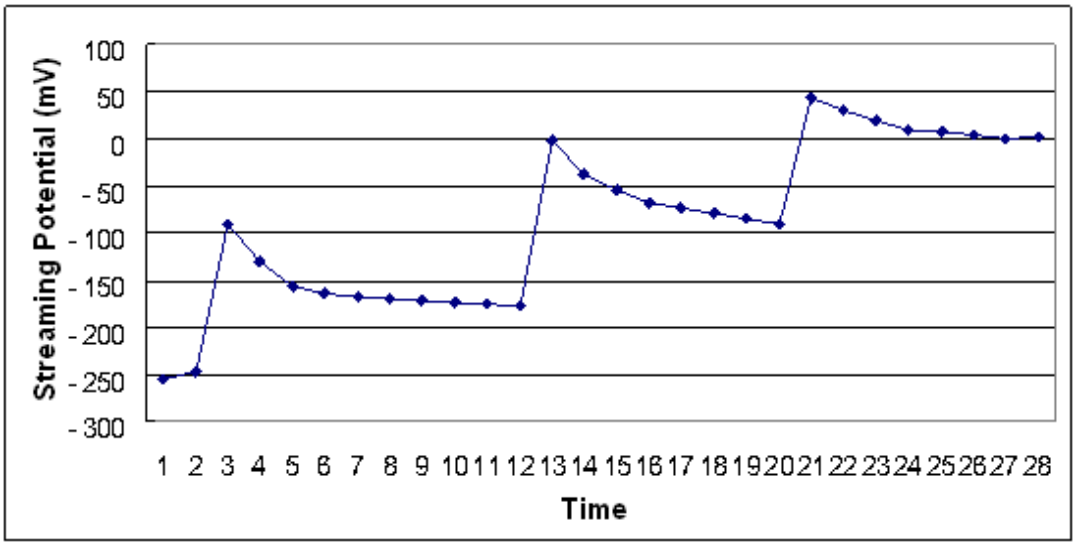

Figure 5.4. Decay of streaming potential with time when adding poly-DADMAC in the 190g/L anionic sample at the 2nd, 12th and 20th min.

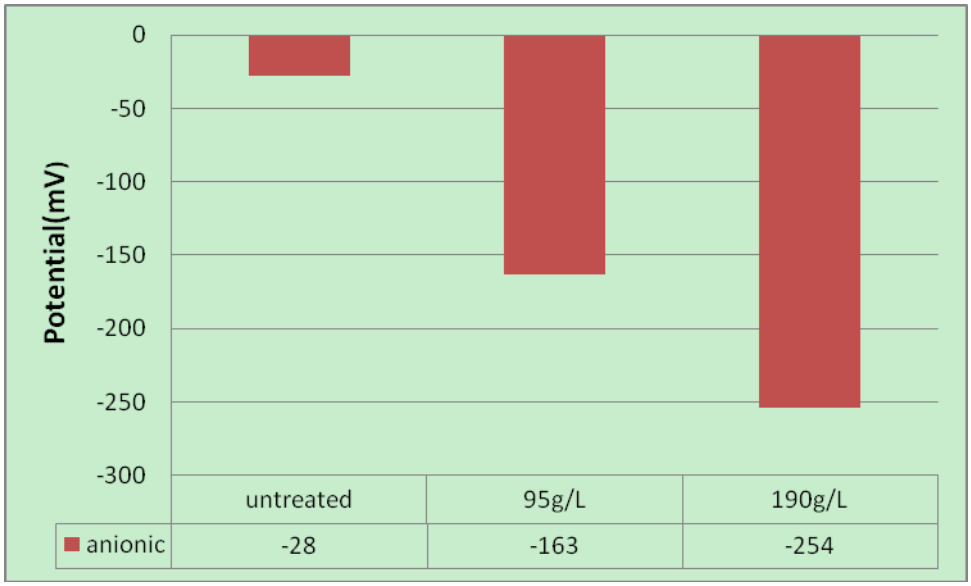

Figure 5.5. The potentials' difference among untreated, 95g/L and 190g/L anionic cotton fibers.

Table 5.2. Surface charge of Anionic Cotton by Different Concentration Treatment

Times	95g/L Treatment (mmol/100g)	190g/L treatment (mmol/100g)
1	15.7	22.43
2	14.95	23.92
3	13.46	20.93
4	14.95	22.43
5	16.44	24.67
Mean	15.1	22.88
STDEV	1.11	1.46

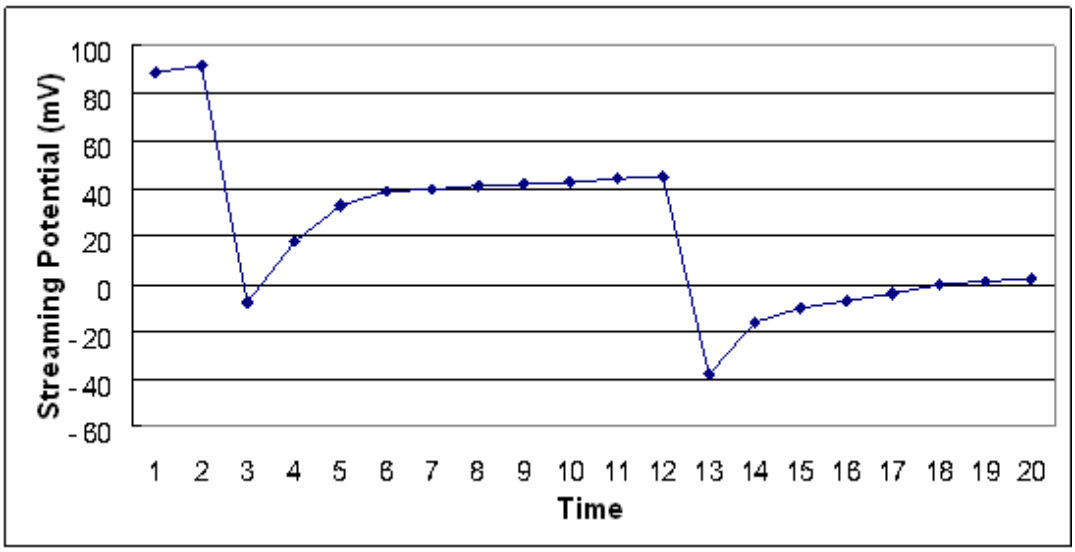

Figure 5.6. Decay of streaming potential with time when adding PVSK in the 188g/L cationic sample at the second and 12th min.

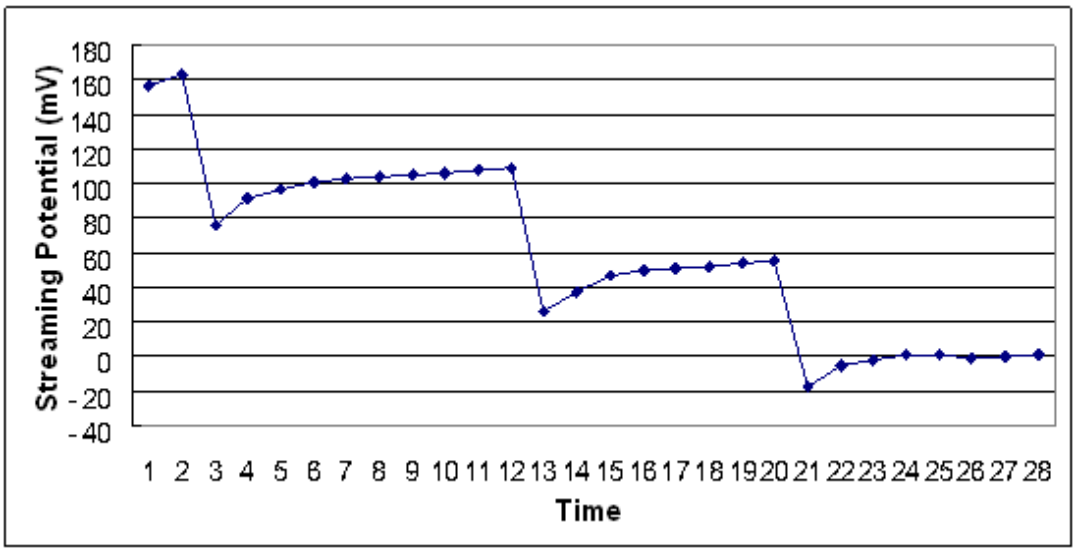

Figure 5.7. Decay of streaming potential with time when adding PVSK in the 376g/L cationic sample at the second and 12th min.

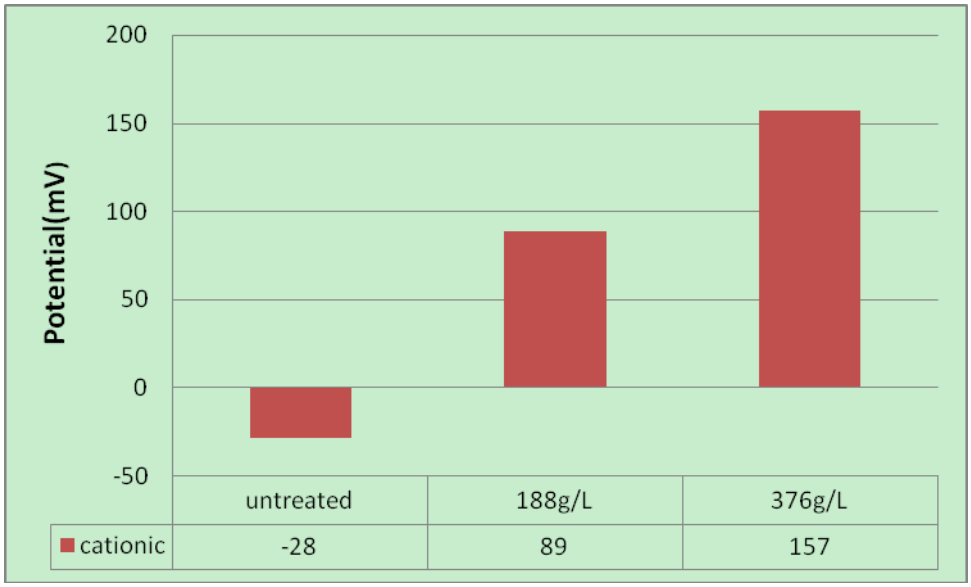

Figure 5.8. The potentials' difference among untreated, 188g/L and 376g/L cationic cotton fibers.

Table 5.3. Surface charge of Cationic Cotton by Different Concentration Treatment

Times	188g/L Treatment (mmol/100g)	376g/L treatment (mmol/100g)
1	11.21	16.82
2	10.09	15.7
3	13.46	17.94
4	11.21	16.82
5	11.21	15.7
Mean	11.44	16.60
STDEV	1.23	0.94

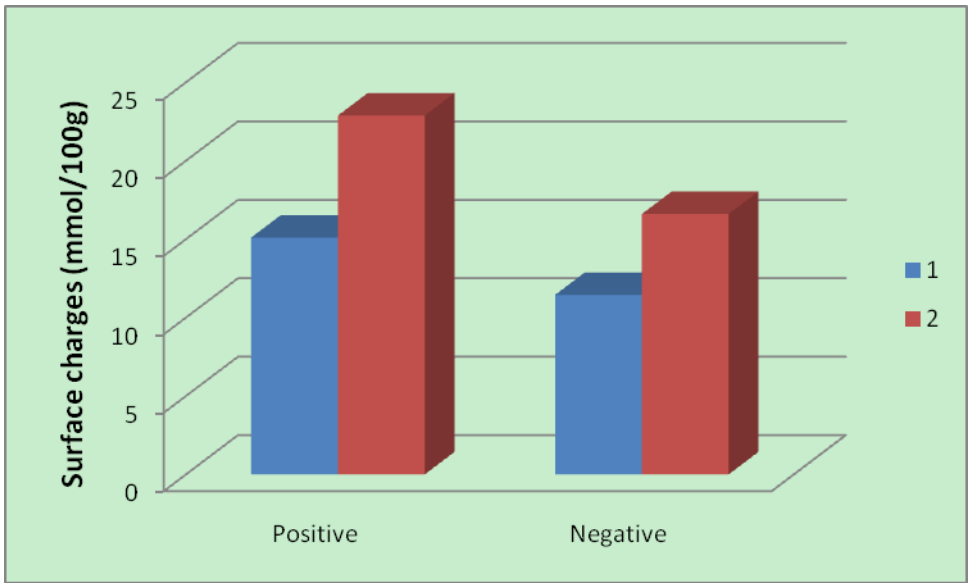

Figure 5.9. Compare the differences of cationic and anionic cotton surface charge between two concentration treatments by streaming potential tests.

1: low concentration

2: high concentration

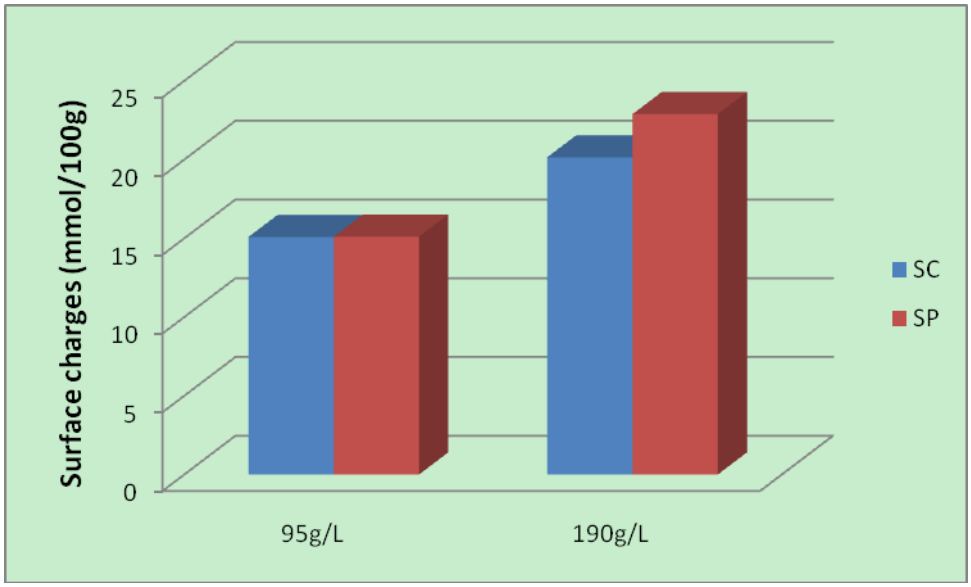

Figure 5.10. Compare the differences of anionic cotton surface charge by two treatments between streaming current and streaming potential tests.

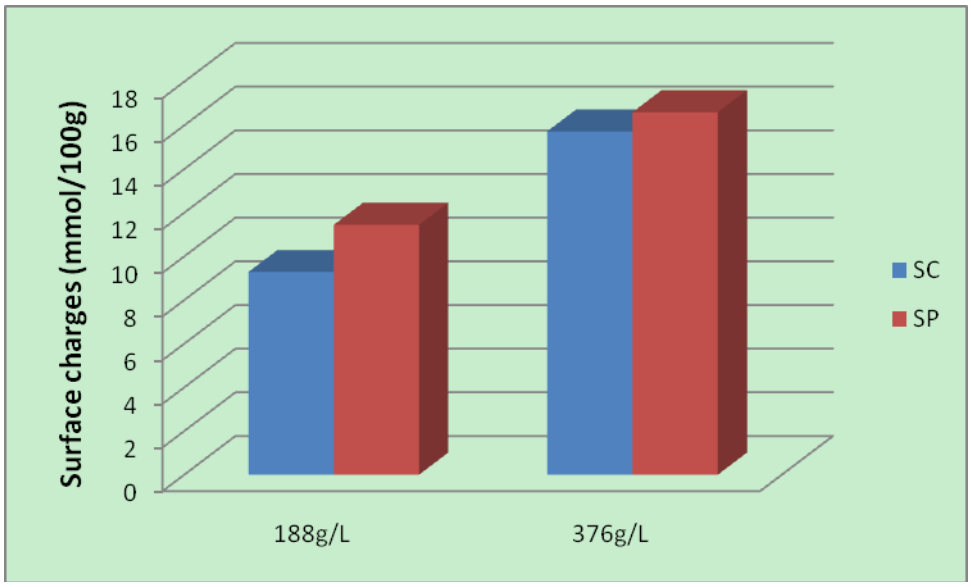

Figure 5.11. Compare the differences of cationic cotton surface charge by two treatments between streaming current and streaming potential tests.

6 LAYER-BY-LAYER POLYELECTROLYTE DEPOSITION ON IONIC FIBER SURFACES (CATIONIC POLYELECTROLYTE INJECTED FIRST)

6.1 Introductions

As introduced in chapter 2, a QCM crystal consists of a thin quartz disc sandwiched between a pair of electrodes. Due to the piezoelectric properties of quartz, it is possible to excite the crystal to oscillation by applying an AC voltage across its electrodes. The resonance frequency (*f*) of the crystal depends on the total oscillating mass of the resonator. When a thin film is attached to the sensor crystal the frequency decreases. If the film is thin and rigid, no or minimum energy dissipation occurs, and the decrease in frequency is proportional to the mass of the film. In order to describe soft adsorbed layers of polymer adsorbing from liquid media, the dissipation value was introduced. QCM-D (Quartz Crystal Microbalance with Dissipation) has the advantage that it can measure the adsorbed amount via Δf and viscoelasticity of adsorbed films via ΔD.

Takeshi et al. [1] focused on electrostatic adsorption of polystyrene particles onto an ultrathin PET film. They quantitatively analyzed the electrostatic adsorption of anionic polystyrene particles on the PET surface by quartz crystal microbalance (QCM) and scanning electron microscopy (SEM) techniques. They studied the effect of the charge density of a particle surface on electrostatic adsorption onto the surface, and the effect of the surface charge of the film on particle adsorption. QCM was used

to calculate the mass of the adsorbed particle according to the frequency shift. Alternate adsorption was performed by using solutions of cationic poly (allylamine hydrochloride) (PAH) and anionic poly (styrene sulfonate) (PSS) each of which contained suitable concentrations of sodium chloride. The chemical structures of PAH and PSS are showed in Figure 6.1.

Recently, Turon et al. [2] studied the enzymatic kinetics of cellulose by using QCM-D. They developed a method to build the cellulose thin film on gold sensors and to monitor the variations of QCM frequency and dissipation of the film to follow the mass and morphological transformations.

To ensure experimental reproducibility and meaningful results, the development of robust cellulose films is of paramount importance. Several techniques have been proposed to create such substrates, the most significants of which involve spin-coating, self-assembly, and Langmuir-Blodgett techniques [3-5].

Surface interface plays an important role in defining the interactions of layer-by-layer adsorption. The interactions between the ionic cellulose film substrate and polyelectrolytes, or counter ionic polyelectrolytes were the focus of our research. Adsorption is a consequence of the balance of the surface energy and the nature of the species involved. In the bulk solution, the conformation of a polymer depends on the chain composition and architecture as well as the chemical environment. At the interface, the conformation also depends on the attraction of polymer segments towards the surface (see Figure 6.2). The “thickness” of a boundary between two

phases, if possible to define, is expected to be extremely narrow. The attraction may involve chemical or physical attraction [6].

In this chapter, earlier investigations were continued involving the use of a piezoelectric sensing technique (QCM-D), which provided a unique way to investigate the adsorption behavior of polymers on cellulose [6-9]. In fact, the mechanical oscillatory nature of QCM-D resonator enabled the measurement of unique properties such as the mass and viscoelasticity of adsorbed polymer films. QCM-D allowed the in-situ and real-time study of interfacial behaviors (including adsorption and desorption) at the nano-scale. It also provided information on the adsorbed mass (from vibration frequency changes) and energy dissipation (related to the conformation of the adsorbed species).

For the study of polyelectrolyte adsorption by QCM-D, the cellulose substrates were prepared by dissolving untreated and ionic cotton and spinning coating on QCM sensors. The ultimate purpose was to achieve insightful information relevant to charge distribution by probing phenomena involved in layer-by-layer deposition of polyelectrolytes on untreated and ionic cellulose substrates.

6.2 Experimental

6.2.1 Materials and Chemicals

The materials and chemicals used in this research were all commercially available and are shown in Table 6.1, along with their descriptions and sources. All chemicals used to manufacture ionic cotton were the same as those presented in

chapters 3 & 4.

All experiments were performed with deionized water produced by an ion-exchange system (Pureflow, Inc.) which was further processed in a Milli-Q® Gradient unit to ensure ultra purification of water to a resistivity greater than 18MΩ. 200ppm aqueous solutions of the polyelectrolytes were made by using sodium chloride (pH 6.9, as background electrolyte).

6.2.2 Ionic Cotton Preparation

Cationic cotton was obtained following the same process described in chapter 3. Fabric samples with the size 12'×15' were soaked in the prepared cationizing solution mixture of CR-2000 and NaOH padded to 100% wet pick-up. The padded samples were then dried at 45^0C for 10 minute, and finally cured at 115^0C for 10 minute in a forced air oven. The cured fabrics were washed with cold water, neutralized with dilute acetic acid (2g/l), washed with cold water again, centrifuged and air-dried.

The anionic cotton was prepared following the same procedure described in chapter 4. Firstly, fabric samples were soaked in 20% NaOH solution for 10 minutes, padded to 100% wet pick-up and dried at 45 °C for 12 minutes. The dried samples had a yellow color. Following, mono chloroacetic acid was neutralized by adding weak base sodium carbonate. The samples from the first step were soaked in aqueous sodium chloroacetate solutions of low level or 1low level concentrations for 5 minute, padded to 100% wet pick-up, cured at 85 °C for 30 minute, washed with water, acidified with 2 g/l acetic acid, washed with water again and then dried in air.

6.2.3 Cellulose Films Preparation

Thin films of untreated and ionic cellulose were used as model substrates. The resonators used in QCM-D consisted of gold-coated AT-cut quartz crystals [3]. The sensors were first cleaned using a mixture of ammonium hydroxide and hydrogen peroxide (Q-Sense Inc., Sweden) followed by UV-ozone plasma treatments. In the plasma treatment, the incident UV light oxidized any spuriously adsorbed organic matter that may have remained on the surface of the sensor and also activated silanol groups required in later coating steps. Cleaned gold sensors were then immersed in a diluted poly (ethylenimine) (PEI) solution before spin-coating. PEI was thus adsorbed from the solution onto the sensor and was used as an anchoring layer between the sensor surface and the cellulose thin film.

Spin coating of the untreated and ionic cellulose solutions on the sensor was then performed to create a uniform, thin film on top of the PEI layer. *N*-methylmorpholine-*N*-oxide (NMMO), which is capable of dissolving cotton fibers, was used to prepare cellulose solutions for spin-coating [9]. In our case, untreated and ionic cotton fibers were cut into very tiny pieces, and then 0.025g of cotton fibers were immersed in a 2.5ml water/NMMO (50% w/w) solution and heated at 115 °C. When the cotton fibers were almost dissolved, 7.5 ml dimethyl sulfoxide (DMSO) was added to adjust the concentration and viscosity of the mixture. Reducing the viscosity allowed the manufacture of thinner films, provided that DMSO was added judiciously to avoid suspension instability [3].

The cellulose solutions were then spin-coated on the sensors at 5000 rpm for 40 seconds (Laurell Technologies model WS-400A-6NPP). The sensors were then removed from the spin-coater and dried in an oven at 80 °C for 2 hours and then soaked in Milli-Q water for at least 4 hours. The cellulose-coated substrates were washed thoroughly with Milli-Q water, dried by nitrogen gas and stored at room temperature in a clean container for future use.

6.2.4 Polyelectrolyte Solution Preparation

DMAPAA (pH 3.6) was used to prepare a cationic polyelectrolyte solution (*cat*), and itaconic acid (pH 4.4) was used to prepare an anionic polyelectrolyte solution (*an*). Both of them were diluted to 200mg/L with 0.1mM sodium chloride solution (pH 6.9), which also acted as background electrolyte. Figure 6.3 illustrates the chemical structures of polyelectrolyte, respectively.

6.2.5 Quartz Crystal Microbalance (QCM) Measurements

Adsorption of polyelectrolyte samples onto the cellulose films was conducted by a Quartz Crystal Microbalance with Dissipation mode, QCM-D300 model (Q-Sense, Gothenburg, Sweden). The temperature in our experiments was controlled within 0.02 °C of the respective set point via a Peltier element that was built in the QCM apparatus. A piezoelectric resonator (quartz) underwent electric polarization due to applied mechanical stresses (piezoelectricity). Resonators consisting of gold-coated AT-cut quartz crystals with a fundamental frequency of 5 MHz were used as sensors. During the measurement, the crystal was mounted in a thermostatic liquid chamber,

which was designed to provide a rapid, non-perturbing exchange of the liquid in contact with one side of the sensor. This system allowed for the measurement of up to 4 harmonics. In this study, the frequency and dissipation responses were recorded at around 15, 25, and 35 MHz, corresponding to the third, fifth and seventh overtones (n = 3, 5, and 7, respectively). For clarity, only the normalized frequency Δf (Δf/n) shifts, , and the dissipation shifts ΔD, for the third overtone (n=3) are presented.

The sensor coated with cellulose film was mounted in the QCM-D equipment with the buffer for 4 hours to allow the cellulose to swell and to reach equilibrium. After running the QCM-D for ten minutes, a constant QCM-D baseline was obtained. Then 1 ml of the polymer solution was injected into the adsorption module at a low rate (0.12ml/min). The frequency and dissipation were monitored until equilibrium was reached. Finally, 3 ml of the buffer solution was used to rinse any loosely bound polyelectrolyte (using the same injection rate). Therefore the net adsorption was accounted for. In this chapter, multilayer self-assembly on cellulose substrates was accomplished by alternating injection of polyelectrolytes: an injection of cationic DMAPAA solution (*cat*) was followed by a subsequent injection of anionic IA solution (*an*). This procedure was repeated as needed to build up polyelectrolyte multilayers.

6.3 Results and Discussion

6.3.1 Thickness of Cellulose Films Manufactured by Spin Coating

Spin coating is a technique used previously to prepare thin cellulose films

because of its efficiency and reproducibility [14-17]. During spin coating, an excessive amount of solution was placed on the substrate, which was then rotated at high speed (usually in the thousands of revolutions per minute), spreading the fluid by centrifugal force. The solvent evaporated simultaneously with rotation. Rotation continues until the desired thickness of the film was achieved. Variables involved in the spin coating process which, influence the thickness and uniformity of the obtained film, included viscosity, concentration, angular frequency of the rotating substrate and operation temperature.

A model which is used to describe the final thickness in term of these factors is the Lawrence's equation which was verified by extensive experimental work [15, 18]:

$$h_f \propto \frac{c_0(\eta_0 D_0)^{1/4}}{\Omega^{1/2}} \qquad (4)$$

Where h_f, final thickness;

c_0, initial polymer concentration;

η_0, initial kinetic viscosity;

D_0, solute diffusivity;

Ω, spinning speed.

From this equation, the final thickness is found to be most sensitive to the initial polymer concentration. The viscosity of solution obviously plays a role also. Oxidizing the polymer at an elevated temperature increased the viscosity of the solution. Based on the model, higher viscosity could lead to an increase thickness of

the thin film. The dependency of thickness to different variables indicates that attention should be paid to the surface preparation in order to keep the same operational conditions and obtain reproducible surfaces.

6.3.2 Adsorption of Polyelectrolytes onto Untreated Cellulose Substrates

The adsorptions of the cationic and anionic polyelectrolytes onto the surface of untreated cellulose film were at the pH conditions of the buffer (pH 6.9). The data plotted in Figure 6.4 presents the frequency change monitored with time, and the change in energy dissipation as recorded by QCM-D. The cationic polyelectrolyte was injected at the 12^{th} minute, leading to an immediate drop in frequency and rise in energy dissipation. These shifts indicated the *cat* adsorbed onto the untreated cellulose surface. Because the untreated cellulose surface has negative charges, as it presents in aqueous condition. These negative charges drive to attract positive charge in *cat* to form the adsorbed polyelectrolyte layer. Such polyelectrolyte adsorption leads to an increase in the mass of the sensor, and therefore a drop of frequency, as showed in Figure 6.4. After rinsing with the buffer, an anionic polyelectrolyte solution was injected. Since this time the outermost layer was positively charged cationic polymers, which attract the anionic polymers in *an*, the data showed that the frequency dropped again. The polyelectrolytes with counter-ions were alternately used for injection in the experiment. Throughout the whole process, a large amount of buffer was used to rinse excessive (loosely adsorbed) polymer from the interface. The buffer was injected into the adsorption chamber at the 15^{th}, 19^{th}, 22^{nd}, 26^{th}, 30^{th} and 37^{th} minute. This process

can also be observed from the changes in frequency and energy dissipation depicted in Figure 6.4.

From Figure 6.5(a), it is clear that the frequency changes in the different adsorption steps. The first injection of *cat* at the 12th minute shifted the frequency 14 Hz. The second turning point was at the 17th minute when *an* was injected, and the frequency descended 23 Hz. All of these phenomena could be attributed to the fact that the untreated cellulose film initially had a negatively charged surface, which could adsorb the positively charged polymer. After the first injection of *cat*, the cationic polyelectrolyte deposited on the untreated cellulose film and formed the first layer. After rinsing, the cellulose film attracted a layer of cationic polyelectrolyte, which further adsorbed the negatively charged polymer when *an* was injected in the sensor.

As shown in Figure 6.5(a), the frequencies were almost the same when the sensor was rinsed with the buffer. Figure 6.5(b) shows that the frequency changes were similar when *cat* was injected for the 1st and 3rd times. At the 4th injection of the anionic polyelectrolyte solution, the frequency change was negative, which is different from the changes after the other injections. These results indicate that the 3rd layer (cationic polyelectrolyte) desorbed from the substrate. At the 5th injection (*cat*), the frequency change was greater than that of the 1st and 3rd injections when the polymer solutions were also cationic. This indicates that the outermost layer had more negative charges than the original substrate or the two layered substrate. When *an* was

injected again after the rinsing, the frequency increased, and the change was greater than at the 4th injection. All of these observations prove that the 3rd layer on the untreated cellulose film was not stable. The desorption happened when *an* was injected onto the three-layered substrate. The negative charges in *an* attracted the outermost layer (3rd layer, with positive charges); while at the same time, the 2nd layer also attracted the 3rd layer due to the reversed charges. The results show that the attracting force between *an* and the 3rd layer were greater than that between the 2nd and the 3rd layers, and therefore lead to the desorption of the 3rd-layer instead of the adsorption of the 4th-layer on the cellulose substrate. The process is shown in Figure 6.6.

The QCM-D results of the untreated cellulose substrate will be compared with the results of the layer-by-layer deposition onto the ionic cellulose substrates in later chapters.

6.3.3 Adsorption of Polyelectrolytes on Cationic Cellulose Substrates

Adsorption studies of polyelectrolytes onto cationic cellulose films were performed at pH 7. The data plotted in Figures 6.7 and 6.9, respectively, represents the frequency changes of two concentrations of cationic cellulose films over time, and the changes in energy dissipation as recorded by QCM-D. These cellulose films were prepared from cotton treated with two concentrations of cationic reagent.

From Figure 6.7, *cat* was first injected at the 9th minute, and the frequency and energy dissipation changed immediately. These changes prove that the cationic

polymer was adsorbed onto the cationic cellulose surface (low level), which means that negative charges exist on the surface to attract the positively charged polymer in *cat*. Though the cationic cellulose surface (low level) bears positive charges due to the cationic treatment, not all hydroxyl groups on the cellulose reacted with the cationic reactant. Some untreated carboxyl groups remained on the cationic cellulose surface, which leads to the adsorption of positively charged polymer. After rinsing, the *an* polymer solution was injected, and the frequency and dissipation changed again. Then, *cat* and *an* were alternately injected into the chamber. Throughout the entire process, a large amount of the buffer was used to rinse excess (loosely adsorbed) polymer from the surface after every injection of the different polyelectrolyte solutions.

As shown in Figure 6.7, the first turning point appeared at the 9^{th} minute, the frequency went down 10 Hz. As discussed in last paragraph, the cationic cellulose film had positive and negative charges on the surface. Therefore, the first frequency change was because the negative charges on the surface attracted the positively charged polymer in *cat*. After rinsing, the second turning point was the 13^{th} minute when the injection solution was changed from *cat* to *an*, and the frequency descended from 30 Hz. The deposition of the anionic polymer on the cationic cellulose film with positively charged polymer (first layer) leads to the second frequency change.

As mentioned in the discussion of the surface charge of cationic cotton fibers in chapter 3, the cotton fibers did not react completely with the cationic reactant, some unreacted hydroxyl groups were still left, due to electrostatic repulsion, reactant

concentration and other reasons. After rinsing, the substrate with adsorbed cationic polymer (first layer) had positive charges on the surface, which attracted the anionic polymer with negative charges when *an* was injected. After the first injection, the cationic cellulose film showed a smaller decrease in the frequency than the untreated cellulose, because the cationic cellulose film had fewer negative charges than the untreated one. The cationic cellulose film had positive charges on the surface, decreasing accordingly the amount of negative charges on the surface. Some hydroxyl groups on the surface were reacted with cationic reactant. Meanwhile, due to the electrostatic repulsion, it is difficult to access the surface characteristics of the cationic polymer adsorbed onto the cationic cellulose.

In Figure 6.8 (b), the second frequency change is almost three times that of the first, which is much larger than the untreated cellulose film (shown in Figure 6.5). Although the frequency of the first cationic polymer deposition on the cationic cellulose film (low level) was smaller than on the untreated one, the frequency of the second anionic polymer deposition on the cationic cellulose film (low level) was larger than on the untreated one. For the cationic cellulose film, the anionic polymer in *an* was attracted by the positive charges of the first layer on the surface and the positive charges of the cationic cellulose film produced from the cationic treatment. Both of them on the cationic cellulose film surface adsorbed more anionic polymer than the untreated cellulose film. Meanwhile, the molecular weight of DMAPAA is smaller than IA. Therefore, even the same mole adsorption of anionic polymer on

untreated cellulose film will yield higher frequency variation than the adsorption of cationic polymer on the untreated substrate.

Figure 6.9 shows the cellulose film prepared from cationic cotton (high level), when the cationic solution was injected at the 11th minute. The frequency dropped immediately when the *cat* flowed into the sensor. This drop indicates that the cationic polyelectrolyte was adsorbed onto the cationic cellulose surface (high level). This process is similar to what observed for cationic cellulose surface (low level). As the polymer solution with oppositely charged ions was injected, the frequency descended again. The counter-ion polyelectrolytes were injected alternately into the sensor. A large amount of buffer was also used at the 15th, 21st, 25th, 31st, 35th, and 42nd minutes to rinse the sensor.

When the cationic solution was injected, the first turning point appeared at the 11th minute, and the frequency went down 6 Hz. After rinsing, the *cat* was replaced with the anionic solution, and the second turning point was at the 19th minute, and the frequency descended from 23 Hz. The cationic polyelectrolyte solution was deposited on the cationic cellulose film with higher concentration. After rinsing, the anionic solution was injected and the second layer adsorption occurred. All the phenomena are similar to those of the low level cationic cellulose film. The obvious difference is that the first frequency change of the high level cationic cellulose film is smaller than that of the low level cationic cellulose film. This proves the high level cationic cellulose film has less negative charges to adsorb cationic solution than the low level

cationic cellulose. In other words, the high level cationic cellulose has more positive charges on the surface because the higher concentration of treatment leads to greater positive charges on the surface. These positive charges repel the positive charges in the cationic solution. Meanwhile, the first frequency change is smaller than the second one. The second frequency change of the high level cationic cellulose film is also smaller than that of the low level cationic cellulose film. This is because the high level cationic cellulose film adsorbed less cationic polymer than the low level cationic cellulose film. The low level cationic cellulose film with one layer has more positive charges outside, which will absorb more anionic polymer.

Figures 6.6 and 6.8 show clearly how the frequency changes by different steps. In Figure 6.10(a), the frequency values were almost the same each time the sensor was rinsed with the buffer. As shown in Figure 6.10(b), the first frequency change of the high level cationic cellulose is smaller compared to the untreated or low level cationic cellulose films. More negative charges on the surface lead to greater frequency changes, and the first layer adsorption affects the second frequency change. The higher the first frequency change, the higher the second frequency change, which means that the second layer deposition partly depends on the first adsorption layer. As discussed before, at the 4^{th} injection, the same deposition occurred.

By such frequency shifts due to sequential adsorptions of cationic and anionic polyelectrolytes, multilayers built up on cationic cellulose film are shown in Figure 6.11. It is found the trend of three curves is similar. First adsorption of positively

charged polymer occurred on untreated and the two level cationic cellulose films. The adsorbed mass on different cellulose film increases with the increase of negative charges on the surface. Growth of the polyelectrolyte multilayers in first three steps is linear.

6.3.4 Adsorption of Polyelectrolytes on Anionic Cellulose Substrates

Studies of polyelectrolyte adsorption on anionic cellulose surfaces with treatments of different concentrations were performed under pH 7 conditions. Two cellulose films were prepared from the anionic cotton with low level and high level concentration treatments. The data plotted in Figures 6.12 and 6.14 represents the frequency changes of two level anionic cellulose films monitored with time, and the changes in energy dissipation as recorded by QCM-D.

Figure 6.12 shows us that *cat* was first injected into the sensor at the 5^{th} minute. The frequency immediately dropped. This decrease indicates that cationic polymer deposition occurred on the low level anionic cellulose surface. After rinsing, the oppositely ionic solution-*an* was injected next, the frequency decreased again. Polymer solutions containing oppositely charged ions were alternately injected into the sensor, and a large amount of buffer was used at the 7^{th}, 13^{th}, 15^{th}, 19^{th}, 22^{nd} and 27^{th} minutes to rinse excess (loosely adsorbed) polymer from the interface.

For the low level anionic cellulose film, the first turning point appeared at the 5^{th} minute, the frequency went down 21 Hz. After rinsing, the injection was changed to *an*, and the second turning point was observed in the 9^{th} minute when the frequency

decreased 29 Hz. The first frequency change happened on the low level anionic cellulose film was greater than that for the cationic and untreated cellulose films. The reason is that the low level anionic cellulose film has more negative charges on the surface than untreated and cationic cellulose due to the anionic reaction. These negative charges on the surface attracted more cationic polymers, and this adsorption make the frequency change. After rinsing, the low level anionic cellulose film with one adsorption layer of positively charged polymer, which attracted the anionic polymer in *an*, leads to the second frequency change. Thus, the second layer is deposited.

Figure 6.13 clearly shows how the frequency changes for the low level anionic cellulose film by different injection steps. As shown in Figure 6.12 (a), the frequency values were almost the same when the sensor was rinsed with the buffer each time. In Figure6.12 (b), the first frequency change of the low level anionic cellulose was bigger than that for the untreated one, which leads to a difference in the second frequency change. The higher the first frequency change is, the higher the second one will also be; which means that the second layer deposition partly depends on the first adsorption layer. At the 4^{th} injection, the frequency change is negative when the injection was *an*. This indicates there were some polyelectrolyte complexes desorbed from the outermost substrate, which had three layers of ionic polymers. This phenomenon also occurred on the untreated and cationic cellulose film. At the 5^{th} injection (*cat*), the frequency change was similar to the 3^{rd} injection for the cationic

polymer solution, but less than that of the 1st injection (*cat*). The deposition of latter layers mostly depends on the outermost layer, but not on the substrate. When *an* was injected again after the rinse, the frequency increased more than the 4th injection. All these results prove that the third layer (cationic polymers) on the anionic cellulose film is not stable. Desorption will occur when *an* is injected onto the substrate with three layers. This may be due to the following reason: on the one hand, the negatively charged polymers in *an* attracted the positive charges on the outermost surface; on the other hand, the positive charges on the substrate attracted the anionic polymers in *an*; the former force is greater than the latter one, due to the polymer adsorption layer being soft and unstable, therefore, desorption rather than adsorption occurs on the anionic cellulose film with three polyelectrolyte layers on the surface.

In Figure 6.14, *cat* was injected into the sensor at the 8th minute when the substrate was the high level anionic cellulose film. The frequency immediately dropped too. This change proves that the cationic polymer is adsorbed onto the high level anionic cellulose film. This process is similar to what happened on all tested cellulose film. When the oppositely charged ionic solution was injected, the frequency had a drop again. Then the counter-ion solutions were alternately injected into the sensor. Meanwhile a large amount of buffer was also used at the 10th, 22nd, 31st, 41st, 50th, and 58th minutes for rinsing loosely adsorbed polymer on the surface.

For the high level anionic cellulose film, the first turning point appeared at the 11th minute when *cat* was injected, and the frequency decreased 30 Hz. After rinsing,

the injection was replaced with *an*, and the second turning point was at the 15th minute, when the frequency dropped 15 Hz. When the first injection was *cat*, the cationic polymer was deposited on the high level anionic cellulose film due to the negative charges on the surface. At the second injection (*an*), due to the first adsorption, the high level anionic cellulose film had positively charged polymer on the outermost to absorb the anionic polymer in *an*. All of these phenomena are the similar to that of the low level anionic cellulose film. The only difference is that the first frequency drop for the high level anionic cellulose film is larger than for the low level anionic cellulose film. According to the frequency change indicates the adsorption of ionic polymers on the surface, this difference between two anionic cellulose films states that the high level anionic cellulose film has more negative charges on the surface to absorb the cationic polymer compared to the low level anionic cellulose film. The higher reagent concentration leads to the higher negative charges on the surface. Therefore, in all cellulose films, the substrate with more negative charges can attract more cationic polyelectrolytes.

Figure 6.15 shows the frequency changes by different injection steps for the high level anionic cellulose film. As mentioned before, in Figure 6.15(a), the frequency values were almost the same each time the sensor was rinsed with the buffer. As shown in Figure6.15 (b), the first layer adsorption affects the second frequency change. The greater the first frequency change, the greater second one is. The deposition of each layer partly depends on the outermost layer. For the high level

anionic cellulose film, the first frequency of it is greater than that of the low level anionic cellulose film. Correspondingly, the second frequency change of it is greater than that of the low level anionic cellulose film. The increase of positive charges on the outermost surface increases the anionic polymer adsorption. The frequency change in the QCM-D depends on the adsorption of mass. For cationic and anionic polymers, the frequency change also depends on their molecular weight if number of moles of adsorption is fixed. Therefore, the anionic polymer adsorption among all tested celluloses films is greater than the cationic polymer adsorption due to the molecule weight of IA being greater than DMAPAA. At the 4th injection, desorption of cationic polymer occurred for all cellulose film substrates, which means that it is not possible to obtain 4 layers under current experimental conditions.

By such frequency shifts due to sequential adsorptions of cationic and anionic polyelectrolytes, multilayers built up on anionic cellulose film are shown in Figure 6.16. It is also found the trend of three curves is similar. First adsorption of positively charged polymer occurred on untreated and the two level anionic cellulose films. Growth of the polyelectrolyte multilayers in first three steps is linear.

6.3.5 Comparison of Adsorbed Mass and Thickness onto Different Substrates

For rigid, ultrathin, and evenly distributed adsorbed layers, the Sauerbrey equation successfully describes the proportional relationship between the adsorbed mass (Δm) and the shift of the QCM crystals' resonance frequency (Δf). Under these conditions, the dissipation value is constant. It doesn't change with time or with

increased adsorbed mass. On the other hand, if the adsorbed material exhibits a viscoelastic behavior, such as for layers of proteins, substantial deviations from the Sauerbrey equation can occur.

Generally, soft adsorption layers dissipate more energy and thus are of higher dissipation value. From this point of view, dissipation value is an indicator of the conformation of the adsorption layers. This is the fundamental basis of the QCM-D technique.

A practical QCM-D system records the signals of the fundamental frequency (5 MHz) and overtones (e.g. 15, 25 and 35 MHz). Each overtone has its own detecting range in thickness. This enables it to measure non-uniform adsorption layers. Theoretical work was done by Voinova and coworkers [19]. A general equation was derived to describe the dynamics of two-layer viscoelastic polymer materials of arbitrary thickness deposited on solid (quartz) surfaces in a fluid environment.

$$\Delta f \approx -\frac{1}{\pi\rho_0 h_0}\left\{\frac{\eta_3}{\delta_3}+\sum_{j=1,2}\left[h_j\rho_j\omega-2h_j\left(\frac{\eta_3}{\delta_3}\right)^2\frac{\eta_j\omega^2}{\mu_j^2+\omega^2\eta_j^2}\right]\right\}$$

$$\Delta D \approx \frac{1}{2\pi f\rho_0 h_0}\left\{\frac{\eta_3}{\delta_3}+\sum_{j=1,2}\left[2h_j\left(\frac{\eta_3}{\delta_3}\right)^2\frac{\mu_j\omega}{\mu_j^2+\omega^2\eta_j^2}\right]\right\} \quad (5)$$

Where: ρ stands for density;

h stands for thickness;

η stands for viscosity;

δ stands for the viscous penetration depth.

The subscripts 0, 1, 2 and 3 denote quartz crystal, layer 1, layer 2 and the bulk solution respectively. From this model, the shift of the quartz resonance frequency and the shift of the dissipation factor strongly depend on the viscous loading of the adsorbed layers and on the shear storage and loss moduli of the layers. These results can be readily applied to quartz crystal acoustical measurements of viscoelasticity polymers, which conserve their shape under shear deformation and do not flow, and also for layered structures such as protein films adsorbed from solution onto the surface of self-assembled monolayers. By measuring at multiple frequencies and applying this model, which has been incorporated in Q-Sense software QTools ™, the adhering film can be characterized in detail: viscosity, elasticity and correct thickness may be extracted even for soft films when certain assumptions are made.

Figures 6.17 to 6.21 show the areal mass and thickness of each layer on different cellulose substrates. These results are based on Voinova's theory and calculated by QTools ™. According to the frequency change of different cellulose film at the first *cat* injection, the adsorbed mass of first layer could be calculated. Figure 6.23 and 6.24 compare the areal mass of first and second layers for different cellulose films. The first layer is built after the adsorption of cationic polymer -DMAPAA. The maximum adsorption mass was for the high level anionic cellulose film, and the minimum adsorption mass was for the high level cationic cellulose film. The anionic cellulose films have the most negative charges on the surface complex with the

cationic polymer. Thus its areal mass was the largest. On the other hand, the high level cationic cellulose film had the fewest negative charges on the surface due to the treatment of higher cationic reactant concentration. Its areal mass was the lowest. The adsorbed mass increased with increasing negative charges on the cellulose surface.

The second layer was built after adsorption of the anionic polymer. The areal mass of the second layer on different surfaces decreased with decreasing the negative charges on the cellulose films, except the low level cationic cellulose films. The adsorption mass for the high level anionic cellulose film was the largest. For the high level cationic cellulose film it was the least because the anionic cellulose film of higher concentration had the most negative charges on the surface, which adsorbed the most cationic polymers on the surface. The higher cationic reactant concentration leads to the greater positive charges on the cellulose films. The high level cationic cellulose film had the least negative charges on the surface and the first adsorption mass was also the lowest. Although the second adsorption not only depended on the first layer but also on the original surface, the positive charges on its outermost surface were still less than other substrates.

For the low level cationic cellulose film, the surface had positive charges, but the amount of these positive charges was less than those on the high level cationic cellulose film. In the other words, the negative charges on the surface of the low level cationic cellulose film were greater than those of the high level cationic cellulose film. Therefore adsorption of the first layer on the low level cationic cellulose film was

greater than on the high level cationic cellulose film; and less than on the untreated one. The second layer on the low level cationic cellulose film depends on the substrate and the first layer. Thus its mass was larger than that for the untreated and the high level cationic cellulose film. How the first and second layers deposited on different cellulose films are illustrated in Figure 6.25.

Although to the second layer, the high level anionic cellulose adsorbed the most anionic polyelectrolytes, the difference of the second layer among all substrates was less compared to the first adsorption. This is because adsorption of the first layer only depended on the substrate, but the adsorption of the second layer depended on the substrates as well as the first layers.

6.4 Conclusion

Adsorption onto untreated and charged cellulose films for two simple polyelectrolytes (anionic and cationic) were measured by using the QCM-D technique. It was found that the charge properties of the substrates and the adsorbing polymer were important in the adsorption mechanism (extent and conformation). The adsorbed polyelectrolytes tend to form multiple, dissipative layers. The further the layer is away from the substrate, the softer and looser it will be. Surfaces of low charge density adsorbed less polyelectrolyte. Adsorption of the first layer depended on the substrate, while adsorption of the second layer depended on the substrate and the production first layer. Overall, the results presented in this chapter allow a better understanding of polyelectrolyte adsorption and reveals that the extension of adsorption and

conformation of the adsorbed species is a result of the charge properties of surfaces.

6.5 Reference

1. Takeshi Serizawa, Satoko Kamimura and Mitsuru Akashi, Electrostatic adsorption of polystyrene particles with different surface charge onto the surface of an ultrathin polymer film, *Colloids and Surfaces A: Physicochemical and Engineering Aspects* **164**: 237–245 (2000)

2. Xavier Turon, Orlando J. Rojas, Randall S. Deinhammer, Enzymatic kinetics of cellulose hydrolysis: a QCM-D study, *Langmuir*, **24** (8): 3880 -3887. (2008)

3. Gunnars, S.; Wagberg, L.; Stuart, M. A. C. Model Films of Cellulose: I. Method Development and Initial Results. *Cellulose*, **9**, pp: 239-249 (2002).

4. Kontturi, E.; Thune, P. C.; Niemantsverdriet, J. W. Novel Method for Preparing Cellulose Model Surfaces by Spin Coating. *Polymer*, **44**, pp: 3621- 3625 (2003).

5. Osterberg, M.; Claesson, P. M. Interactions between Cellulose Surfaces: Effect of Solution pH. *J. Adhesion Sci. Technol.*, **14**, 603-618 (2000).

6. Edvardsson, M.; Rodahl, M.; Kasemo, B.; Hook, F., A dual-frequency QCM-D setup operating at elevated oscillation amplitudes. *Analytical Chemistry,* **77**, (15), pp: 4918-4926 (2005).

7. Marx, K. A.; Zhou, T.; Sarma, R., Quartz crystal microbalance measurement of selfassembled micellar tubules of the amphiphilic decyl ester of D-tyrosine and their enzymatic polymerization. *Biotechnology Progress* **15**, (3), pp: 522-528 (1999).

8. Rodahl, M.; Kasemo, B., Frequency and dissipation-factor responses to localized liquid deposits on a QCM electrode. *Sensors and Actuators B-Chemical*, **37**, (1-2), pp: 111-116 (1996).

9. Rodahl, M.; Kasemo, B., On the measurement of thin liquid overlayers with the quartzcrystal microbalance. *Sensors and Actuators a-Physical*, **54**, (1-3), pp: 448-456 (1996).

10. Rosenau, T.; Potthast, A.; Sixta, H.; Kosma, P. The Chemistry of Side Reactions and Byproduct Formation in the System NMMO/Cellulose (Lyocell Process), *Prog. Polym. Sci.*, **26**, pp: 1763-1837 (2001).

11. Rodahl, M.; Hook, F.; Fredriksson, C.; Keller, C. A.; Krozer, A.; Brzezinski, P.; Voinova, M.; Kasemo, B. Quartz-Crystal Microbalance Setup for Frequency and *q*-Factor Measurements in Gaseous and Liquid Environments. *Re*V. *Sci. Instrum.*, **66**, pp: 3924-3930 (1995).

12. Stockbridge, C. D. Effect of Hydrostatic Pressure on Rotated Y-Cut Quartz Crystal Resonators. *Vac. Microbalance Tech.*, **5**, pp: 179-191 (1966).

13. Rodahl, M.; Kasemo, B. On the Measurement of Thin Liquid Overlayers with the Quartz-Crystal Microbalance, *Sens. Actuators, A*, **54**, pp: 448-456 (1996).

14. Kontturi, E.; Johansson, L. S.; Kontturi, K. S.; Ahonen, P.; Thune, P. C.; Laine, J., Cellulose nanocrystal submonolayers by spin coating. *Langmuir*, **23**, (19), pp: 9674-9680 (2007).

15. Lawrence, C. J., The Mechanics of Spin Coating of Polymer-Films, *Phys Fluids*, **31**, (10), 2786-2795(1988).

16. Levinson, W. A.; Arnold, A.; Dehodgins, O., Spin-Coating Behavior of Polyimide Precursor Solutions. *Polym Eng Sci,* **33**, (15), 980-988 (1993).

17. Meyerhofer, D., Characteristics of Resist Films Produced by Spinning. *J Appl Phys*, **49**, (7), 3993-3997 (1978).

18. Sczech, R.; Riegler, H., Molecularly smooth cellulose surfaces for adhesion studies. *J Colloid Interf Sci*, **301**, (2), 376-385 (2006).

19. Voinova, M. V.; Rodahl, M.; Jonson, M.; Kasemo, B., Viscoelastic acoustic response of layered polymer films at fluid-solid interfaces: Continuum mechanics approach. *Physica Scripta*, **59**, (5), 391-396 (1999).

20. Junlong, Song. Ph.D. Thesis *Adsorption of Amphoteric and Nonionic Polymers on Model Thin Films* (North Carolina State University, Raleigh, NC, 2008)

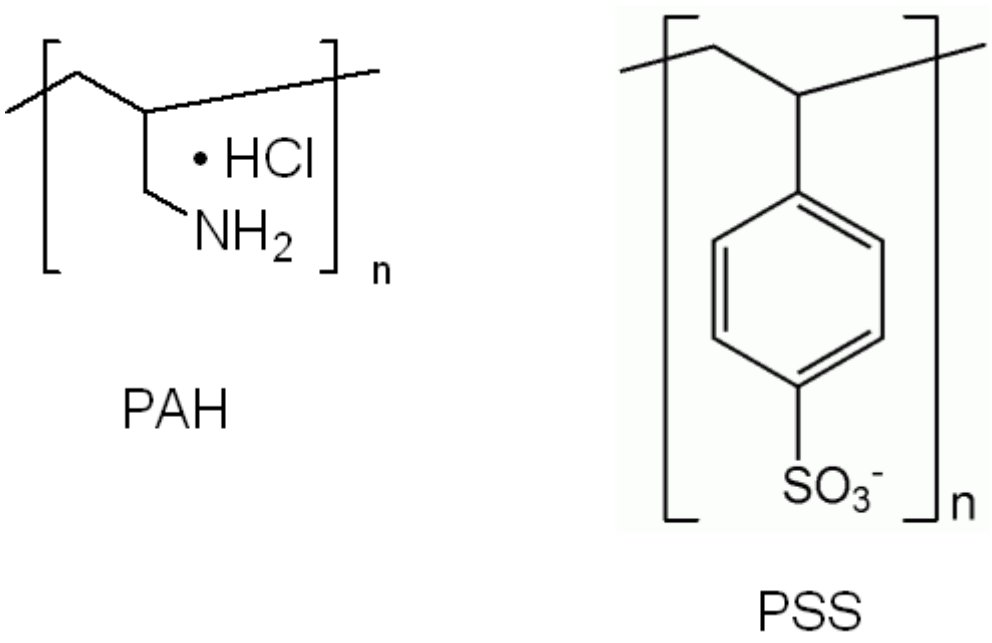

Figure 6.1. The chemical structures of PAH and PSS

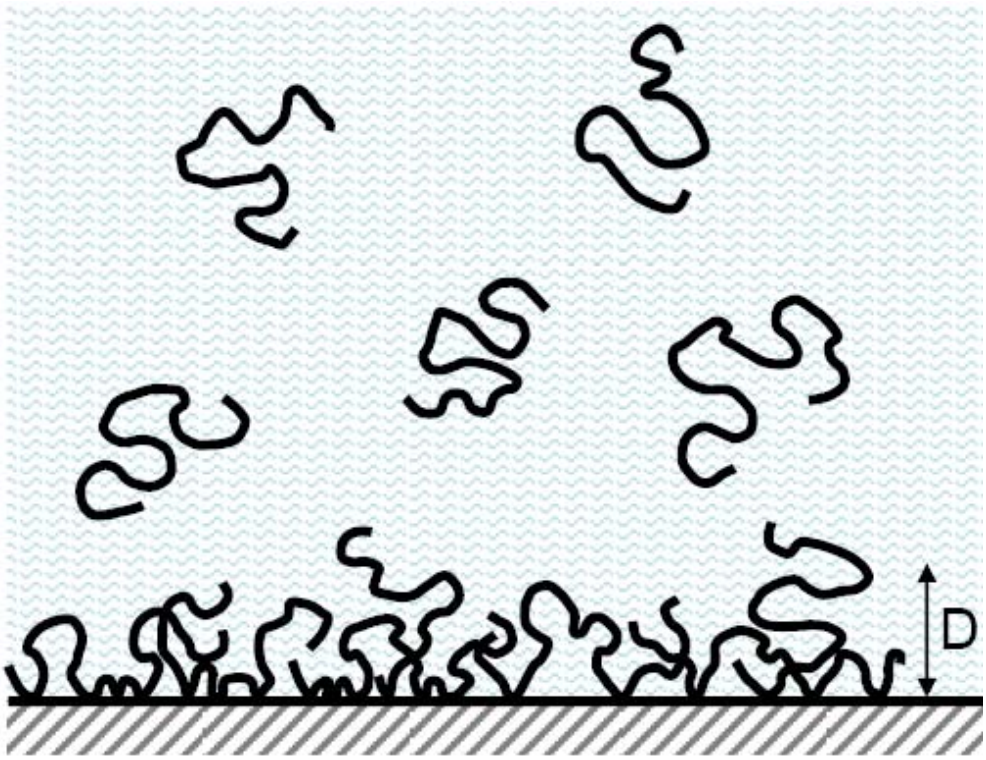

Figure 6.2. Polymer adsorption onto surfaces from solution, D is the thickness of adsorbed polymer layer. [20]

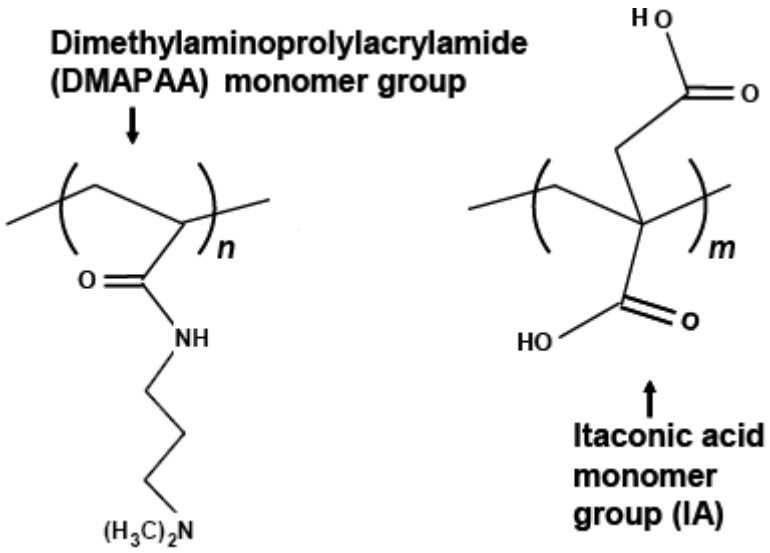

Figure 6.3. The chemical structures of cationic and anionic polyelectrolytes.

Table 6.1. Test materials and chemicals

Name or Group	**Description**	**Manufacturer**
Cotton Fabric	Standardized TIC-400 woven cotton fabrics	Textile Innovators, Inc.
Cationic Polyelectrolyte	DMAPAA, N, N-dimethyl aminopropyl acrylamide (wt%=15%)	Harima Chemicals, Inc.
Anionic Polyelectrolyte	IA, Itaconic acid (wt%=15%)	Harima Chemicals, Inc.
Cleaning Chemicals	50% Ammonium hydroxide 30% Hydrogen peroxide	LabChem Inc.
	DMSO, Dimethyl sulfoxide	Fisher Scientific
	NMMO, 50%*N*-methylmorpholine-*N*-oxide	Sigma-Aldrich Inc.
	PEI, Poly (ethylenimine)	BASF

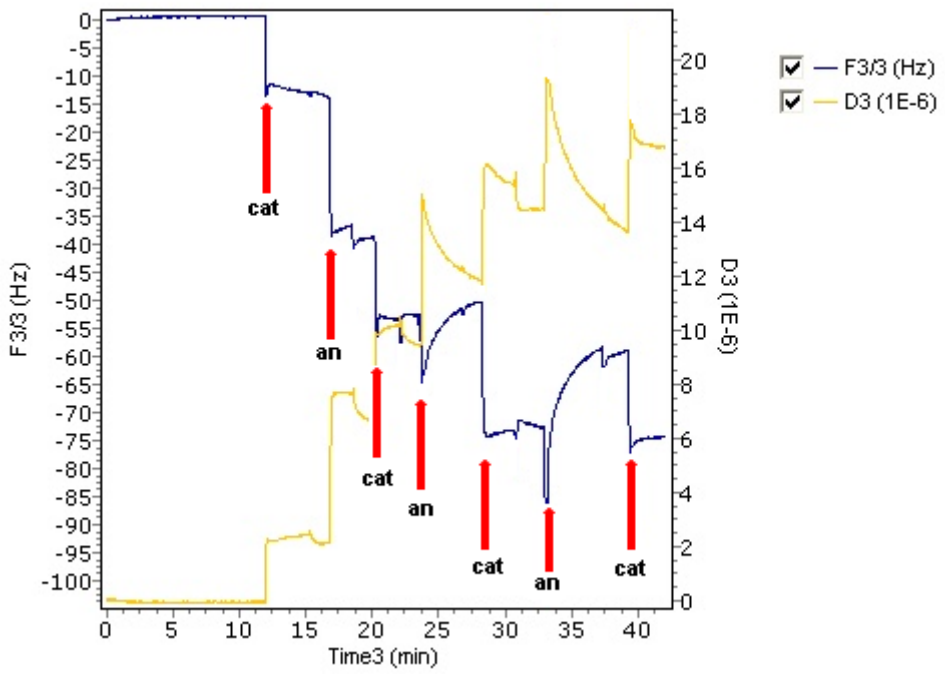

Figure 6.4. Frequency and Energy dissipation change curves for polyelectrolytes adsorbed on untreated cellulose substrates. Cationic polyelectrolyte injected first.

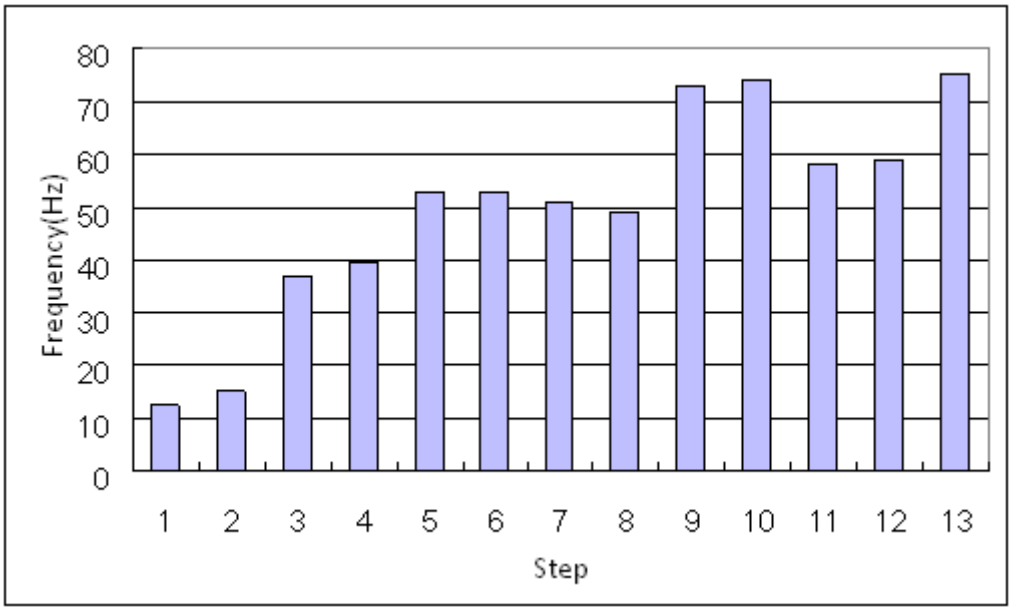

(a)

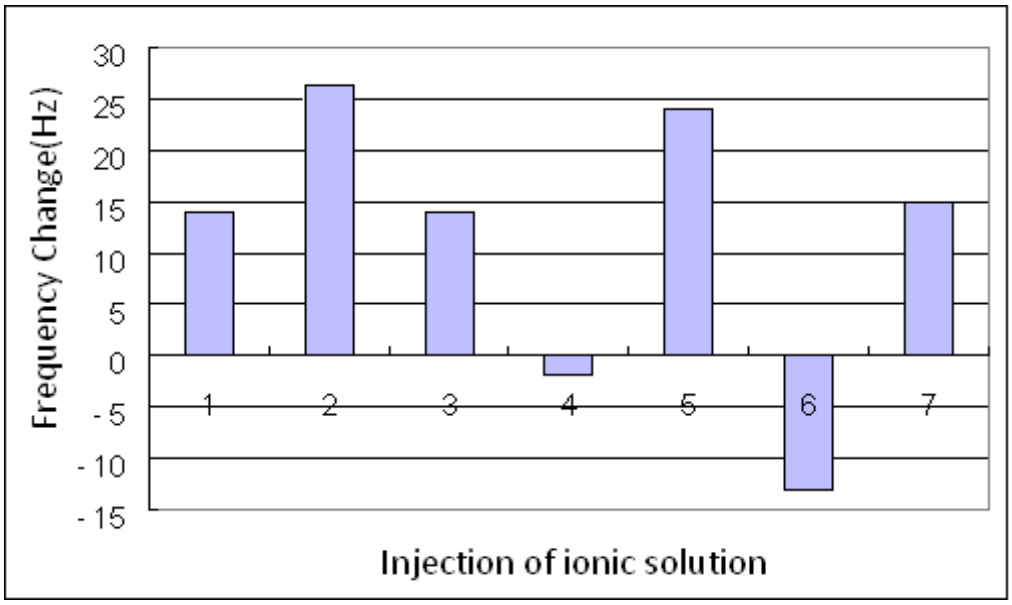

(b)

Figure 6.5. Untreated Cellulose: (a) Frequency values in each injection step; even numbers on x axis represent injecting buffer, step 1, 5, 9, 13 represent injecting cationic solution and step 3, 7, 11 represent injecting anionic solution; (b) Frequency change with the conversion of ionic solution; even numbers on x axis represent injecting anionic solution and odd numbers represent injecting cationic solution.

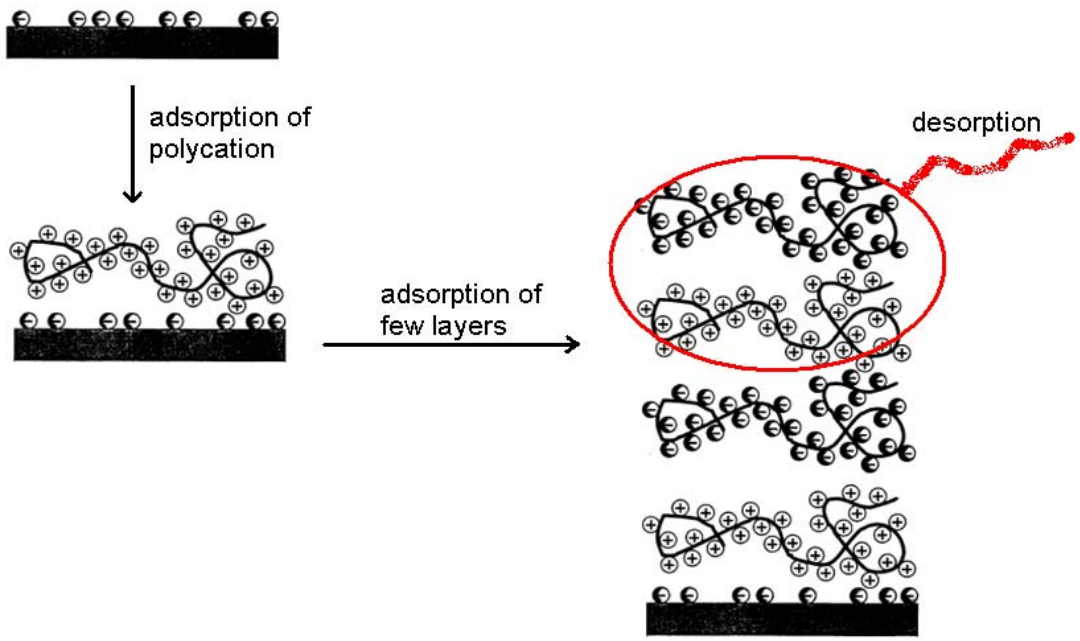

Figure 6.6. The hypothesis of polyelectrolyte adsorption on the untreated cellulose film after few layers deposition.

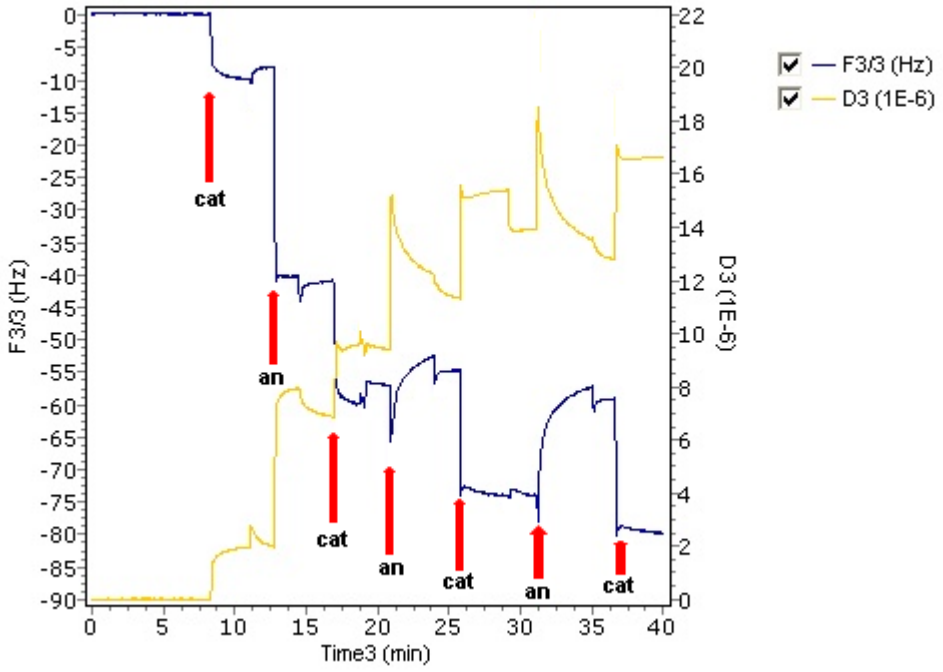

Figure 6.7. Frequency and Energy dissipation change curves for polyelectrolytes adsorbed on cationic cellulose substrates with low level treatment. Cationic polyelectrolyte injected first.

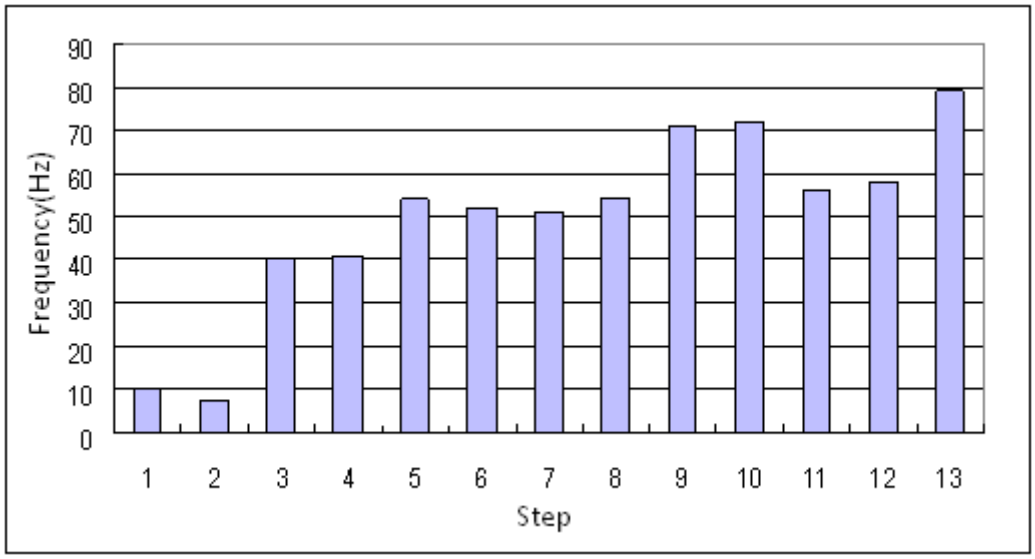

(a)

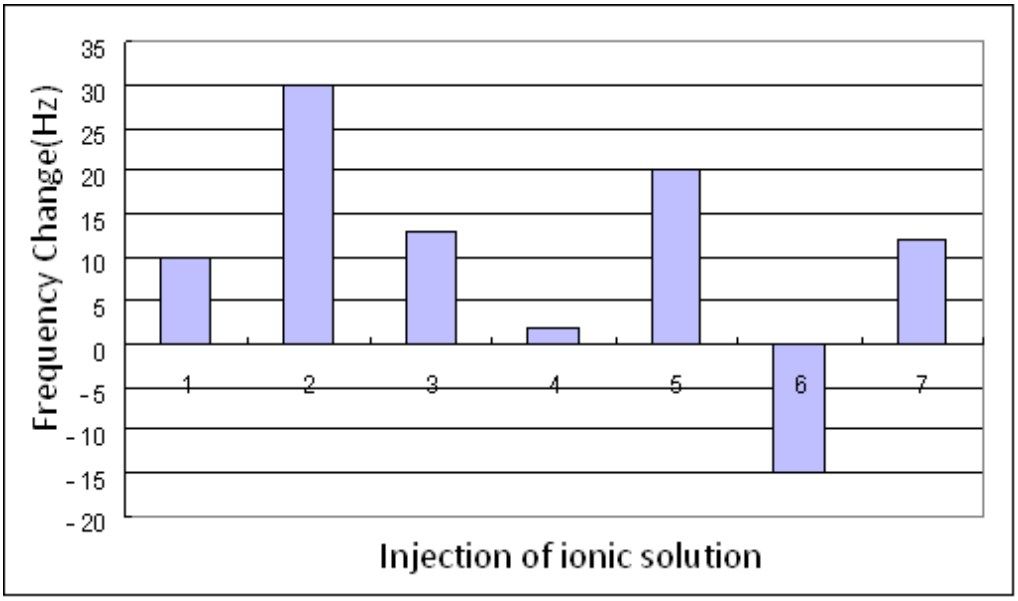

(b)

Figure 6.8. low level Cationic Cellulose: (a) Frequency values in each injection step; even numbers on x axis represent injecting buffer every time, step 1, 5, 9, 13 represent injecting cationic solution and step 3, 7, 11 represent injecting anionic solution; (b) Frequency change with the conversion of ionic solution; even numbers on x axis represent injecting anionic solution and odd numbers represent injecting cationic solution.

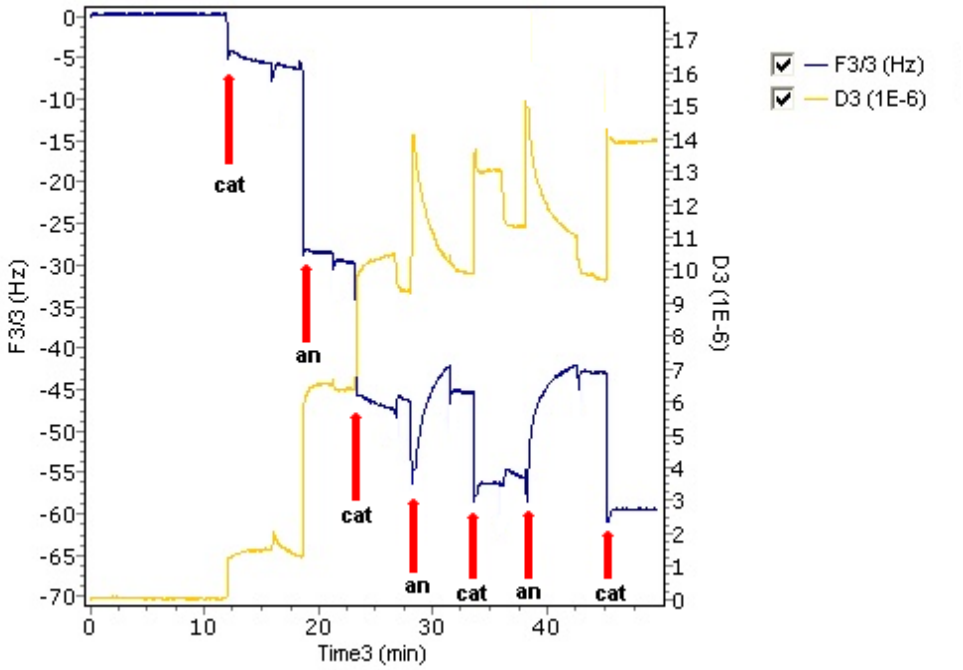

Figure 6.9. Frequency and Energy dissipation change curves for polyelectrolytes adsorbed on cationic cellulose substrates with high level treatment. Cationic polyelectrolyte injects first.

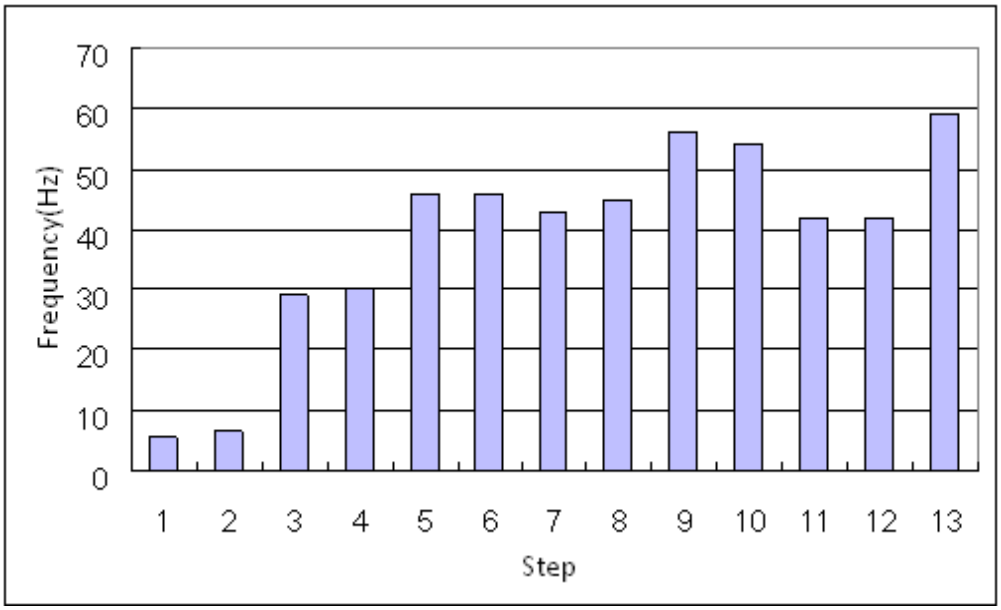

(a)

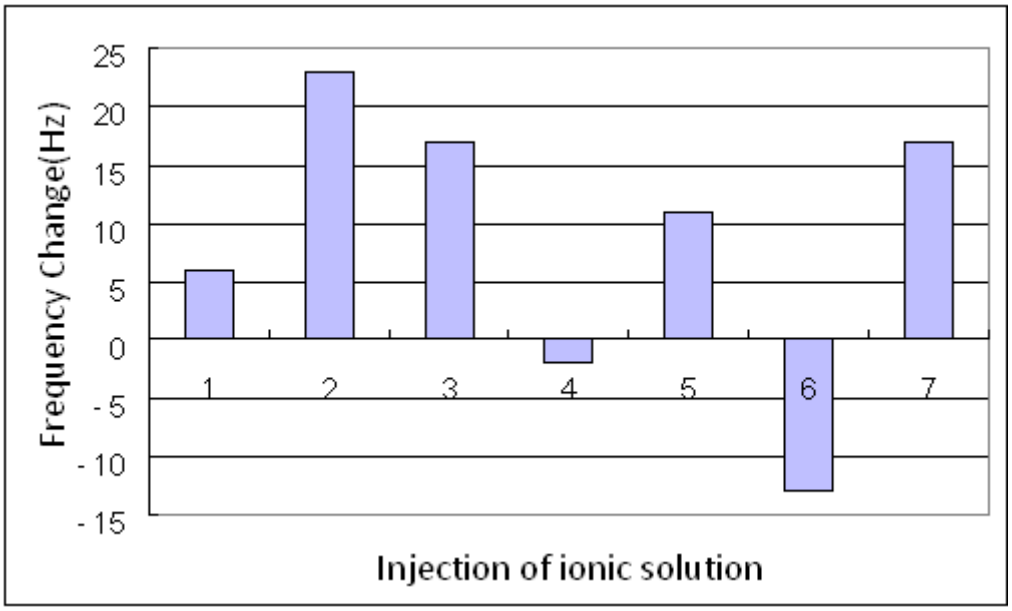

(b)

Figure 6.10. High level cationic cellulose: (a) Frequency values in each injection step; even numbers on x axis represent injecting buffer every time, step 1, 5, 9, 13 represent injecting cationic solution and step 3, 7, 11 represent injecting anionic solution; (b) Frequency change with the conversion of ionic solution; even numbers on x axis represent injecting anionic solution and odd numbers represent injecting cationic solution.

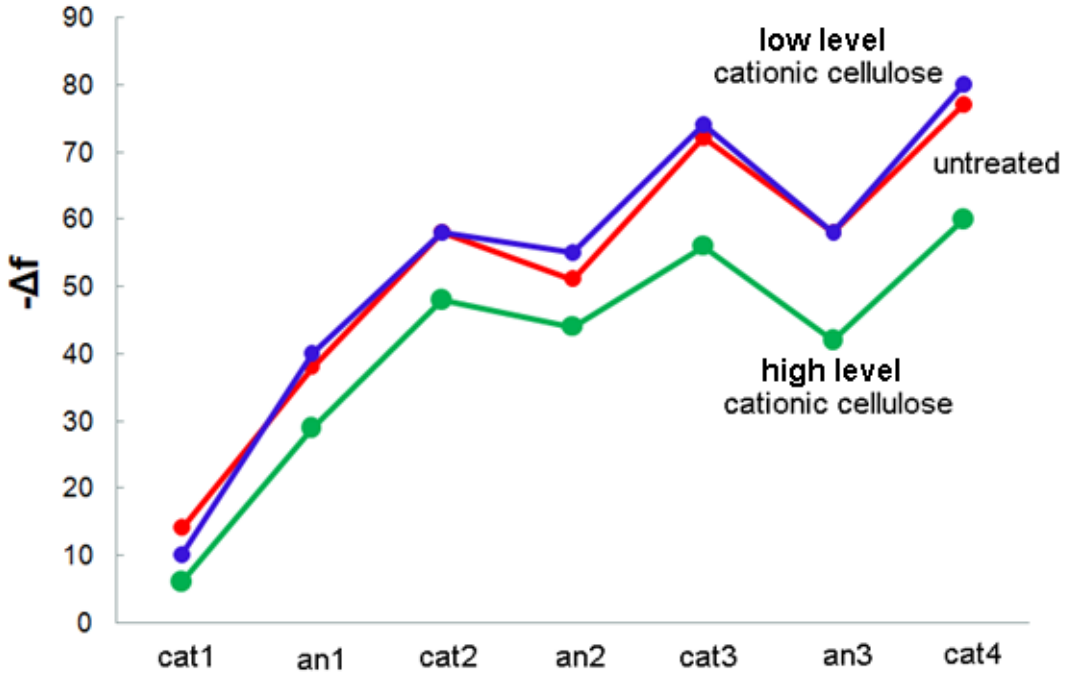

Figure 6.11. Build up of Multilayers on Cationic Cellulose (*cat* first).

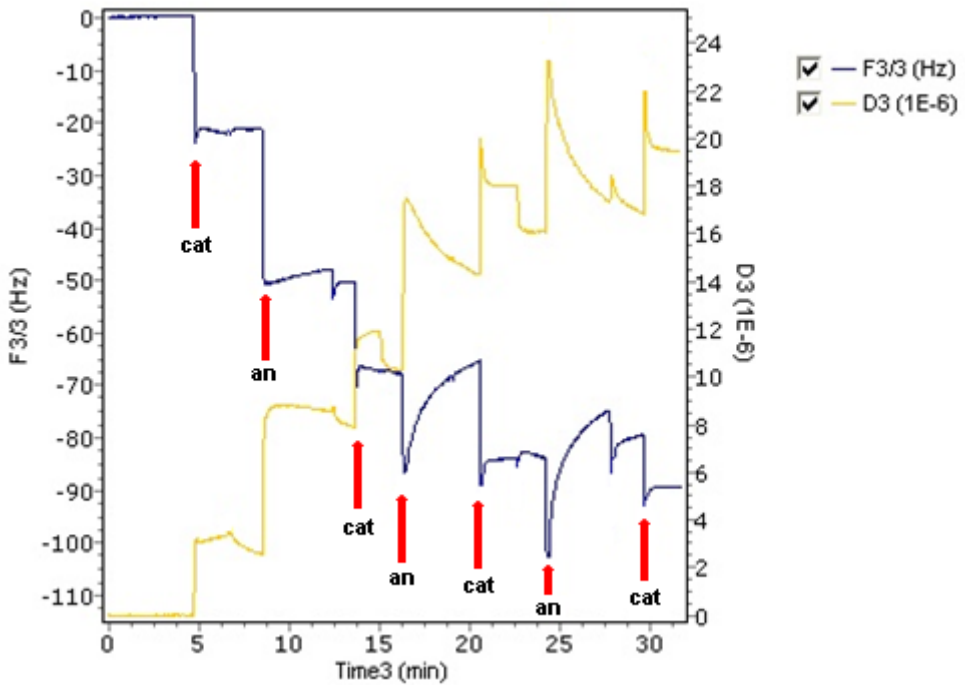

Figure 6.12. Frequency and Energy dissipation change curves for polyelectrolytes onto anionic cellulose substrates of low level treatment. Cationic polyelectrolyte injects first.

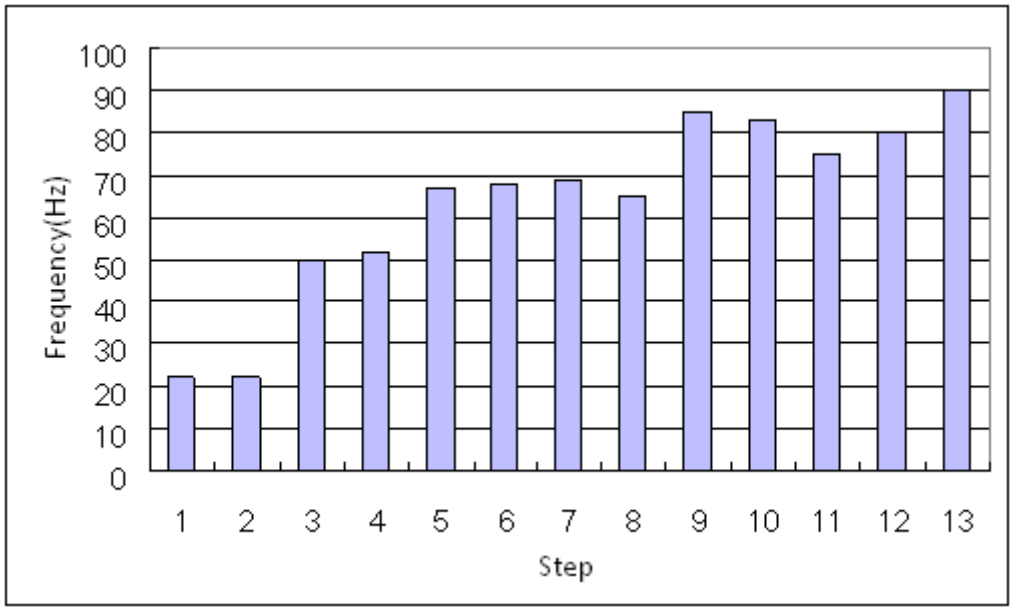

(a)

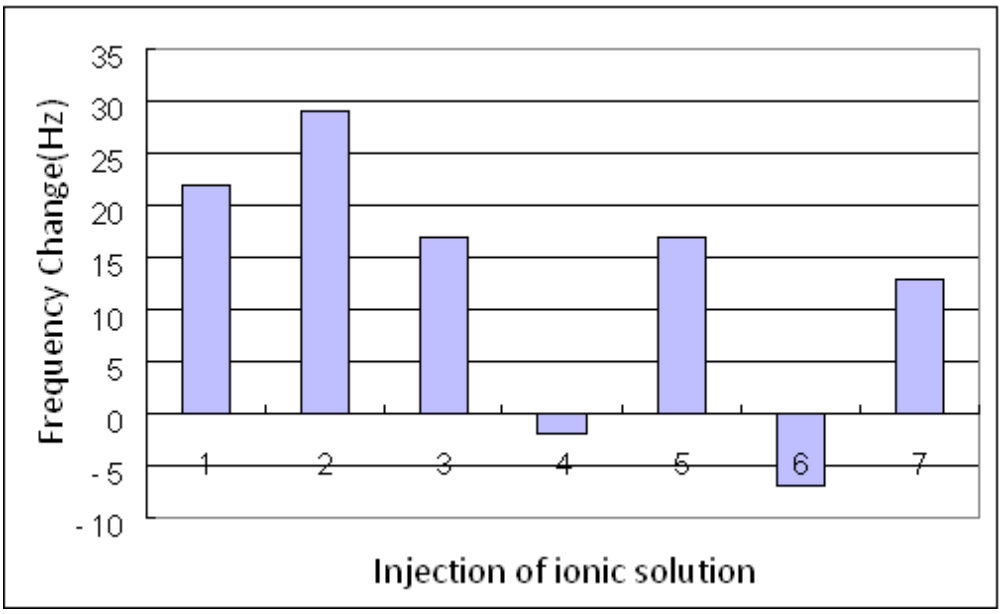

(b)

Figure 6.13. low level Anionic Cellulose: (a) Frequency values in each injection step; even numbers on x axis represent injecting buffer every time, step 1, 5, 9, 13 represent injecting cationic solution and step 3, 7, 11 represent injecting anionic solution; (b) Frequency change with the conversion of ionic solution; even numbers on x axis represent injecting anionic solution and odd numbers represent injecting cationic solution.

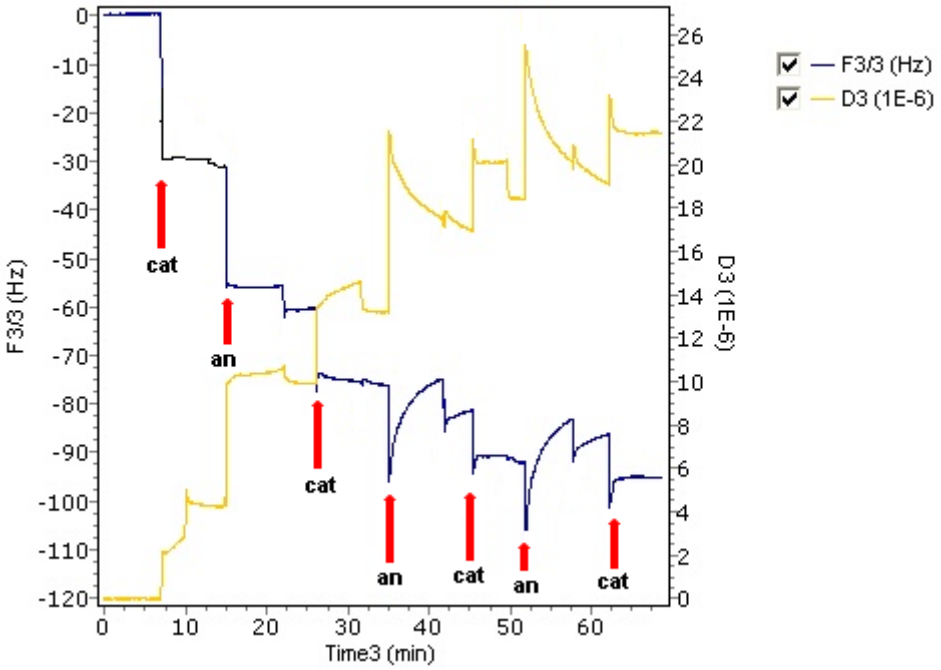

Figure 6.14. Frequency and Energy dissipation change curves for polyelectrolytes onto anionic cellulose substrates of high level treatment. Cationic polyelectrolyte injects first.

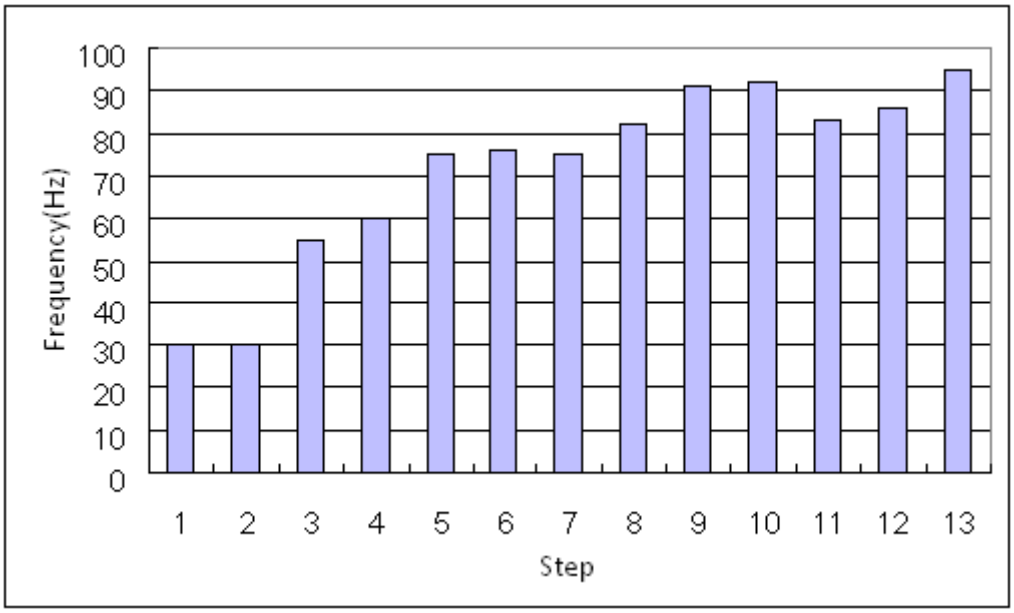

(a)

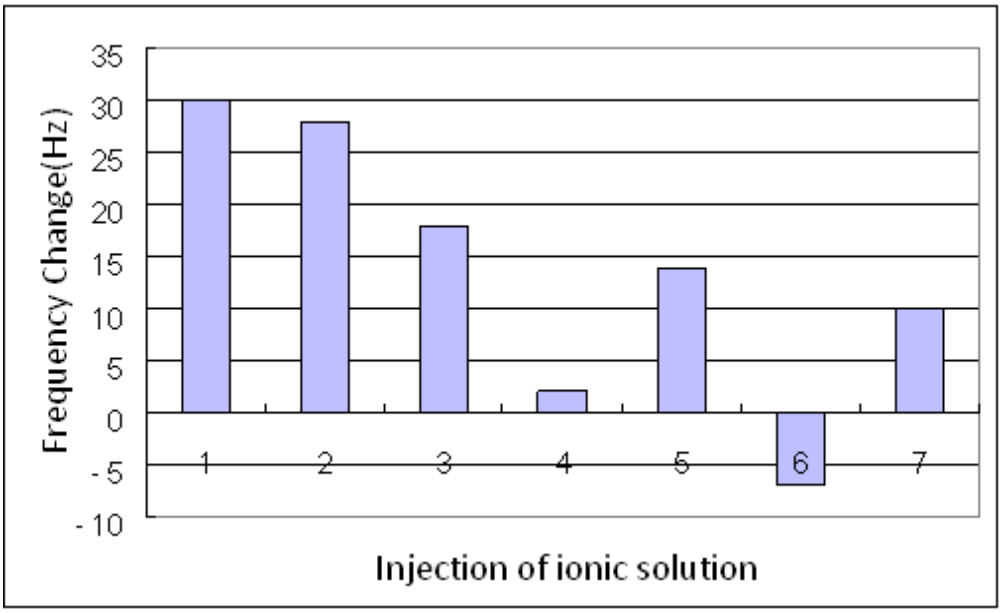

(b)

Figure 6.15. High Level Anionic Cellulose: (a) Frequency values in each injection step; even numbers on x axis represent injecting buffer every time, step 1, 5, 9, 13 represent injecting cationic solution and step 3, 7, 11 represent injecting anionic solution; (b) Frequency change with the conversion of ionic solution; even numbers on x axis represent injecting anionic solution and odd numbers represent injecting cationic solution.

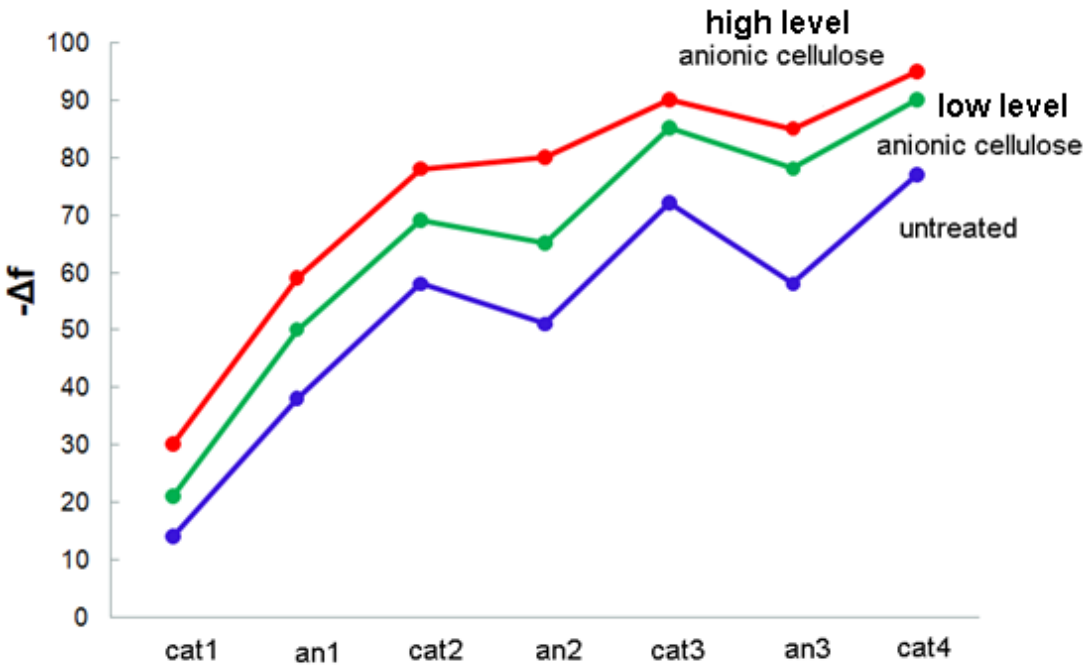

Figure 6.16 Build up of Multilayers on Anionic Cellulose (*cat* first)

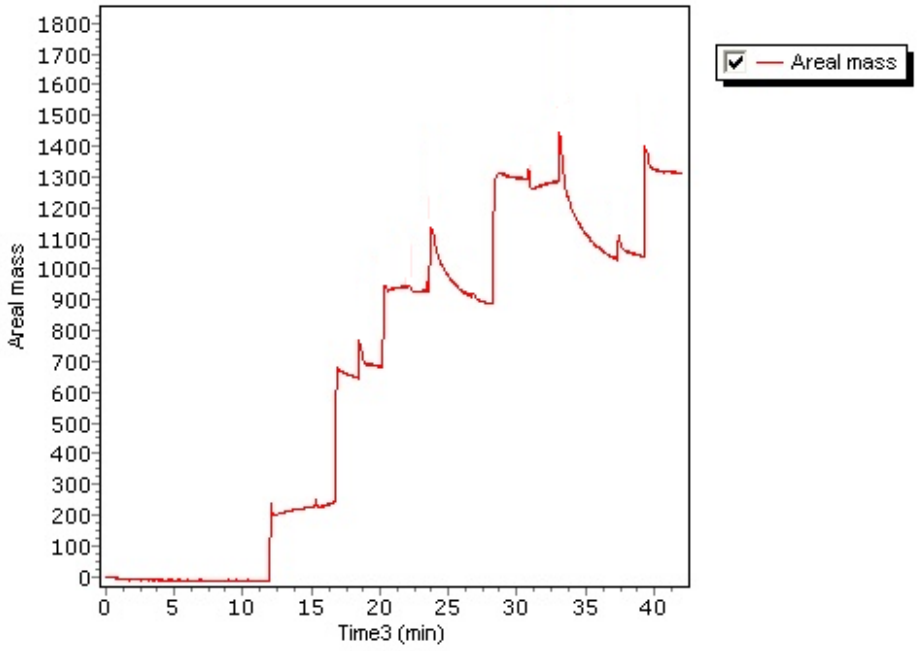

(a)

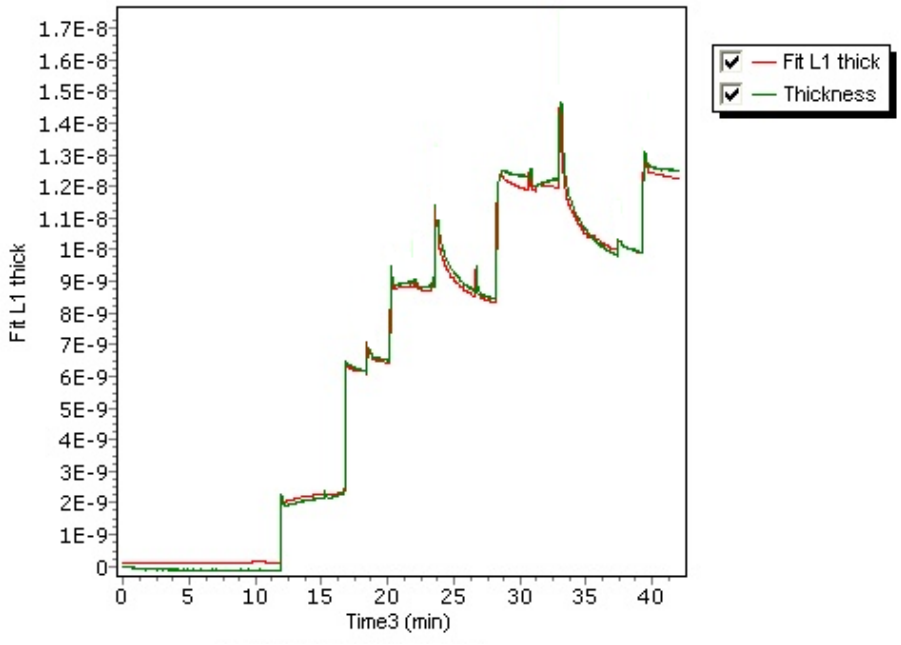

(b)

Figure 6.17. (a) Areal mass (ng/cm2) and (b) thickness (m) of polyelectrolyte adsorption on untreated cellulose substrates

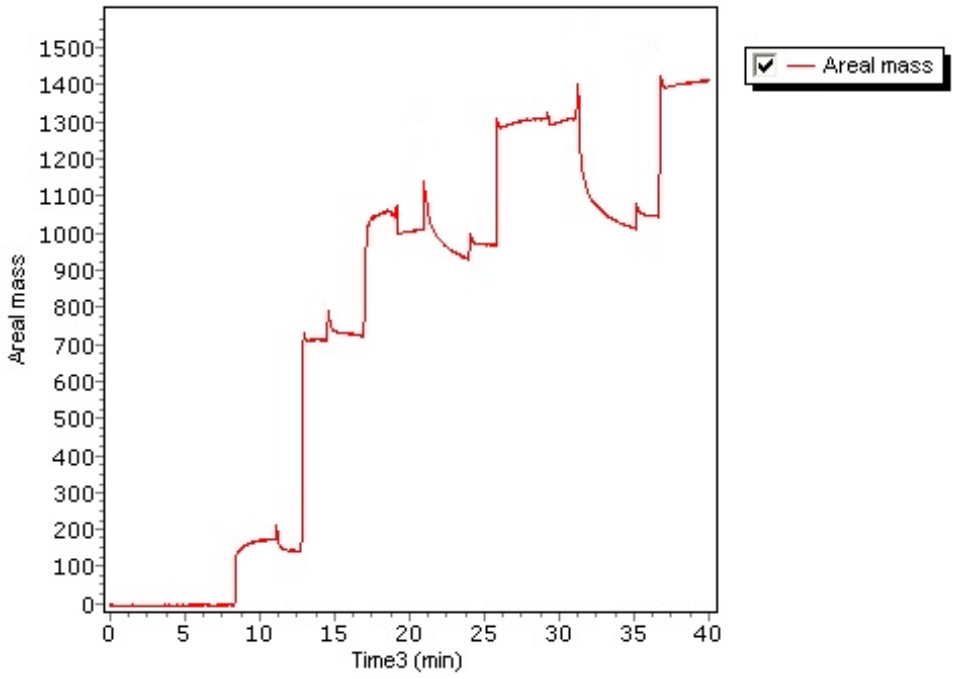

(a)

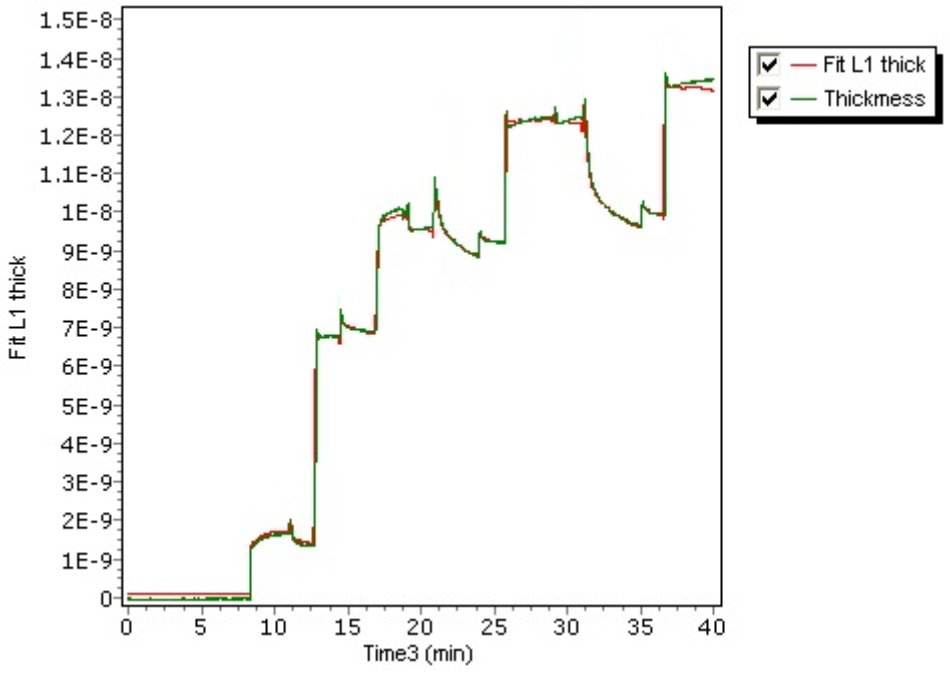

(b)

Figure 6.18. (a) Areal mass (ng/cm2) and (b) thickness (m) of polyelectrolyte adsorption on cationic cellulose substrates (low level)

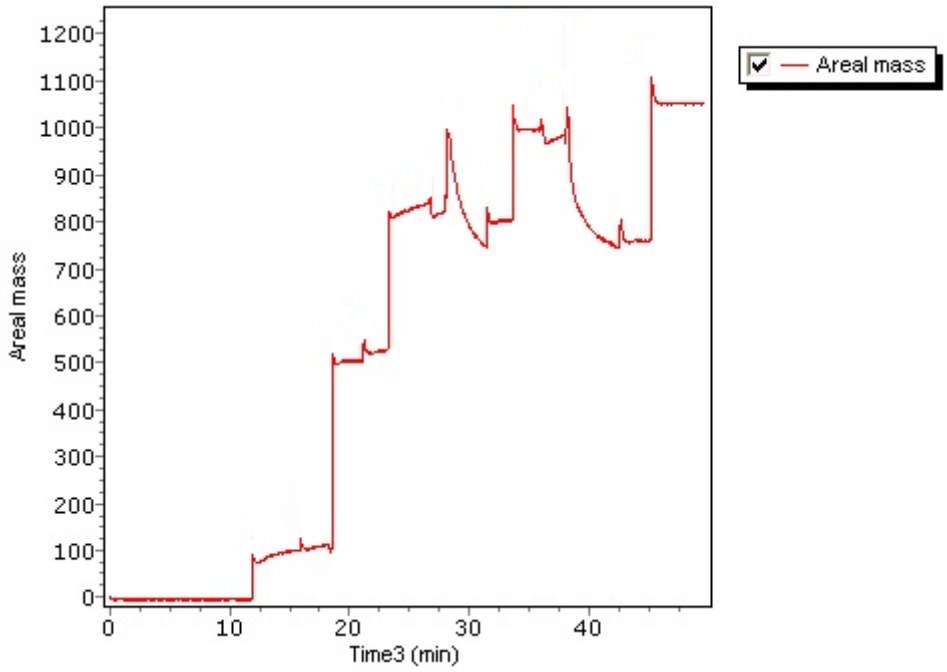

(a)

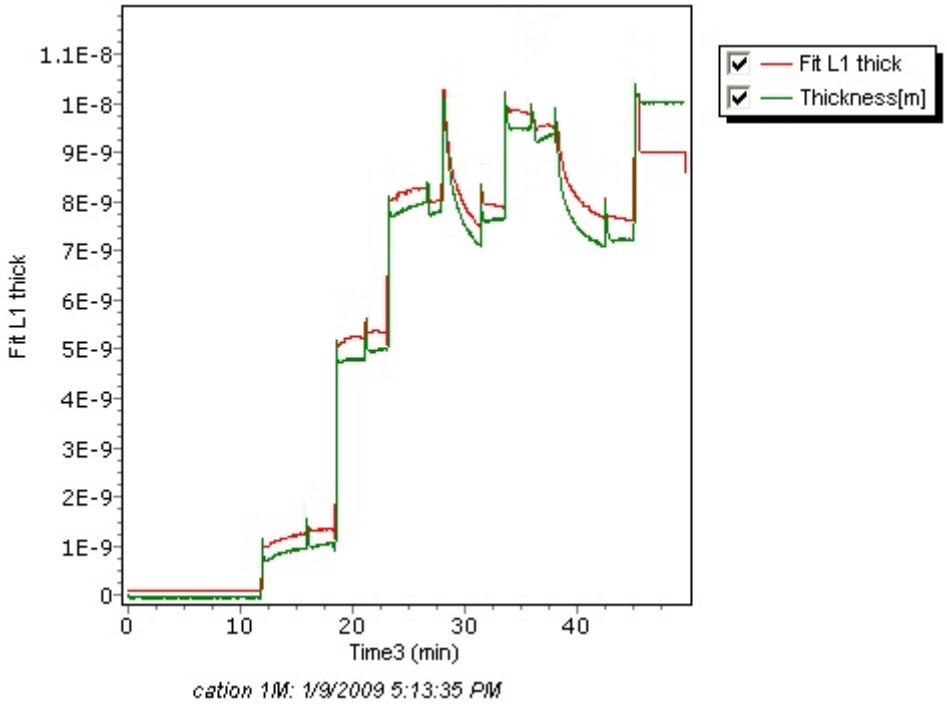

(b)

Figure 6.19. (a) Areal mass (ng/cm2) and (b) thickness (m) of polyelectrolyte adsorption on cationic cellulose substrates (high level)

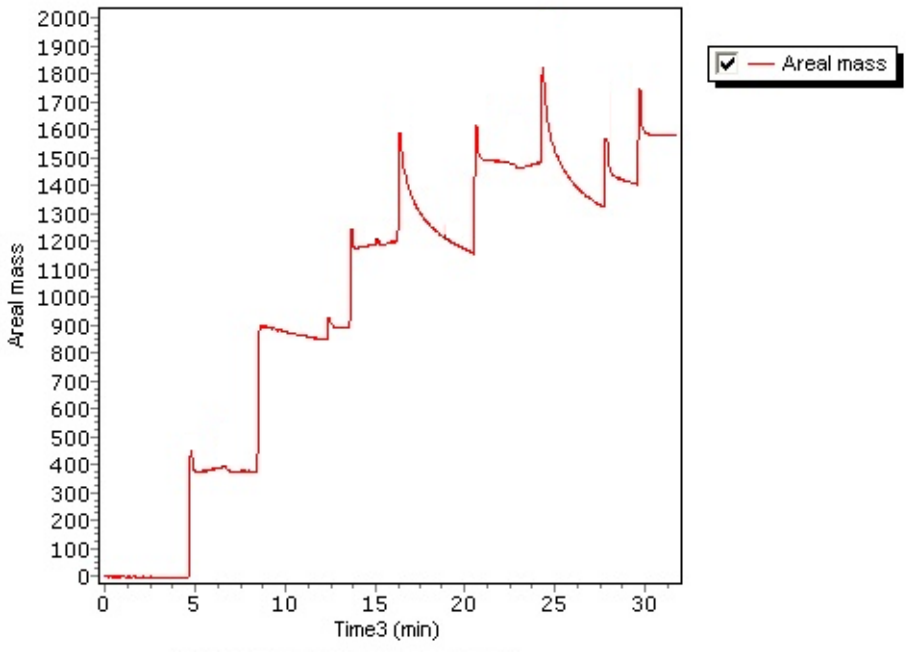

(a)

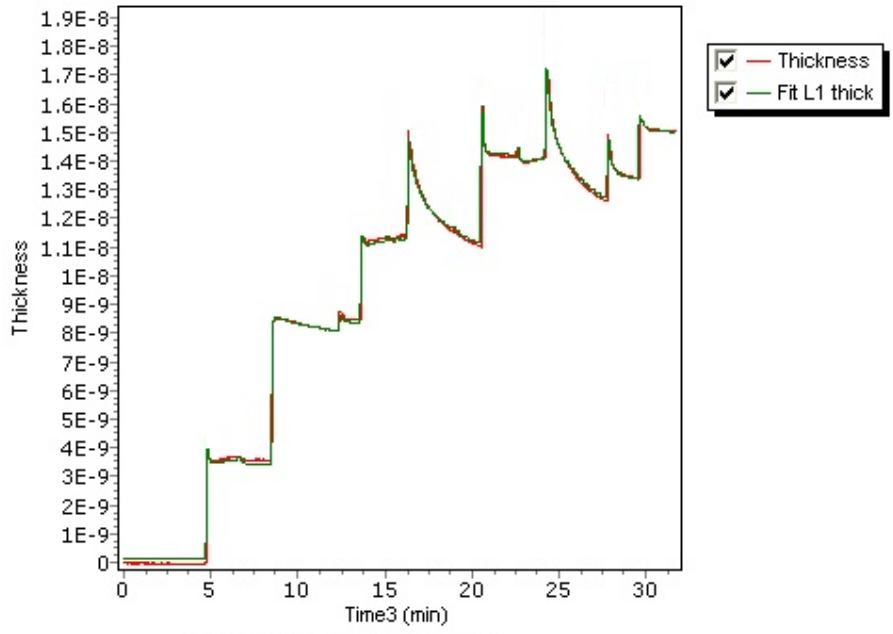

(b)

Figure 6.20. (a) Areal mass (ng/cm2) and (b) thickness (m) of polyelectrolyte adsorption on anionic cellulose substrates (low level)

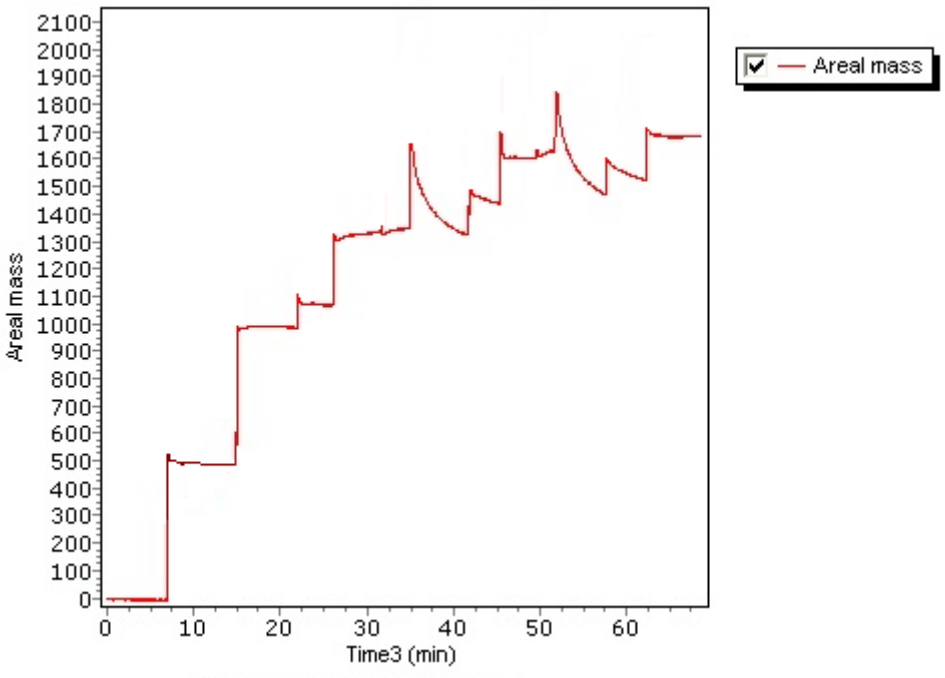

(a)

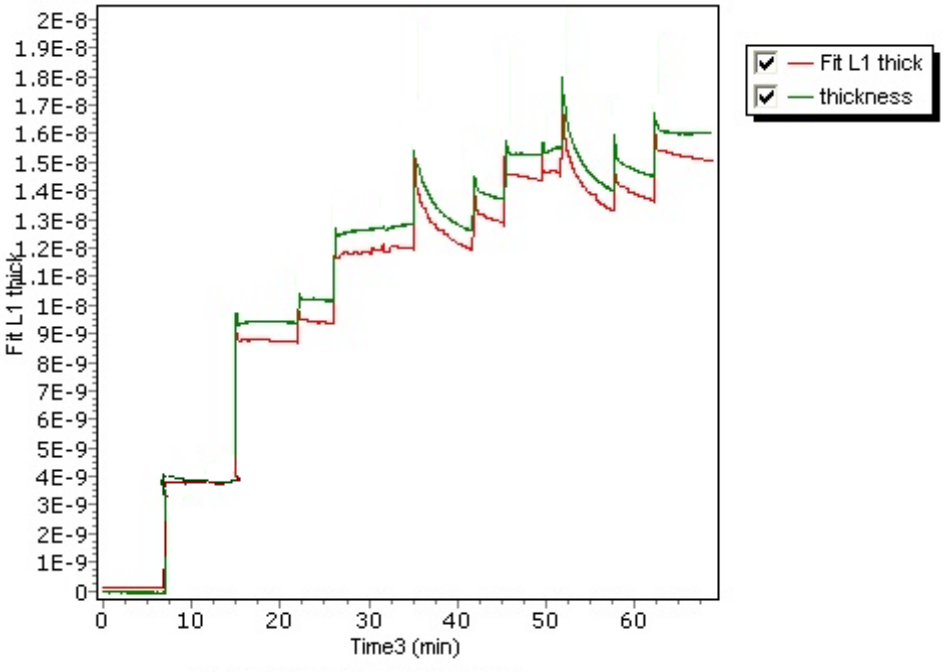

(b)

Figure 6.21. (a) Areal mass (ng/cm2) and (b) thickness (m) of polyelectrolyte adsorption on anionic cellulose substrates (high level)

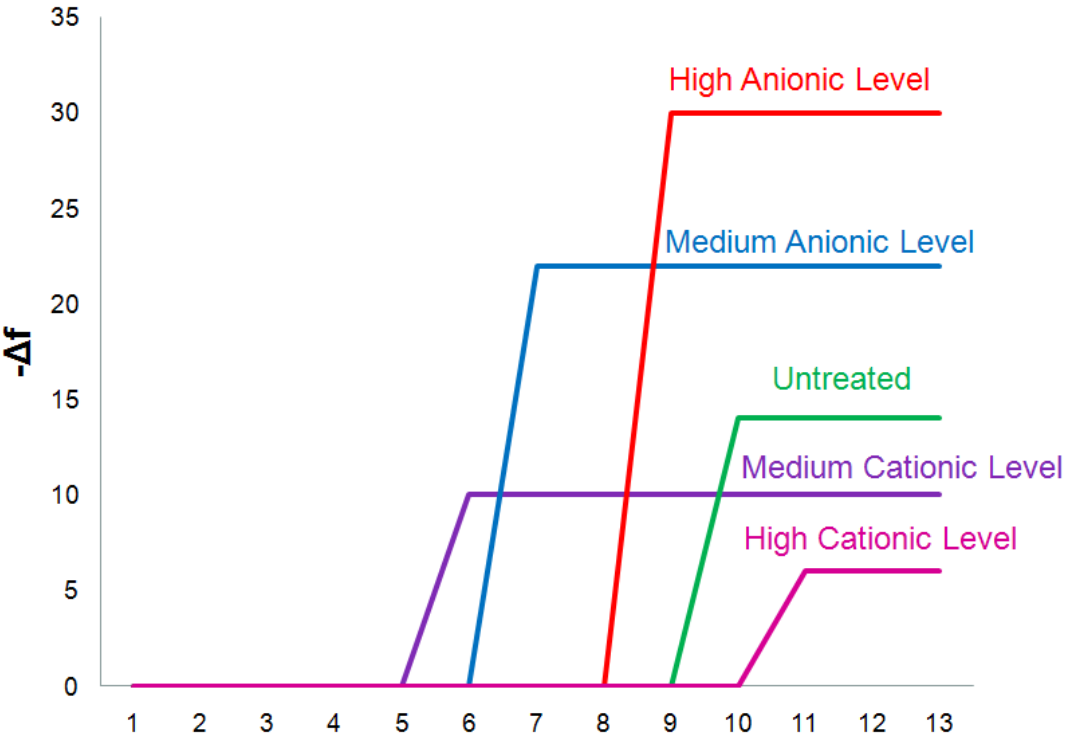

Figure 6.22. At the first *cat* injection, frequency changes of different cellulose films.

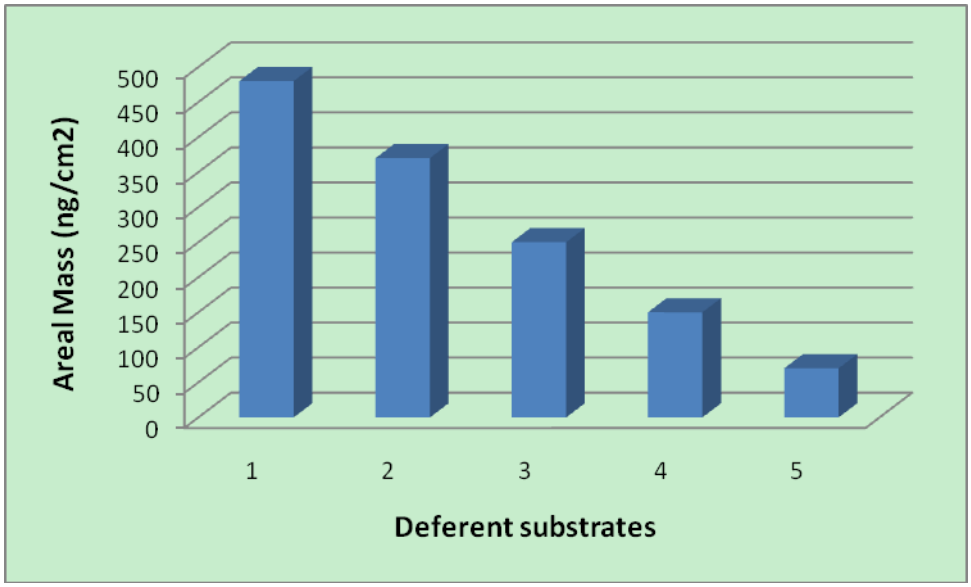

Figure 6.23. Comparision of the areal mass of first layer adsorption (DMAPAA) on different substrates. 1, 2, 3, 4, 5 represent anionic cellulose (high level), anionic cellulose (low level), untreated cellulose, cationic cellulose (low level), cationic cellulose (high level) respectively.

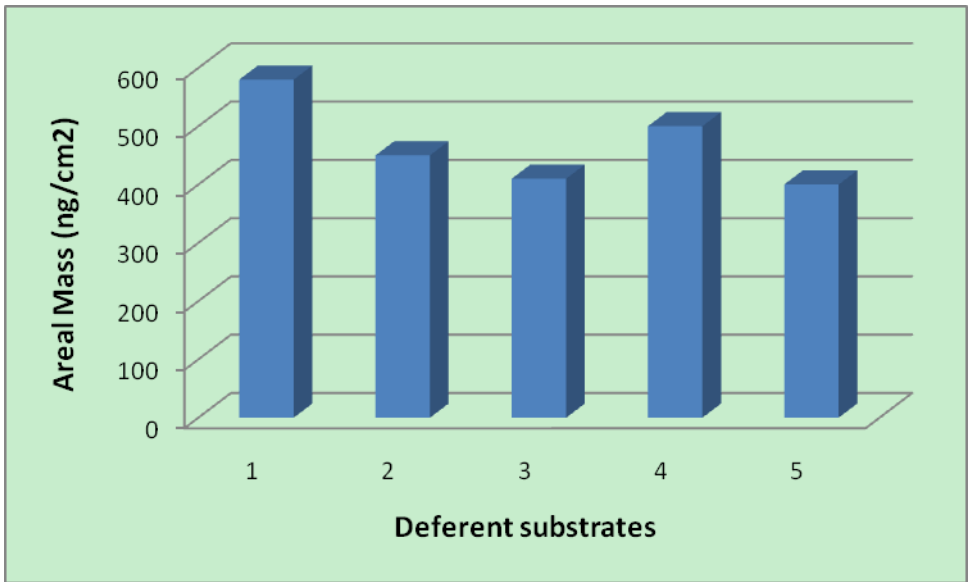

Figure 6.24. Comparision of the areal mass of second layer adsorption (IA) on different substrates. 1, 2, 3, 4, 5 represent anionic cellulose (high level), anionic cellulose (low level), untreated cellulose, cationic cellulose (low level), cationic cellulose (high level) respectively.

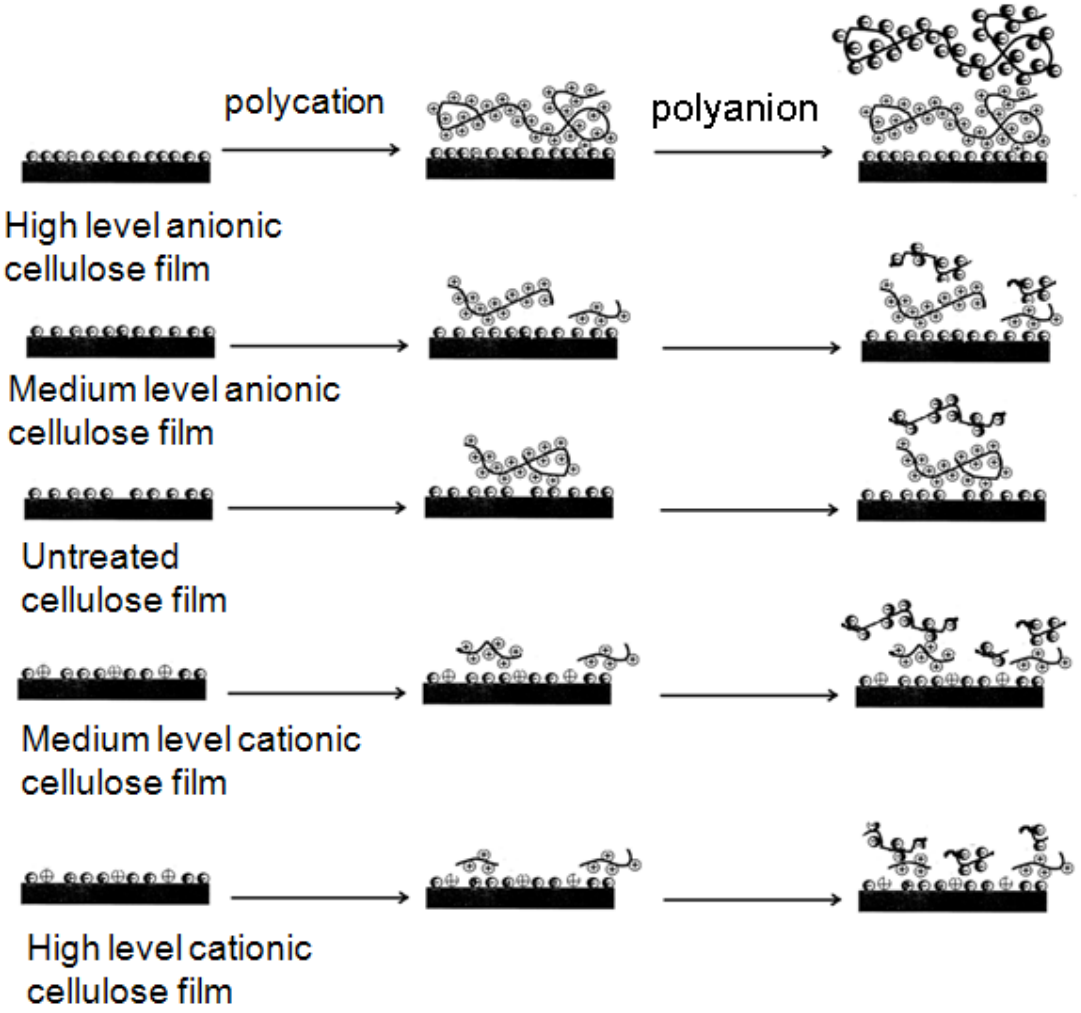

Figure 6.25. Adsorptions of the first and second layers onto the different cellulose films.

CHAPTER7: LAYER-BY-LAYER POLYELECTROLYTES DEPOSITIONS ON IONIC FIBER SURFACES (ANIONIC POLYELECTROLYTE INJECTED FIRST)

7.1 Introduction

With QCM-D, a real-time monitoring of two parameters (frequency and energy dissipation) can be carried out simultaneously, as molecular layers form onto the surface of the sensor. A general raw data plot is shown in Figure 7.1 [1]. In step 1, the blue pentagons (small molecules) adsorbed on the sensor, reflected by the small changes of frequency and dissipation; in step 2, red symbols (large elongated molecules) bond to form a softer and thicker layer, which can be observed by higher Δf and ΔD; in step 3, after rinsing with the buffer, the elongated molecules were removed, so that frequency and dissipation were reduced again.

In this study, polyelectrolytes were the charged macromolecules carrying acidic or basic groups. Under appropriate conditions, these groups dissociate in aqueous solution, producing ionic segments on the polymer chain and the respective counter-ions. These polymers can deposit on the ionic cellulose films layer by layer.

In chapter 6, based on QCM-D, the adsorption phenomena of two ionic polymers (DMAPAA and IA) on different cellulose substrates (prepared from untreated, cationic and anionic cotton) was studied by alternating sequential injections of counter ionic polyelectrolyte solution. After the first injection (cationic DMAPAA solution-*cat*), because all cellulose films bear negative charges, these groups attracted

the positively charged polymers in *cat*. The adsorption of *cat* on any kind of cellulose substrates was monitored by the changes of frequency and energy dissipation in QCM-D. However, the cationic cellulose films, the cotton treated at two concentrations, also have positive charges onto the surface by cationic reaction, besides negative groups which are not reacting with the cationic reagent. Theoretically, the cationic cellulose films were able to adsorb the anionic polymers due to their outermost charges. However, there is a lack of experimental data to confirm the proposed theories and to directly allow the elucidation of the polyelectrolyte adsorption phenomena when the first injection is the anionic IA solution. In this study adsorption experiments with polyelectrolytes (DMAPAA and IA) were carried out on a series of cellulose films. All processes used in this experiment were the same as in chapter 6, except for the sequence of polyelectrolyte injection. There the anionic IA solution (*an*) was injected first.

7.2 Experimental

7.2.1 Materials

The materials and chemicals used in this research were the same as in chapter 6. All experiments were performed with deionized water from an ion-exchange system (Pureflow, Inc.), and the deionized water was further processed in a Milli-Q® Gradient unit to ensure ultrapure with resistivity greater than 18MΩ. The 200ppm aqueous solutions of the polyelectrolytes were made by using sodium chloride (pH 6.9).

7.2.2 Ionic Cotton Preparation

All ionic cotton used in this chapter was the same sample as in chapter 6.

7.2.3 Polyelectrolyte Solution Preparation

The protocol of how to prepare the polyelectrolyte solution was addressed in detail in Chapter 6.

7.2.4 Cellulose Films Preparation

The protocol of how to prepare cellulose films on the sensor was addressed in detail in Chapter 6. For the experiments in this chapter, the cellulose films were prepared from untreated, anionic (high level) and cationic (high level) cotton.

7.2.5 Quartz Crystal Microbalance (QCM) Measurements

Adsorption of polyelectrolyte samples onto the cellulose films was conducted with a Quartz Crystal Microbalance with Dissipation mode, QCM-D300 model (Q-Sense, Gothenburg, Sweden). The temperature in the experiments was controlled within 0.02 °C of the respective set point via a Peltier element that was built in the QCM apparatus. A piezoelectric resonator (quartz) underwent electric polarization due to applied mechanical stresses (piezoelectricity). Resonators consisting of gold-coated AT-cut quartz crystals with fundamental frequency of 5 MHz were used as sensors. During the measurement, the crystal was mounted in a thermostated liquid chamber, which was designed to provide a rapid, non-perturbing exchange of the liquid in contact with one side of the sensor. This system allows for the measurement of up to 4 harmonics. In this study, the frequency and dissipation responses were

recorded at around 15, 25, and 35 MHz, corresponding to the 3rd, 5th and 7th overtones (n = 3, 5, and 7, respectively). For clarity, only the normalized frequency shifts, normalized Δf (Δf/n), and the dissipation shifts ΔD, for the third overtone were presented.

In the experiments, fresh polymer solutions (200mg/L) were prepared with the buffer of a 0.1mM background ionic strength. Before running the polymer solutions, the instrument was stabilized with the buffer. The sensor with cellulose film was immersed in the QCM-D equipment with the buffer for 4 hours to allow the cellulose to swell. After running the QCM-D for 10 minutes, a constant QCM baseline was obtained, and then 1 ml polymer solution was injected in the adsorption module at a low rate (0.12ml/min). The frequency and dissipation were monitored until equilibrium was reached. Finally, 3 ml of the buffer was used to rinse the adsorbed layer (using the same injection rate). By running this rinsing procedure, any loosely bound polymer was removed from the interface and the net adsorption was therefore accounted for. As in chapter 6, multilayer self-assembly on cellulose substrates by alternating polyelectrolytes was used: an injection of an anionic IA solution (*an*) was followed by subsequent injection of cationic DMAPAA solution (*cat*); steps will be repeated as needed.

7.3 Results and Discussion

7.3.1 Anionic Polymers adsorption (first injection) on Different Cellulose Substrates

In Figure 7.2, 7.4 and 7.6, *an* was first injected to all cellulose substrates at the 5th minute. The frequency and dissipation of untreated and anionic cellulose (high level) film stayed unchanged, which proves there is no anionic polymer adsorption on the untreated or anionic cellulose films because their surfaces only had negative charges and could not attract the negatively charged polymers. However, for the cationic cellulose (high level) film, the frequency and dissipation had an obvious shift when *an* was first injected. This result indicates that the cationic cellulose film had positive charges onto the surface by the cationic reaction. The high level cationic reagent modified the charge density of cotton fibers. These positive charges on the cotton surface contributed to the layer-by-layer deposition of polyelectrolytes. In addition to the results from chapter 6, due to the hydration, this cationic cellulose film also had negative charges onto the surface which enabled to it adsorb positively charged polymers in *an*.

As shown in Figure 7.3 and 7.5, the areal masses of the first adsorption of anionic polymers onto untreated and anionic cellulose (high level) film were almost zero, indicating the adsorption of negatively charged polymers didn't happen due to the presence of negative charges on the surface. Figure 7.7 shows that the areal mass of the first anionic polymers adsorption on cationic cellulose (high level) film was

about 220ng/cm2. The anionic polymers deposited on the cationic cellulose film were due to the outermost positive charges. All these results are the same as the changes of frequency and dissipation at the first injection.

7.3.2 Cationic polymers adsorption (second injection) on Different Cellulose Substrates

After the first injection of *an* and rinsing, *cat* was injected to all cellulose films. In Figure 7.3, the areal mass of cationic polymer adsorption (second injection) on untreated cellulose film was about 300ng/cm2. However on the anionic cellulose (high level) film, the areal mass of cationic polymers (second injection) was almost 500ng/cm2, as shown in Figure 7.5, while Figure 7.7 shows 280ng/cm2 areal mass of cationic polymers on the cationic cellulose (high level) film. The areal mass comparison of cationic polymers on different cellulose surfaces is shown in Figure 7.8, of which the mass adsorption of cationic polymers on anionic cellulose (high level) film has the maximum value in three films. Figure 7.9 illustrates more negative charges onto the surface of anionic cellulose film than those onto the surface of untreated and cationic cellulose films (note only negative charges onto the surfaces of untreated and anionic cellulose films) leads to more adsorption of cationic polymers. For untreated and anionic cellulose films, after the first injection of *an*, the surface charge distribution were almost the same as the beginning. However, there was a new layer deposited on the cationic cellulose film. The cationic polymer deposition mostly depended on the amount of outermost negative charges. The anionic polymers

attracted by the positive charges on the cationic cellulose film are less than the negative charges on the untreated and anionic cellulose film. Therefore, the adsorption mass of cationic polymers on the anionic cellulose film was the largest.

7.3.3 Adsorptions of Polyelectrolytes onto Different Cellulose Substrates

Figure 7.10, 7.11 and 7.12 show the frequency change with the different steps. The frequencies of untreated, anionic and cationic cellulose substrates were affected by the buffer rinsing, especially after the deposition of few layers onto the surfaces. The buffer swept away the polymers not firmly deposited onto the surface, and twisted and superimposed the polymer chains. Correspondingly, the adsorption of ionic polymers at the beginning layers were not easily rinsed by the buffer. After a few layers, the last adsorption of any of cellulose substrates became unstable and was rinsed away with the buffer.

For all cellulose substrates, the frequency increased at the 5th injection (*an*), Similar phenomenon occurred when the injection was changed to *an*: in chapter 6, the frequencies of all cellulose films increased at the 4^{th} injection of *an*. In this chapter, *cat* was used as the 2^{nd} injection; while in chapter 6, it was used as the 1^{st} injection. Therefore, the 5^{th} injection of *an* in this chapter is the same purpose as the 4^{th} injection in the chapter 6.

A hypothesis to explain this phenomenon is illustrated in Figure 7.14. The substrate is assumed to be a cationic cellulose film. Because the adsorption layers of polyelectrolytes on the cellulose film are very soft, when the 5^{th} injection is anionic

solution after the deposition of a few layers, the anionic polymer with negative charges will attract the positive charges on the outermost layer, and then desorb the polyelectrolyte complex from the sensor. After desorption, the outermost layer is anionic again, and therefore react with positive charges in cationic polymers. The same phenomenon was also be observed only by altering the polyelectrolyte solution. Based on these observations, the polyelectrolyte adsorption on the sensor with cellulose film is not unlimited. After the deposition of a few layers, it is difficult to adsorb more polyelectrolytes by electrostatic layer-by-layer assembly.

Figure 7.13 showed multilayers were built up on cationic, anionic and untreated cellulose film. It is found first adsorption of negatively charged polymer occurred on cationic cellulose films, but not on untreated and anionic cellulose film. Growth of the polyelectrolyte multilayers in first four steps is linear. At the third *an* injection, the frequency decreased as that described in chapter 6.

7.3.4 Comparison of the adsorption process by different injecting sequence

In Figure 7.15, when the first injection was *cat* (S1), the mass adsorption of cationic polymers descended with the decrease of negative charges on different cellulose films. Because the anionic cellulose film had the most negative charges in three samples, it adsorbed the most cationic polymers onto the surface. However, when the first injection was *an* (S2), the mass adsorption of cationic polymers (2^{nd} injection) depended on the negative charges of substrates and the outermost layer.

On the anionic cellulose film, the areal mass of cationic polymers (2^{nd} injection)

was almost 500ng/cm2, which was similar to the areal mass of cationic polymers when *cat* was injected firstly. Meanwhile, the areal mass of S1 was the same as of S2 on the untreated cellulose film. The reason is the anionic polymers didn't deposit on the anionic and untreated cellulose films at the first injection of *an*, so that the density of negative charges on their surfaces didn't change. The areal mass of S1 on the cationic cellulose film was 100ng/cm2, while it reached 300ng/cm2 for S2. For the same cationic polymer injection, the mass adsorption of *cat* on the cationic cellulose film with one *an* layer was higher than the original cationic cellulose film. After the first injection (*an*), the cationic cellulose film adsorbed polymers with negative charges, and therefore more negative to adsorb cationic polymers, as shown in Figure 7.15. But to the original cationic cellulose film, if the first injection is cationic DMAPAA solution, only negative charges left from cationic reaction attract positive charges, while the positive charges repel the polymers with the same charges as they approach. Therefore, more negative groups onto the surface leads to more adsorption of cationic polymers.

Comparing the results of different injecting sequences of polyelectrolyte solutions, the frequency and dissipation changes of the same cellulose sample look similar, except that the untreated and anionic cellulose substrates had no adsorption when the first injection was *an*. Without this step, all kinds cellulose substrates had desorption at the 4^{th} layer when the polyelectrolyte solution was anionic. From the results in the chapters 6 & 7, it can be stated that no more than four polyelectrolyte

layers would be built up in our experiments onto the untreated, cationic and anionic cellulose substrate.

7.4 Conclusion

Adsorption of anionic polyelectrolyte electrolyte in the first layer of cationic cellulose was confirmed. Compared to the cationic cellulose film, the surface of untreated and anionic cellulose films didn't adsorb anionic polymer in the first layer. The first layer on the untreated or anionic cellulose film is formed when the cationic DMAPAA solution was injected. After the first injection of anionic IA solution, the areal mass of cationic polymer deposition was similar to that when the first injection was cationic. The anionic cellulose film had the greatest adsorption mass of positively charged polymers.

7.5 Reference

1. http://www.q-sense.com/applications--2.asp

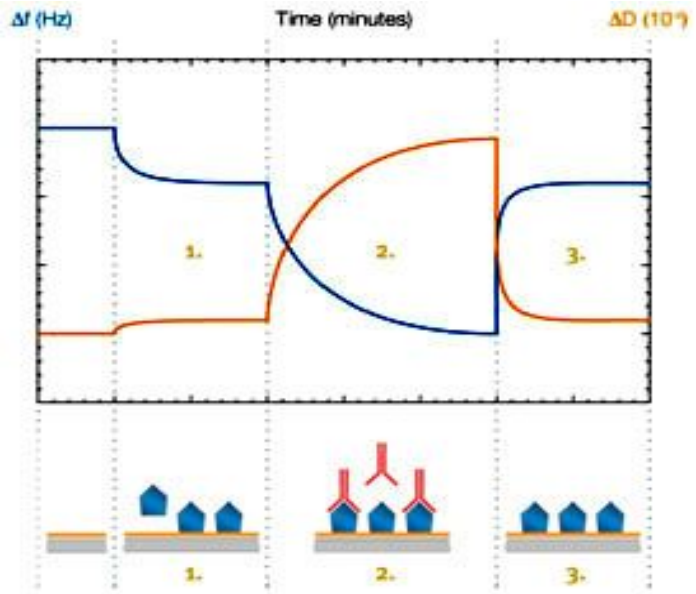

Figure 7.1. A general raw data plot of different injection in QCM-D. [1]

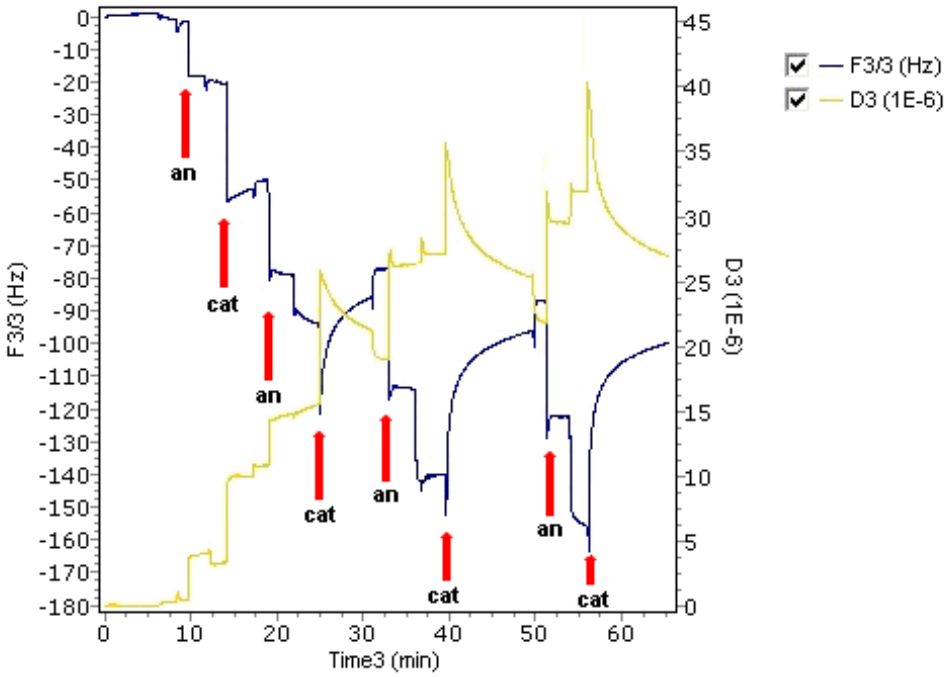

Figure 7.2. Frequency and Energy dissipation change curves for polyelectrolytes onto untreated cellulose substrates. Anionic polyelectrolyte injects first.

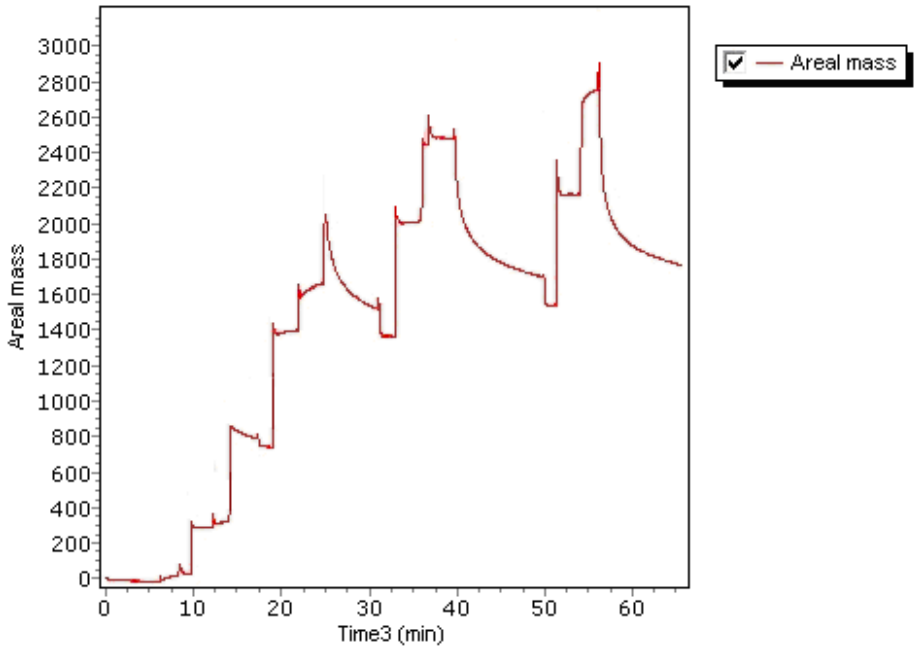

Figure 7.3. Areal mass (ng/cm2) of polyelectrolyte adsorption on untreated cellulose substrates

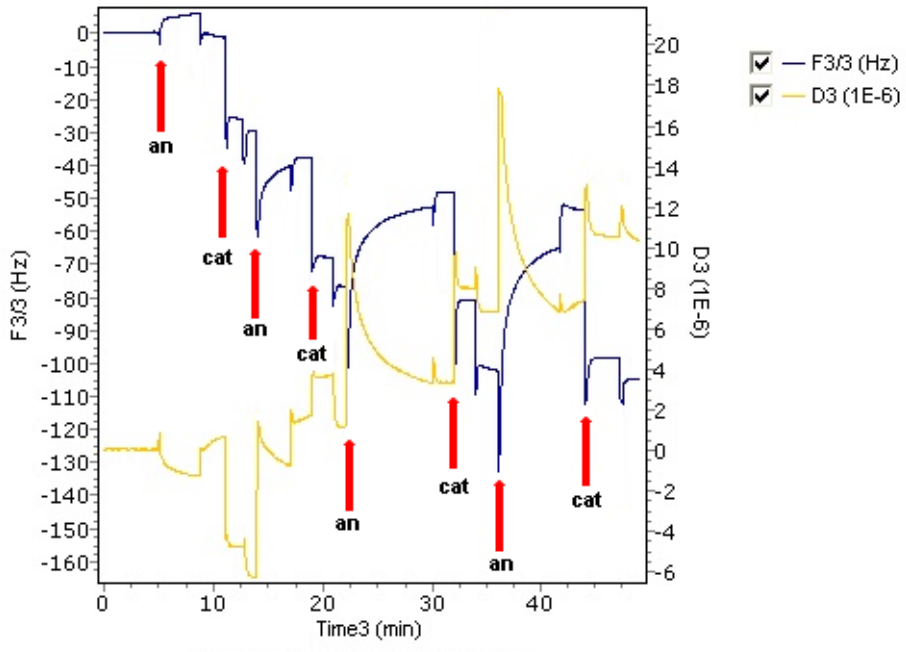

Figure 7.4. Frequency and Energy dissipation change curves for polyelectrolytes onto high level anionic cellulose substrates. Anionic polyelectrolyte injects first.

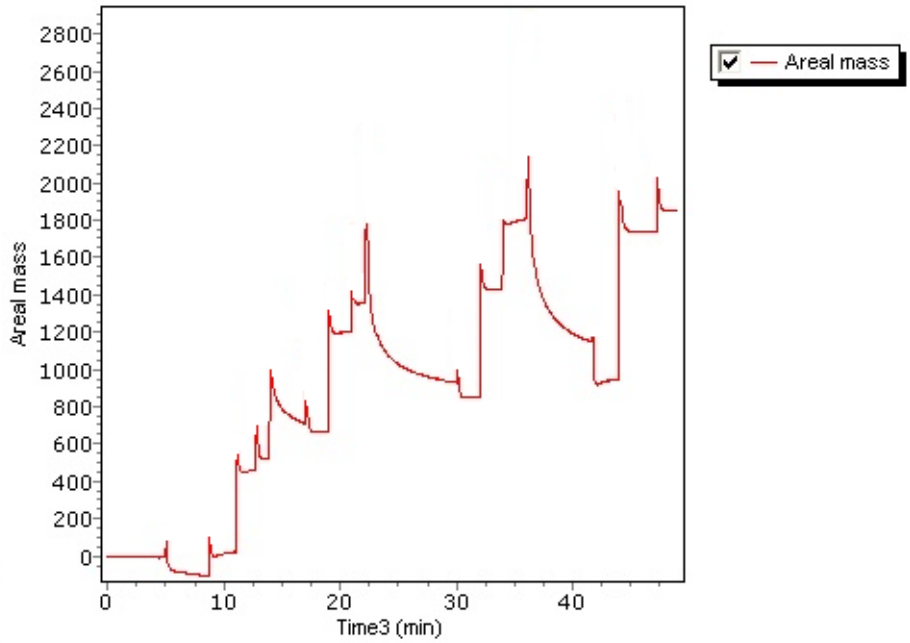

Figure 7.5. Areal mass (ng/cm2) of polyelectrolyte adsorption on high level anionic cellulose substrates

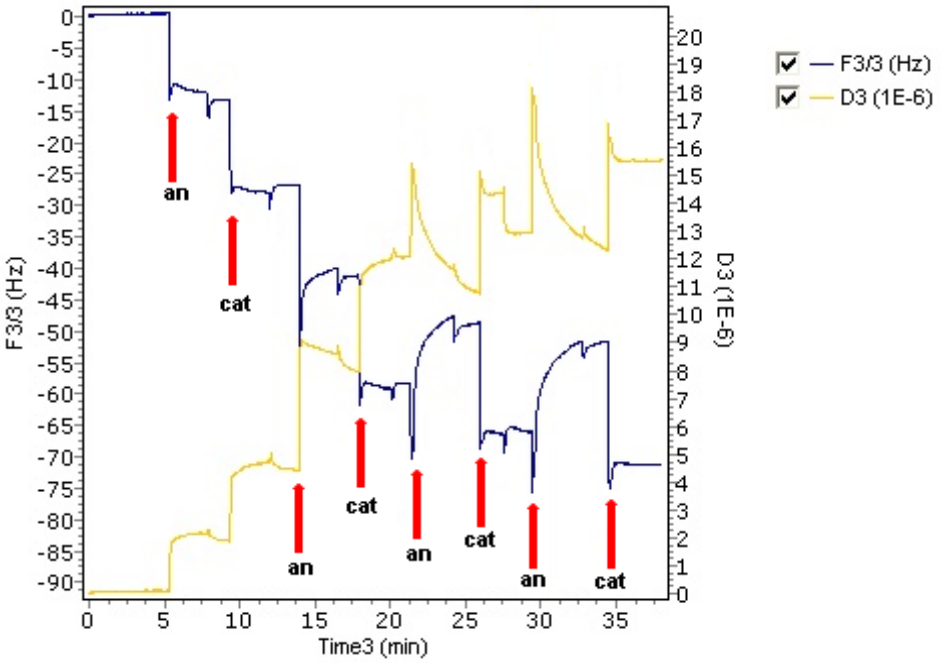

Figure 7.6. Frequency and Energy dissipation change curves for polyelectrolytes onto high level cationic cellulose substrates. Anionic polyelectrolyte injects first.

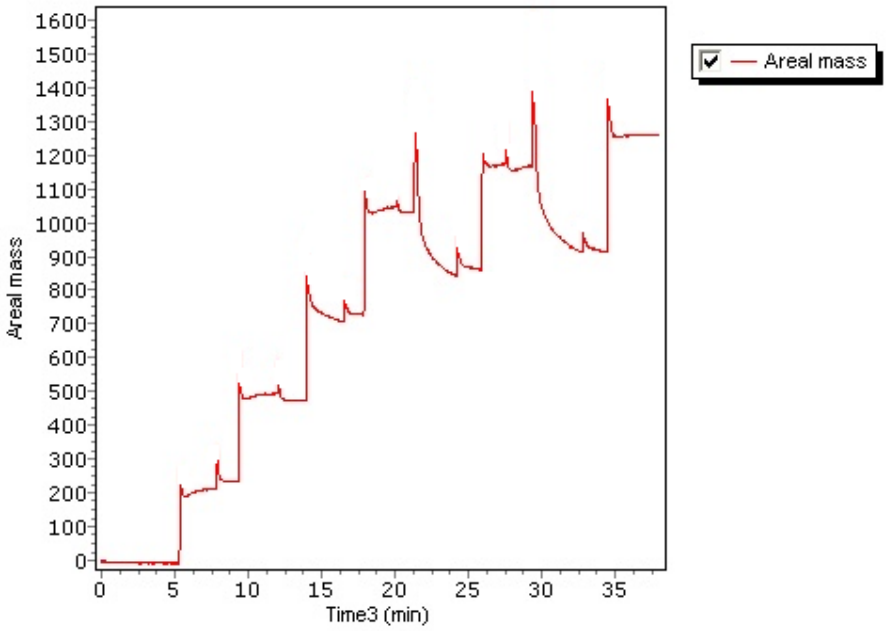

Figure 7.7. Areal mass (ng/cm2) of polyelectrolyte adsorption on high level cationic cellulose substrates

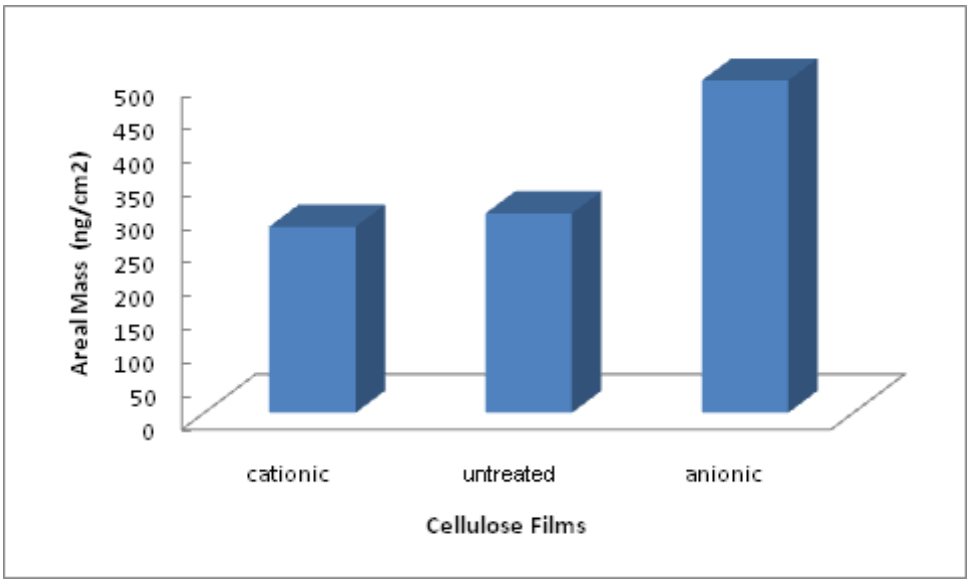

Figure 7.8. Comparison the mass of adsorbed cationic polymers (second layer) on different cellulose surfaces.

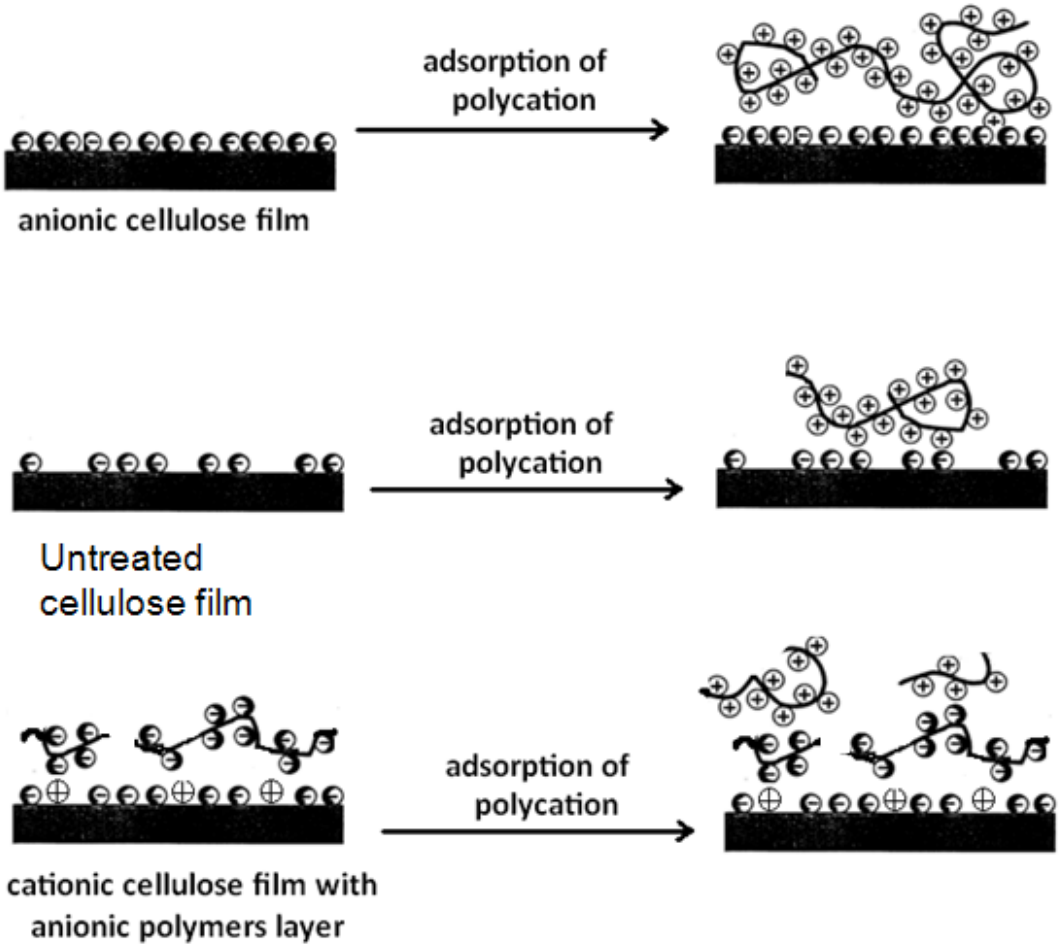

Figure 7.9. Polyelectrolyte first and second adsorbed layer on different cellulose films.

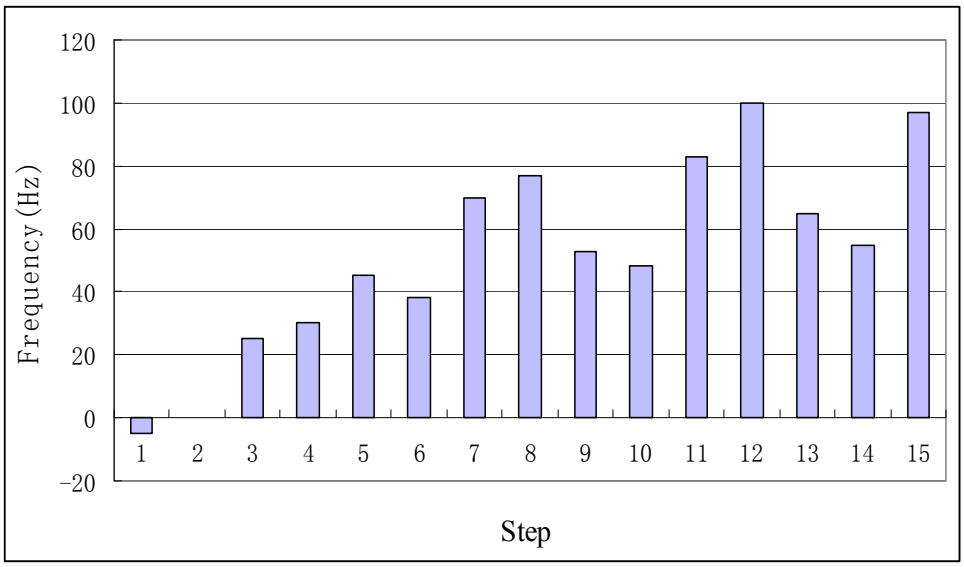

(a)

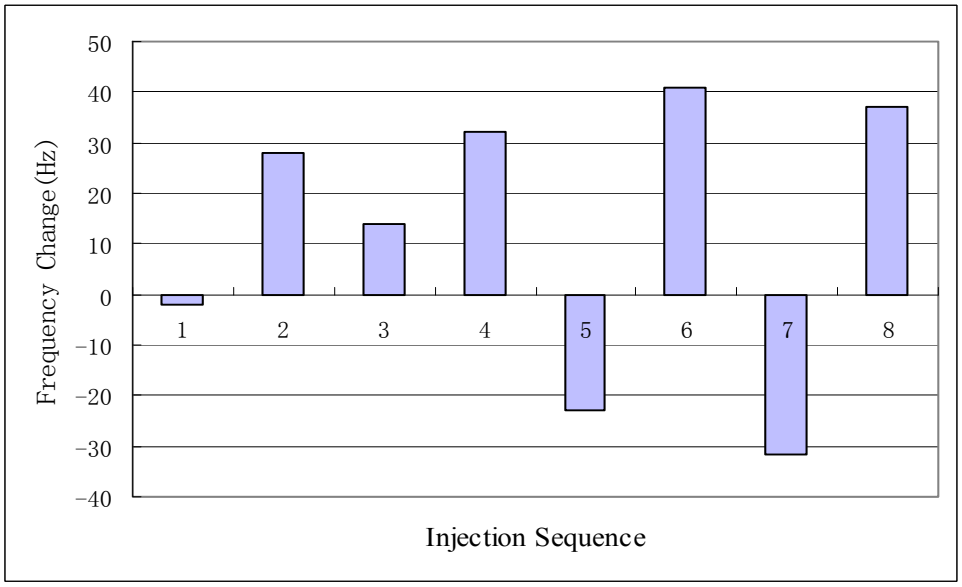

(b)

Figure 7.10. Anionic Cellulose (high level): (a) Frequency values in each injection step; even numbers on x axis represent injecting the buffer every time, step 1, 5, 9, 13 represent injecting anionic solution and step 3, 7, 11, 15 represent injecting cationic solution; (b) Frequency change with the conversion of ionic solution; even numbers on x axis represent injecting cationic solution and odd numbers represent injecting anionic solution.

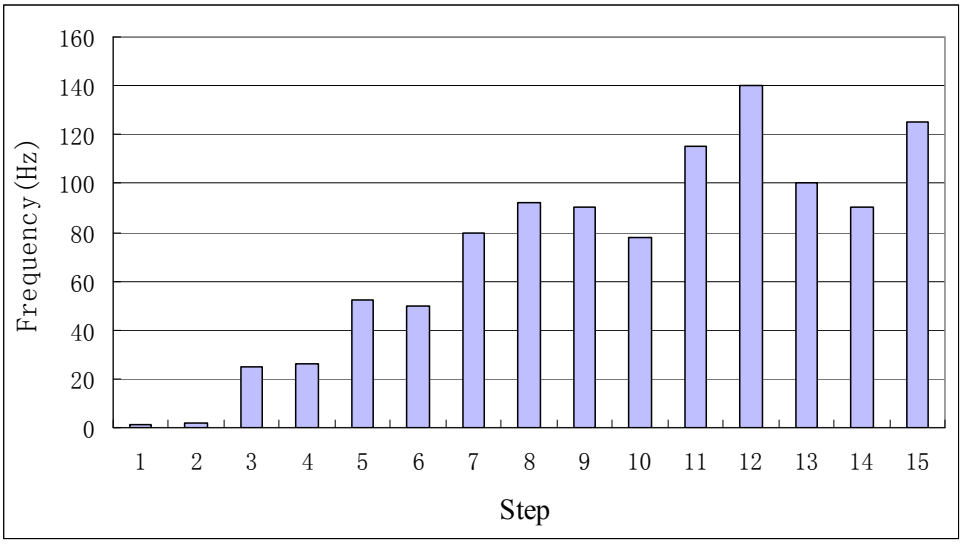

(a)

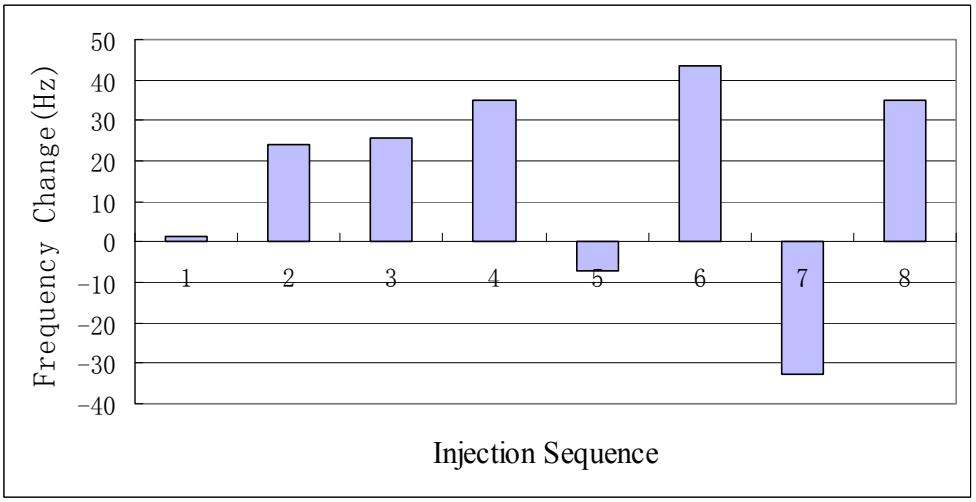

(b)

Figure 7.11. Untreated Cellulose: (a) Frequency values in each injection step; even numbers on x axis represent injecting buffer every time, step 1, 5, 9, 13 represent injecting anionic solution and step 3, 7, 11, 15 represent injecting cationic solution; (b) Frequency change with the conversion of ionic solution; even numbers on x axis represent injecting cationic solution and odd numbers represent injecting anionic solution.

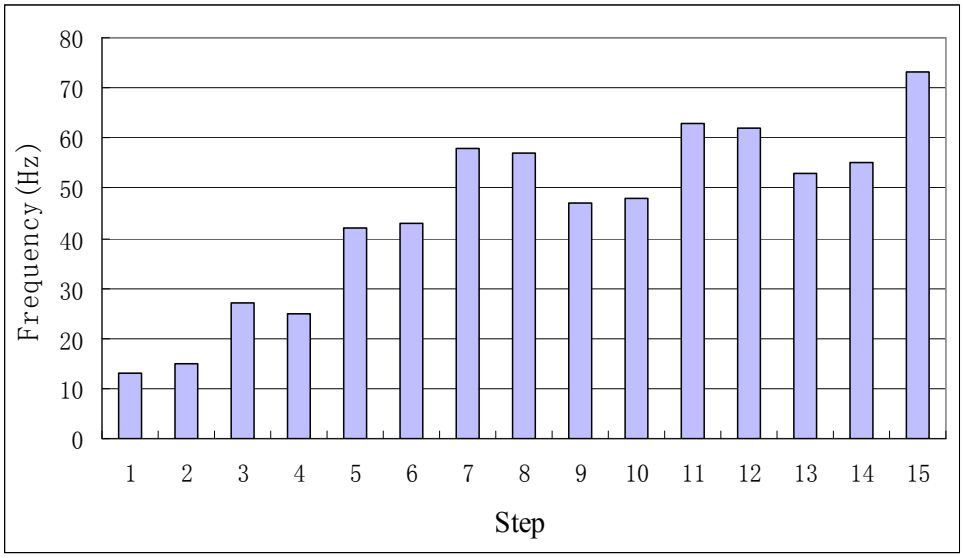

(a)

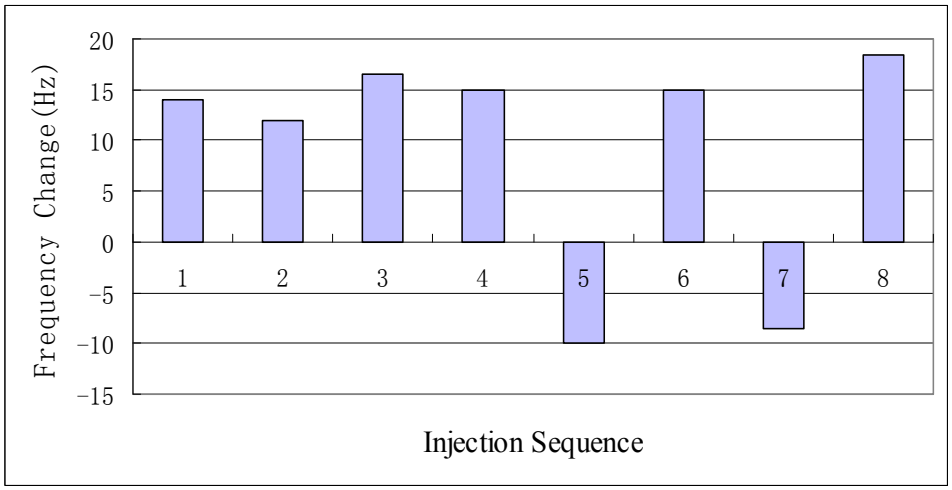

(b)

Figure 7.12. Cationic Cellulose: (a) Frequency values in each injection step; even numbers on x axis represent injecting buffer every time, step 1, 5, 9, 13 represent injecting anionic solution and step 3, 7, 11, 15 represent injecting cationic solution; (b) Frequency change with the conversion of ionic solution; even numbers on x axis represent injecting cationic solution and odd numbers represent injecting anionic solution.

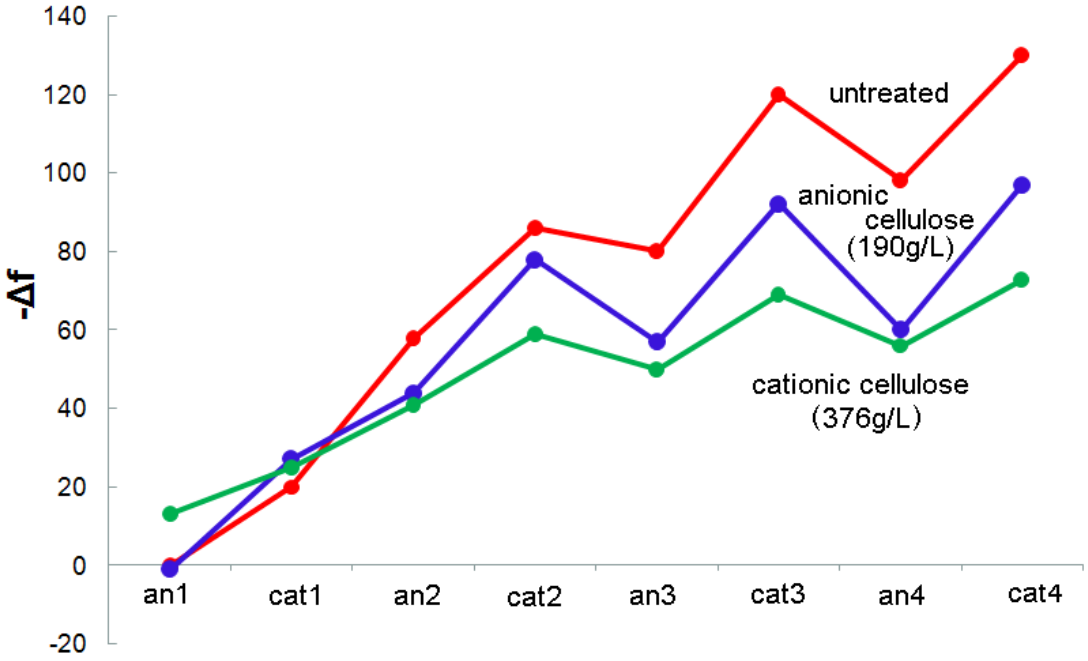

Figure 7.13. Build up of Multilayers on Cationic Cellulose (*an* first)

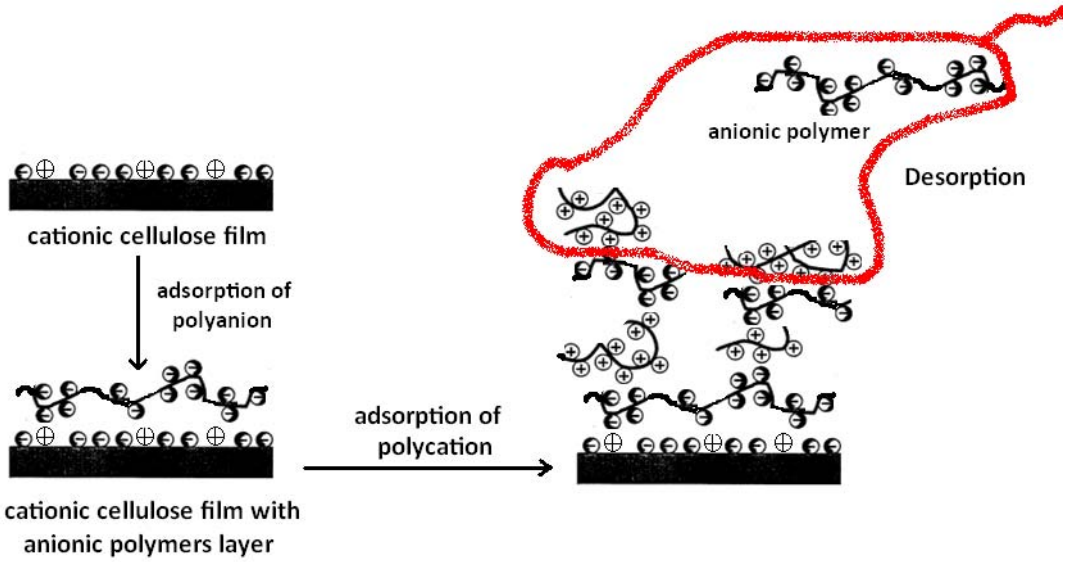

Figure 7.14. The hypothesis of polyelectrolyte adsorption on the cellulose film after few layers deposition.

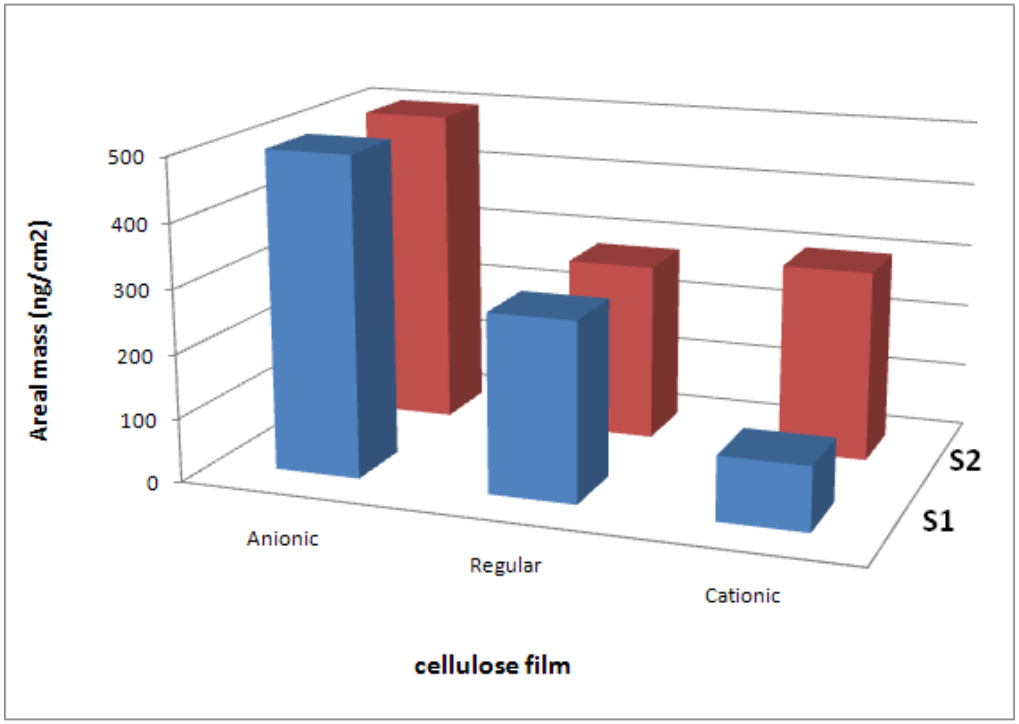

Figure 7.15. Areal mass (ng/cm2) of cationic polymers (DMAPAA) deposition on different cellulose substrates; S1: the first injection is DMAPAA, S2: the first injection is IA.

CHAPTER 8: CONCLUSIONS AND FUTURE WORK

This work has further established the charge distribution of ionized cotton. Polyelectrolyte layer deposition was shown to be determined by the surface charge distribution of ionic cellulose film. The deposited thin layers are capable of changing the macro-scale properties of the substrates. The use of nano-scale deposition techniques, Layer-by-layer deposition, provides a new range of materials to be used in textile applications. A few possible applications for conformal nano-scale coating on textile substrates include new platforms for photovoltaic and fuel cell devices, nano-magnetic structures, scaffolds for tissue engineering, drug delivery systems, and high performance nano and biomolecule filtration and separation structures. The fundamental knowledge generated by this project has helped improve the understanding of surface and total charge of ionic cotton. This work could also help to understand layer-by-layer deposition process affected by substrates with different charge densities.

Table 8.1 shows how much of the charges are on the surface and how much are internal for the untreated, anionic and cationic cotton. Our results have demonstrated that ionic cotton obtained more charges groups by chemical treatments than untreated cotton. The amount of internal charge is much greater than it of the surface charge. Cotton treated with the higher concentration of cationic or anionic reactant leads to the higher surface and total charge density. As the concentration of ionic reactant increases, the internal and surface charge of the cotton increase. An excess of cationic

reactant seemed not to produce an equivalent increase in charge. Saturation in the level of charge modification is expected. The amount of negative charges of the anionic cotton was greater than that of the amount of positive charges of cationic cotton. At the same time, the study has pointed out that adsorption of positively charged polymer occurred on all substrates, including the cationic, anionic and untreated cellulose films. The adsorbed mass on different cellulose film increased with the increase in negative charge density on the surface. Adsorption of negative charged polymer only occurred on the cationic cellulose film. The first layer deposition depended on the charge density of cellulose film, but the second layer depended both on the substrate and the first adsorbed layer. After three layers on the cellulose film, the outermost layer was found to soft and unstable, and the subsequent layers were difficult to adsorb from polyelectrolyte solution.

In future experiments, XPS can be used to determine the charge density of ionic groups on the fiber surface by measurement of nitrogen content (cationic groups), and carboxyl content (anionic groups). Comparing the results from streaming current and streaming potential measurements results from XPS could give more information to understand the charge distribution on the ionic cotton's surface.

In future study, pH or kind of polyelectrolyte could be changed when studying its adsorption on cellulose film by QCM-D. Or at the same experimental condition, compare with polyelectrolyte adsorption on cellulose model surface or silica surface. Meanwhile, many new substrates could be investigated in future research. Synthetic

materials such as polypropylene and nylon and natural materials such as silk are just a few of the possible choices of substrates.

A variety of coatings could also be studied. Atomic layer deposition of metals such as silver, copper, nickel and ruthenium would be of great interest. Many different materials and polymers can also be deposited on the textile fibers by LbL deposition. It will be necessary to employ a variety of analysis techniques to determine the effect of the coatings on the structural, physical, and chemical properties of the modified materials.

Table 8.1 The ratios of internal and surface charge to total charge for the untreated, anionic and cationic cotton.

	Internal Charge/ Total Charge	**Surface Charge/ Total Charge**
Untreated Cotton	76.9%	23.1%
low level Cationic Cotton	82.5%	17.5%
high level Cationic Cotton	79.6%	20.4%
low level Anionic Cotton	81.6%	18.4%
high level Anionic Cotton	79.1%	20.9%